A STUDY OF THE KINETICS AND MECHANISMS OF MATERIALS EJECTION FROM A BASIC OXYGEN FURNACE

A STUDY OF THE KINETICS AND MECHANISMS OF MATERIALS EJECTION FROM A BASIC OXYGEN FURNACE

by

STEVE LACIAK, B.ENG.

A Thesis

Submitted to the School of Graduate Studies

in Partial Fulfilment of the Requirements

for the Degree

Master of Engineering

McMaster University

November, 1977

MASTER OF ENGINEERING (1977)
(Metallurgy and Materials Science)

McMASTER UNIVERSITY
Hamilton, Ontario

TITLE: A Study of the Kinetics and Mechanisms of Materials Ejection from a Basic Oxygen Furnace

AUTHOR: Steve Laciak, B.Eng. (McGill University, Montreal)

SUPERVISOR: Dr. W-K. Lu and Dr. D. Cosma

NUMBER OF PAGES: xii, 230

ABSTRACT

A production basic oxygen furnace installation at Dominion Foundries and Steel Ltd., Hamilton, Ontario was used to develop and evaluate a method of measuring the rates of materials ejection during steelmaking. These rates are determined by periodic sampling at the mouth of the BOF with a tubular sampler during the oxygen blow.

The materials ejected are classified into two categories, slopping and metal ejection. From the measured rates and analyses of ejected materials, combined with the composition of the slag and metal bath as obtained by direct sampling, certain insights are made about the mechanisms of materials ejection. Among the process variables examined, the metal bath level, oxygen flow and course of slag development showed the largest influence on ejection rates.

ACKNOWLEDGEMENTS

The author wishes to express his gratitude to the following:

The National Research Council for the award of a 1967 Science Scholarship, McMaster University for some financial support and Dofasco for sponsorship of the project.

Dr. D. Cosma, the research supervisor at Dofasco, for his continued guidance throughout all phases of the work.

Dr. W-K. Lu, the research supervisor at McMaster, for his guidance in the project.

Brian Morris, Eric Partelpoeg, Steve Walsh and Dan Sofrenevic for their assistance in the various stages of sampling.

Dr. P. Apté, Fred Goetz and Kenzo Yamada for their discussions on the subject material.

Dominion Foundries and Steel Company Ltd., for extensive use of plant equipment and generous assistance of the following departments:

Melt Shop Personnel, Mr. T. Wright, General Foreman, in particular.

Research Department Analysis Lab.

Research Department Steelmaking Group, Dr. B. A. Strathdee, Manager, Applied Research, in particular.

Jackie Lazenby for her careful typing of the manuscript.

TABLE OF CONTENTS

LIST OF FIGURES

LIST OF TABLES

LIST OF SYMBOLS

g	=	gravitational acceleration = 981	(cm sec^{-2})
μ_L	=	liquid viscosity	(gm $cm^{-1} sec^{-1}$)
ρ_L	=	liquid density	(gm cm^{-3})
σ_L	=	liquid surface tension	(gm sec^{-2})
$\bar{n}_c$	=	critical cavity depth	(cm)
$\dot{Q}$	=	mass flow rate of gas	(gm sec^{-1})
$\dot{V}_j$	=	sonic gas velocity	(cm sec^{-1})
h	=	lance height	(cm)
n_o	=	cavity depth	(cm)
K	=	constant	(unitless)

1. INTRODUCTION

Since its inception in the early fifties, the basic oxygen steelmaking process has been applied worldwide to the point where today it accounts for the majority of steel production. Its phenomenal growth is attributable to the speed of the refining reactions. The process reaction scheme is very complex since it involves mass and heat transfer between several phases. The rapidity and complexity of the process make it difficult to control, occasionally resulting in such untimely problems as slopping and metal ejection. These two interfering factors are of industrial importance because they contribute to loss in yield. They also intensify such operating problems as lance failure, vessel refractory wear, and general furnace mechanical maintenance. These problems all signify a decreased steel productivity. For this reason the abatement of slopping and metal ejection is a major concern in all modern steelworks. In this thesis, the nature and causes of these interferences in the process are examined.

In this thesis "slopping" corresponds to the physical ejection from the basic oxygen furnace (BOF) of the gas-metal-slag emulsion formed during the course of refining. The force of ejection comes from the explosive evolution of CO gas in localized areas. Slopping generally occurs during the first half of the blow. Slopping represents an out of control state in the furnace. Certain changes of operating parameters may alleviate slopping while it is happening, but cannot completely eliminate it until the process is once again stabilized through its natural course. The occurrence of slopping is dependent on many factors; the more important ones are thought to be lance operation, vessel size, slag development and raw material quality. The exact quantitative

influence of these parameters in commercial furnaces has not been determined. Even the cause of slopping and its dependence on the interplay of physical and chemical phenomena are highly debatable subjects.

If the BOF is operated properly at its design capacity slopping will only occur sporadically. The degree of slopping when it occurs varies from a "light" slop where only small fragments are thrown out to a "heavy" slop where large pools of emulsion are ejected. In many steelplants where the need arises for increased production, the BOF's are overcharged since efficiency and operation stability are easily sacrificed for the want of a larger installation. These types of operation are subject to more persistent slopping, both in terms of its duration during a heat and its frequency of occurrence. In some steelplants that work in the upper ranges of furnace loading (maximum is about 50% above design capacity), slopping recurs in every heat to different degrees. The reduction in metal yield that results from slopping normally ranges from 0.4 to 1.0%, but can rise in cases of high overloading to 5%.[1-3] The need therefore exists to minimize slopping since the financial benefits are remunerative.

Metal ejection from the BOF exists in two forms, either as molten metal splash or as fine metal droplets entrained in the off gases by drag forces. The more common industrial terminology for metal ejection is "sparking" since this material burns brightly as it oxidizes in the surrounding air atmosphere. Any metal ejection or fine emulsion particles from slopping can be carried into the operation's dust cleaning system if it is fine enough to be entrained in the gas stream. However the majority of metal ejection and slop falls over the sides of the vessel into the surrounding slag pit (See figures 1 and 2).

Metal ejection arises from the combined physical and chemical action of the oxygen jet on the metal bath. Depending on the extent of control a furnace

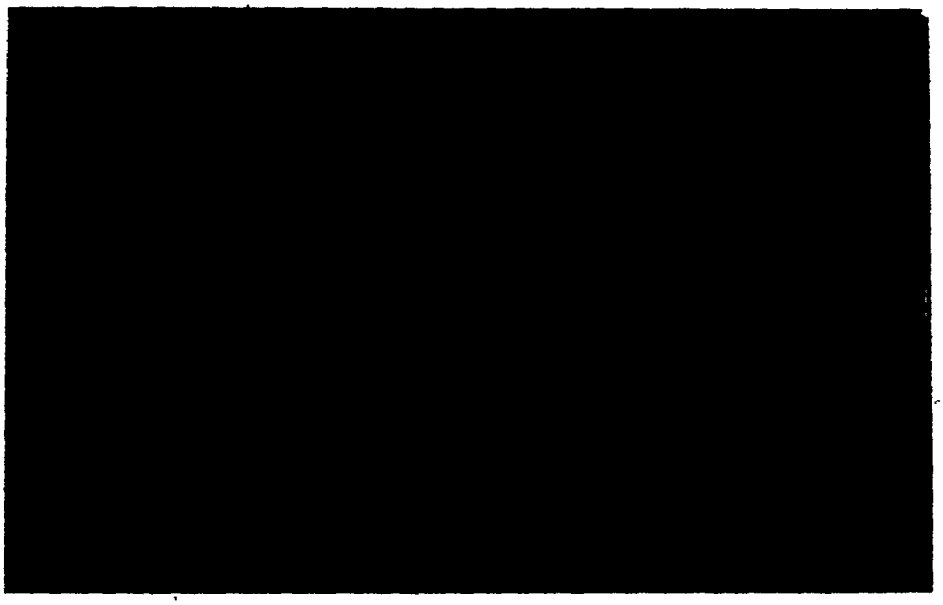

Fig. 1. A view of heavy slopping at the 10 minute mark from the back of the furnace at Dofasco.

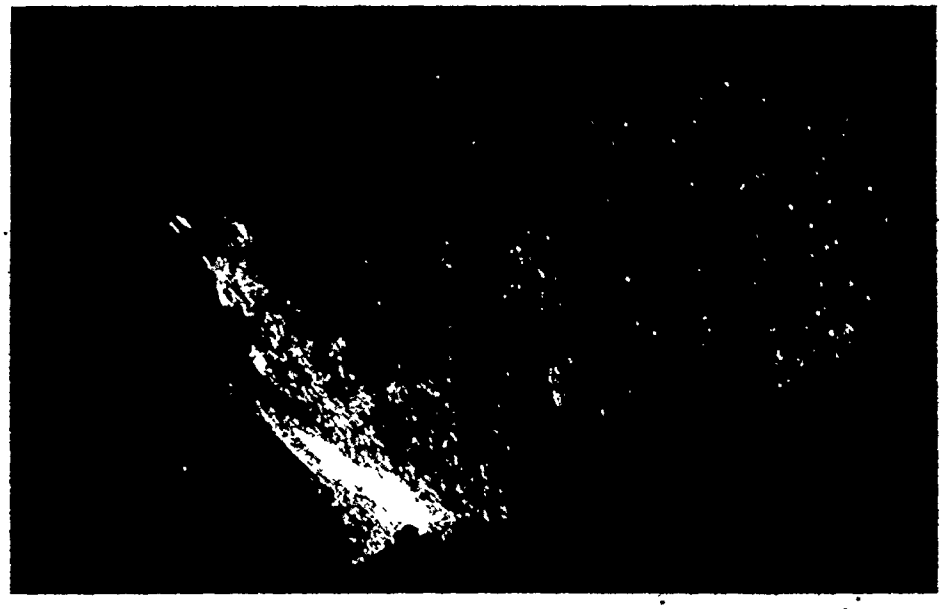

Fig. 2. A view of metal ejection at the 18 minute mark from the back of the furnace at Dofasco.

operator has on the process, the yield losses by metal ejection can vary from 0.2 to 1.8%.[4] The previously mentioned parameters which were said to affect slopping are also the main factors determining ejection rates, but their exact influence is again unresolved. The main reason for this is that these phenomena are not well understood since they have not been studied in great detail in commercial vessels. Very many model studies[5-29] have been conducted on this subject using low temperature liquid mediums with the belief that physical forces were predominant. The contributions due to chemical reactions were neglected. A greater understanding of the mechanical parameters affecting ejection has resulted from these studies, but they cannot simulate all the conditions giving rise to metal ejections in commercial furnaces. Even hot model studies[30-38] using iron-carbon baths have proved inadequate since their operation was under idealized conditions of very thin slag cover. Such a state is present in real BOF's only in the initial segments of the blow.

These two phenomena - slopping and metal ejection - comprise a large part of the material losses from the BOF mouth during a blow. They can account for large metal yield losses, up to a maximum of 5%, and thus must be minimized. Before any improvement can be achieved, their nature and causes must be identified. Very little useful information, particularly of the industrial variety is presently available. For this reason, this investigation was limited to studies of a commercial BOF operation. The extent and nature of these material losses from one particular installation - Dominion Foundries and Steel Ltd. - was studied by direct sampling during the blowing process. Techniques and instruments of sampling were developed to carry out this work. In an effort to further the understanding of the causes of these phenomena, simultaneous sampling of the slag and metal bath was undertaken.

2. LITERATURE SURVEY

Since there are no generally accepted explanations for slopping or metal ejection, it is necessary to examine the main factors that may be responsible. In this survey, these variables are reviewed both in the manner that they can cause these phenomena to occur and their actual quantitative effects based primarily on cold model studies since actual furnace data is lacking. Current explanations for the cause of these phenomena and possible methods of their control are also examined.

The process variables that are thought to exert the greatest influence on slopping and metal ejection include lance practice, vessel size and geometry, and raw material quality. Slag development[39-107] during the blow is another major factor, possibly the most important, but it cannot rightly be considered an independent parameter since it is entirely controlled by the prior three. Figure 3 shows schematically the inter-relationships that exist between these variables, their spheres and magnitudes of influence, and their net effects. Stability of operation and refining efficiency are seen to be the main process goals.

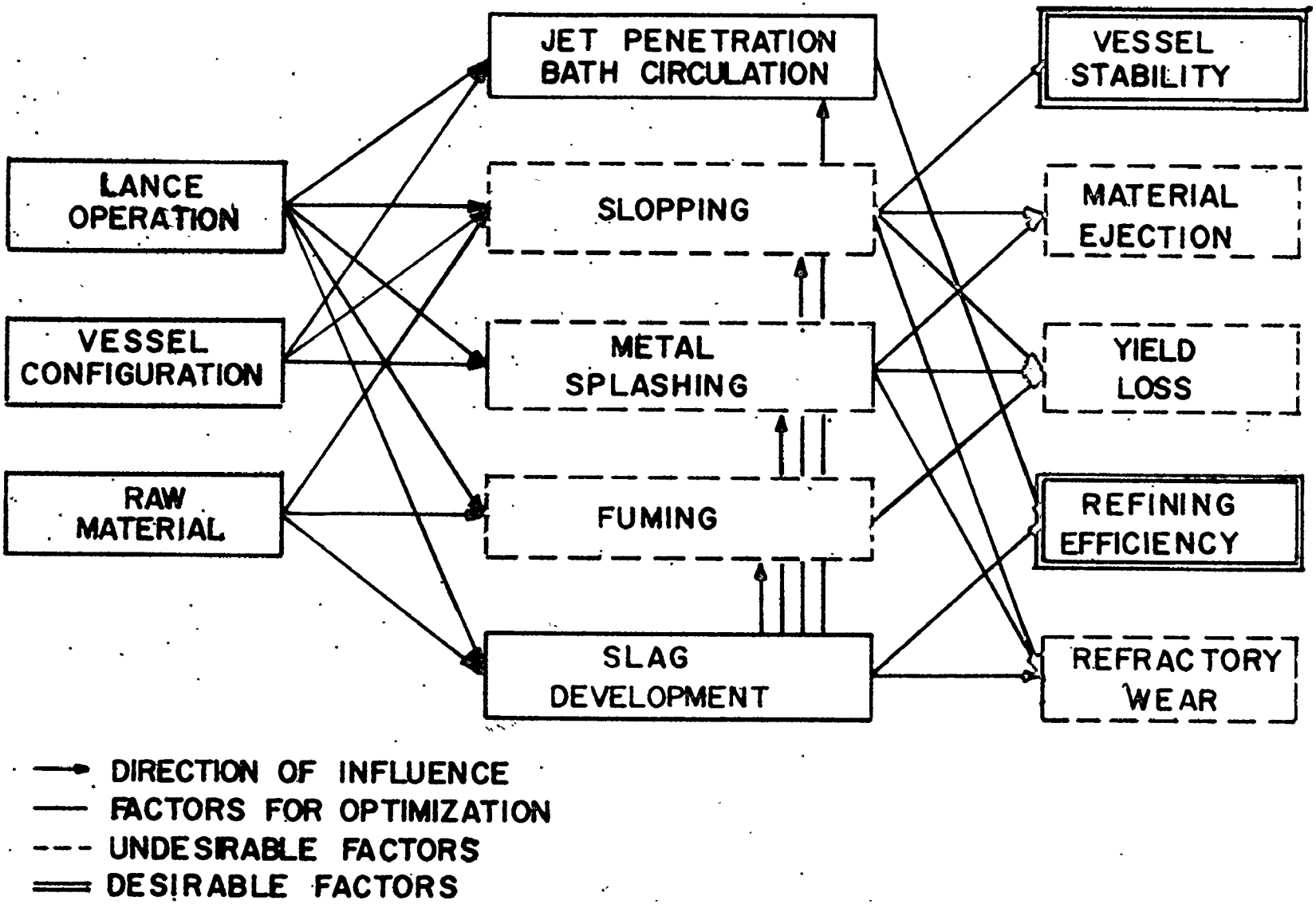

Fig. 3. Interrelationships between the main process variables in BOF operation and the various avenues of material loss.

2A. SLAG DEVELOPMENT

Slag evolves dynamically during the blowing process as the various elements in the hot metal are oxidized and the different flux additions dissolve to form the slag. A stable refining operation free of slopping can only be achieved if the slag is formed in a proper way. Though the importance of slag development has been realized, the question of optimal compositional course to minimize slopping is highly debatable[3, 39-45]. The slag, if it provides a good cover over the metal bath, will substantially minimize the extent of metal ejection since it will serve to physically entrap this material. In addition the slag contains metal droplets in its normal course of development as has been discovered by various authors[46-75]. These metal droplets are the basis for the slag-metal-gas emulsions formed in the furnace during the blow and it is their reaction with the slag to generate large amounts of gas that can cause slopping. Metal droplets are always present in the slag to different extents and their role in the refining reactions is discussed later.

The course of slag development can be altered by changes in blowing practice, hot metal and scrap chemistry and flux additions. Since steelmakers must accommodate their operation to these different conditions, there are many established slag evolution paths considered to be acceptable. Figures 4, 5 and 6 show the "normal" courses of slag development at three BOF shops. They are similar in most respects, but intrinsic differences exist due to varied operation. A general outline of these slag courses and the accompanying proposed reaction mechanisms is now given.

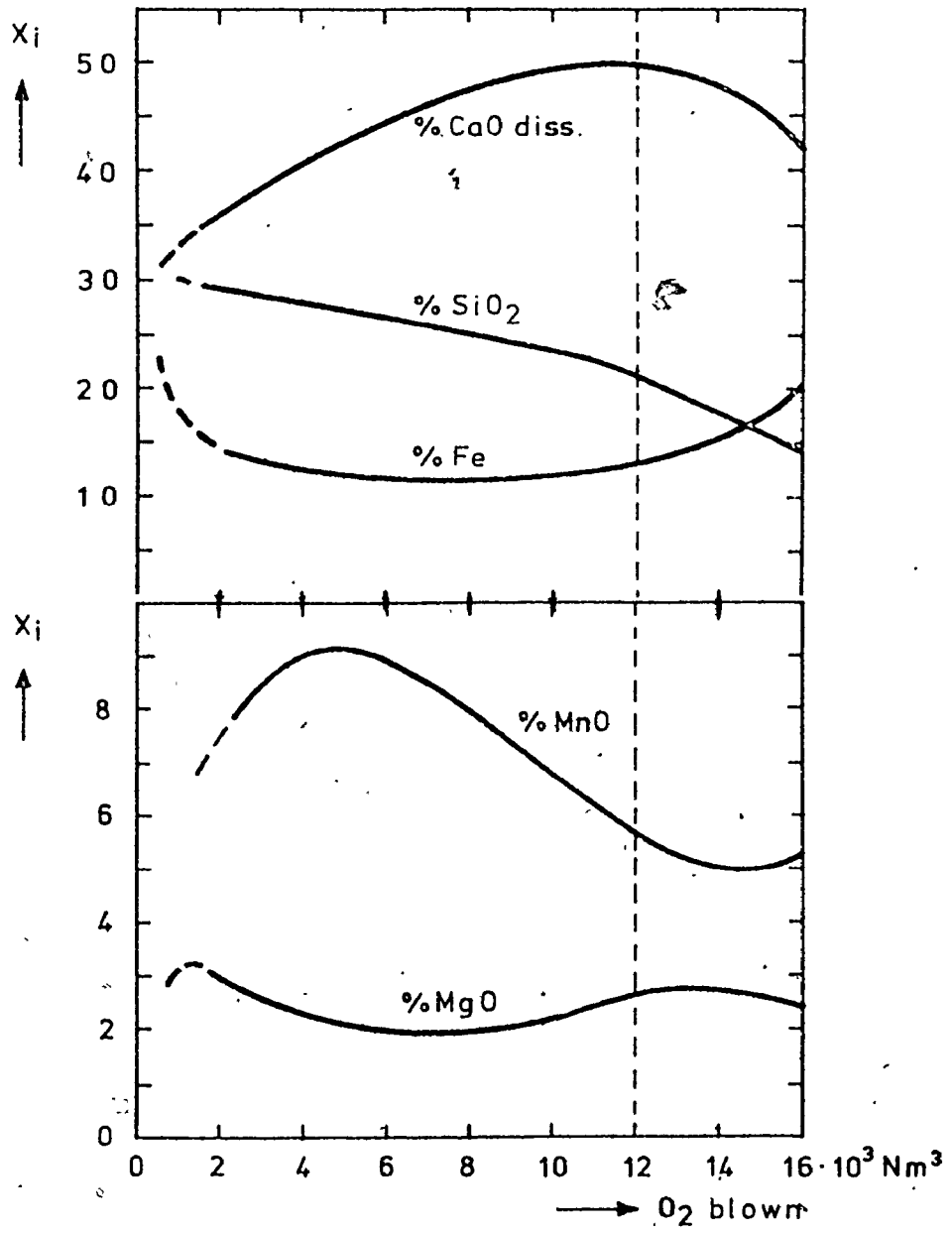

Fig. 4. Evolution of the slag composition during the blow at Hoog ovens. (after van Hoorn (47)).

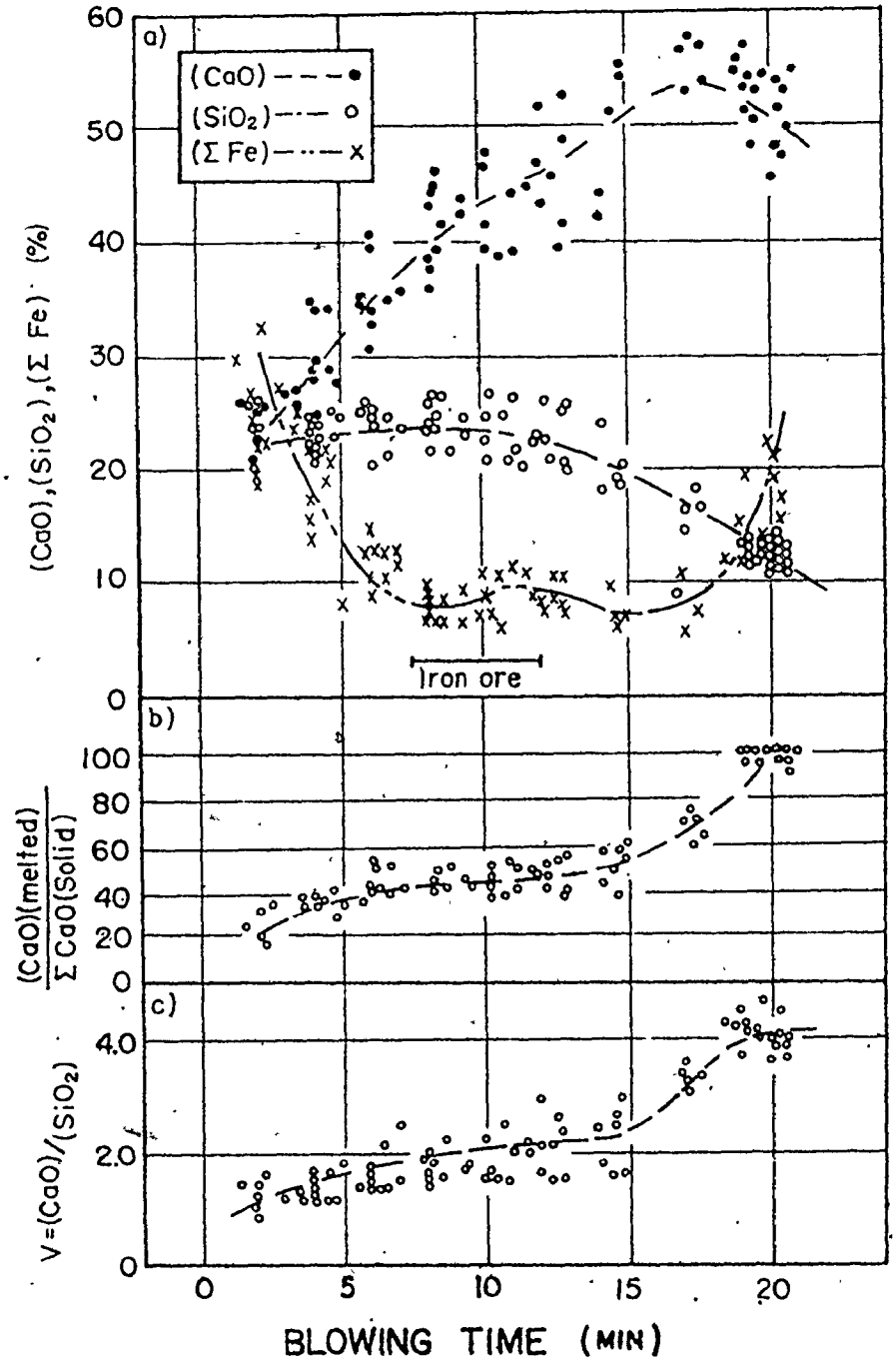

Fig. 5. Change in a) compositions, b) degree of melting of lime in slag, and c) basicity during the blow at NKK. (after Kawakami (107)).

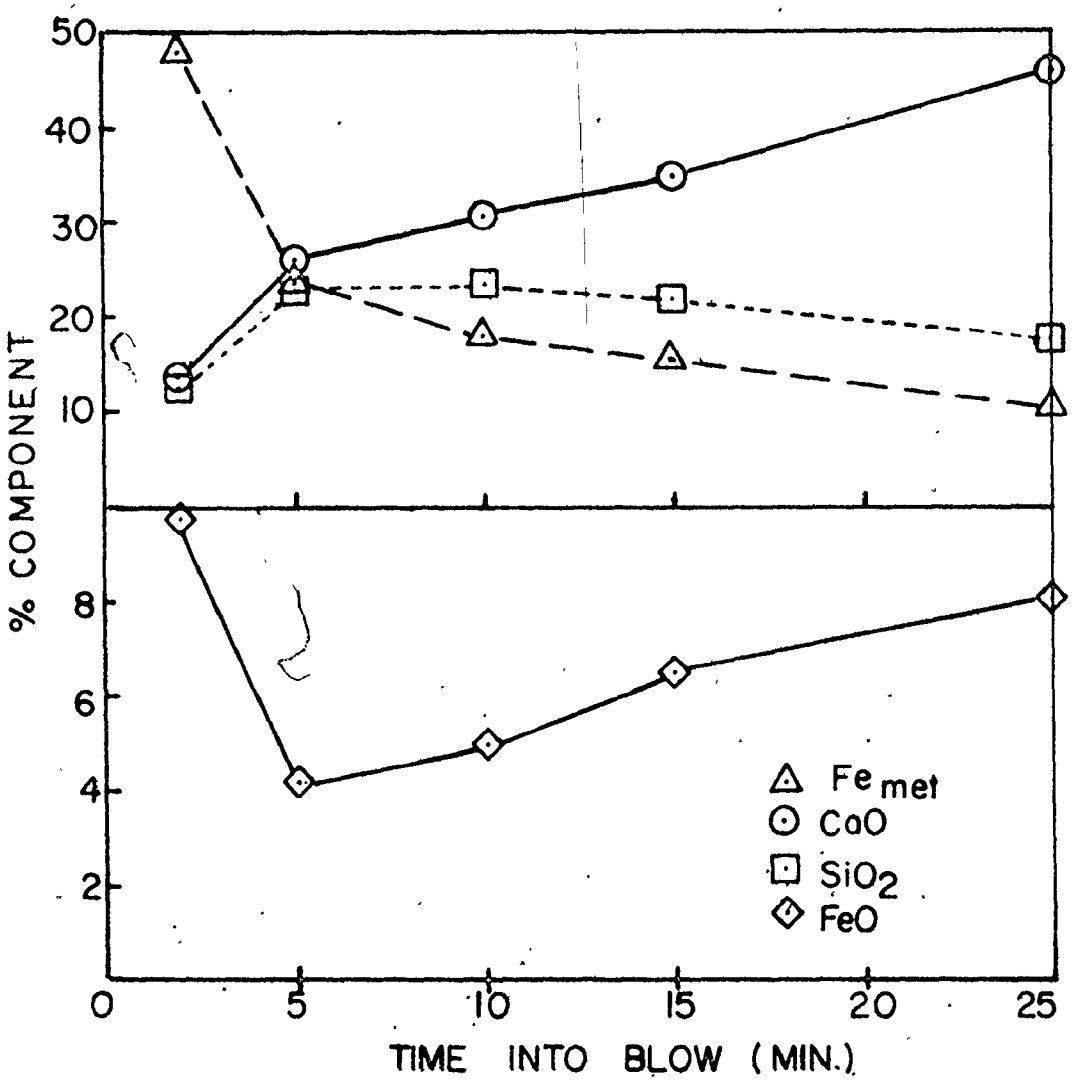

Fig. 6. Slag and emulsion development during the blow at Bofasco. (after Cosma (48)).

At the beginning of the blow a small amount of slag rich in iron, silicon and manganese oxides is produced beneath the lance by direct oxidation of the bath. The metallic iron content in figure 6 illustrates that as this slag is being formed, metal droplets (.1 to 1mm. radius[56, 57, 63]) are ejected into it by the mechanical action of the impinging oxygen jet. These droplets that form the slag-metal emulsion initially contain all original impurity elements. The silicon and manganese in these droplets is preferentially removed by reaction with FeO or Fe_2O_3 contained in this highly oxidizing slag. A continual cycle of droplet formation, reaction and settling to the bath because of its higher density takes place. These refining reactions also occur simultaneously by different mechanisms in the jet impact area and at the slag-metal bath interface. The partition of the total extent of individual reactions among these sites cannot be determined yet. The lime added to the furnace is seen to dissolve very rapidly in the initial acidic slag, but thereafter the dissolution rate slows down. This is considered to be due to the formation of an impervious calcium orthosilicate shell (15-70μ thick[48]) around the lime and dolomite particles. As blowing proceeds, this layer is gradually infiltrated by ferrous and manganese oxides[65]. This brings about the degradation of this barrier and allows further lime dissolution. During the early stage of the blowing period decarburization proceeds slowly because it is hindered kinetically by the low hot metal temperature and oxygen availability for carbon. It is thermodynamically more favorable for certain other impurity elements above certain concentrations to be oxidized.

All the silicon is essentially removed in the first quarter of the blowing time. The bath manganese concentration reaches a minimum at the end of this first quarter. This corresponds to a maximum in the SiO_2 and MnO content

of the slag. This point is further marked by a minimum in the dissolved iron oxide content of the slag. The decrease is brought about by the rise in the decarburization rate. Carbon in the emulsion droplets and at the slag-metal bath interface reacts with iron oxides in the slag, thereby expending it. The period of constant iron oxide level represents a balance between the rate of iron oxidation by the jet and the rate of consumption by the refining reactions. During this period lime slowly dissolves increasing the slag volume and thereby gradually diluting the slag to give lower SiO_2 and MnO levels. The MnO concentration is seen to decrease more rapidly because of the manganese reversion to the metal bath in addition to slag dilution. The decarburization rate, after gradually building up in the early blowing period, reaches its highest level during the middle segment of the blow. A typical pattern for the decarburization rate is given in Figure 7. At the maximum the efficiency of oxygen utilization for decarburization is around 100%. The circumstances giving rise to this rapid reaction rate are the higher metal bath temperatures (above 1400°C) and the beneficial mixing between slag and metal phases as promoted by the fast CO evolution rates. Decarburization occurs in inestimable proportions at all these reaction sites: directly under the jet, in the slag-metal-gas emulsion, along the trajectory of CO bubbles within the bulk metal, and at the slag-metal bath interface.

The last stage of slag development is marked by an increase in the lime dissolution rate causing the MnO and SiO_2 levels to fall off rapidly. The decarburization rate tapers off as carbon content decreases. The oxygen that is still supplied at a constant rate now serves primarily to oxidize the iron in the metal bath, thereby increasing the dissolved iron oxide content of the slag. The emulsion decarburization mechanism has been reported to slow down considerably in this time period. The primary mechanism of carbon monoxide

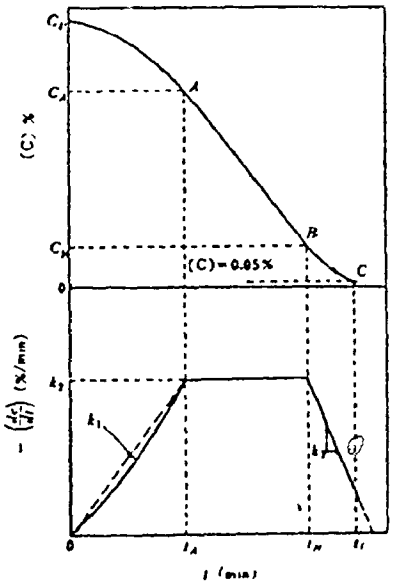

Fig. 7. Schematic diagram of a typical decarburization rate curve for a BOF heat. (after Okano (66)).

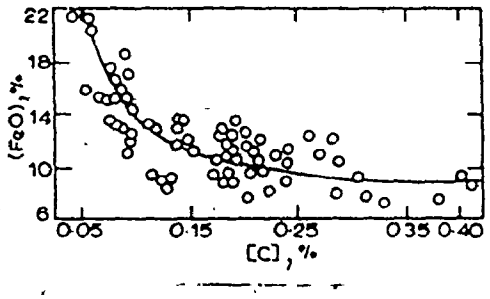

Fig. 8. Relationship between ferrous oxide content of slag and carbon content of metal of a BOF bath. (after Didkovskii (136)).

evolution would be direct jet impingement on the bath. The actual concentrations of slag components at turn down are dependent on the extent of dilution by iron oxide formation which is directly dependent on the final bath carbon concentration (Figure 8).

The evolution of the BOF slag mass can be calculated on the basis of a silicon balance. The curves for two operations are given in figure 9. The slag weight is almost constant for the major portion of the blow. A rapid rise in slag weight occurs at the end of the decarburization period due to iron oxide formation and residual lime dissolution.

The slag-metal-gas emulsion that serves to enhance the refining reactions will vary in amount during the blowing process. In the main decarburization period this emulsion can occupy a large fraction of the furnace volume if the proper stabilizing conditions are met. A schematic of the measured emulsion height during a blow in an experimental furnace is given in figure 10. The destruction of the emulsion is caused by the coalescence of the liquid metal droplets, and the subsequent gravity separation of the larger units. The durability of emulsions is therefore enhanced by any condition that hinders droplet coalescence. One obvious stabilizing factor is a high viscosity of the slag medium. The viscosity of a homogeneous slag increases with silica content (see Figure 11) at a given temperature. However, BOF slags normally contain less than 25% silica and in this range one would not expect slag viscosity to be much of a stabilizing factor. If a solid suspension is present in the slag, its apparent viscosity will increase. Undissolved lime and calcium orthosilicate (V-ratio = 1.75) found in slags could act in this manner. Indirect evidence of this effect is available from an experimental work[76] measuring the capability of commercial furnace slags for foaming (See figure 12) when gas is bubbled through them.

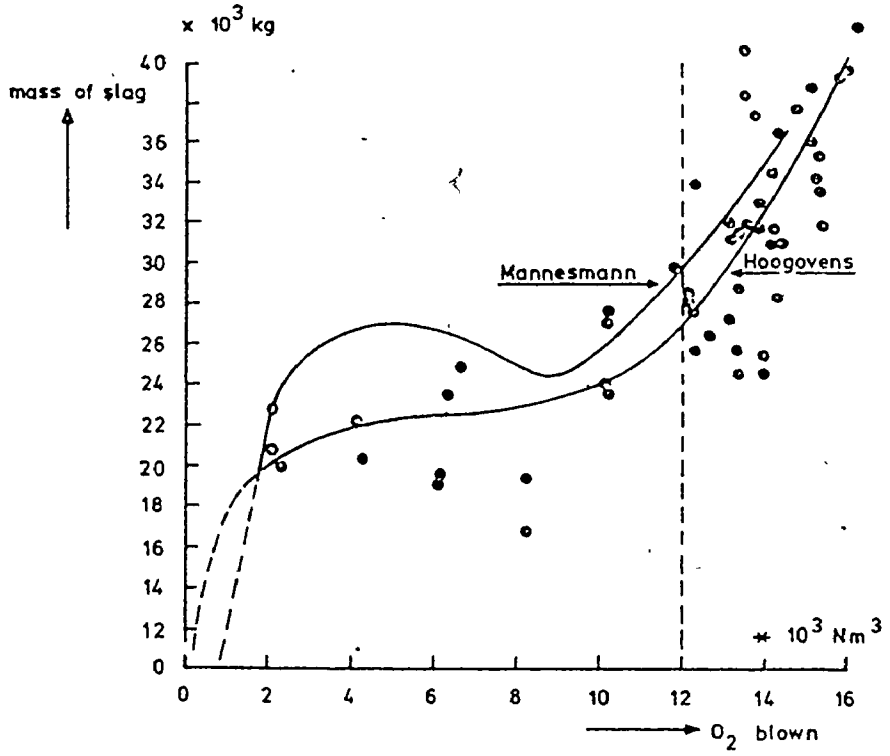

Fig. 9. Evolution of slag weight during the blow for two BOF operations. (after van Hoorn (47)).

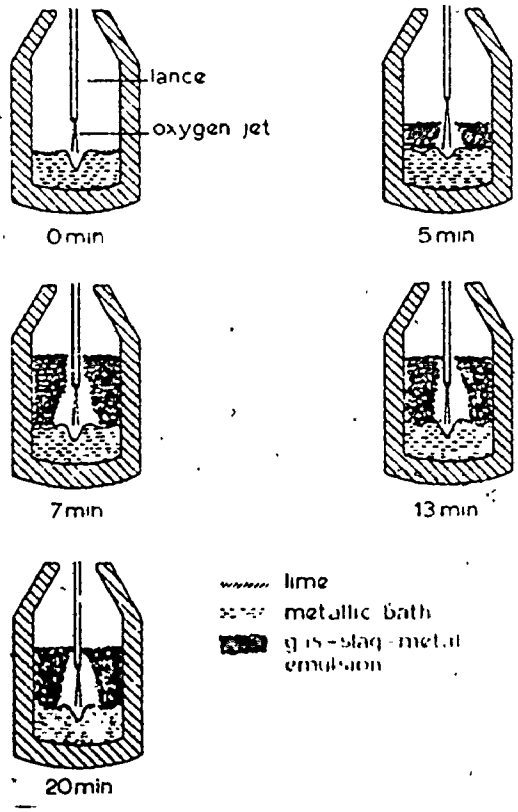

Fig. 10. Sections through a BOF showing emulsion heights at various stages of the blow. (after Chatterjee (38)).

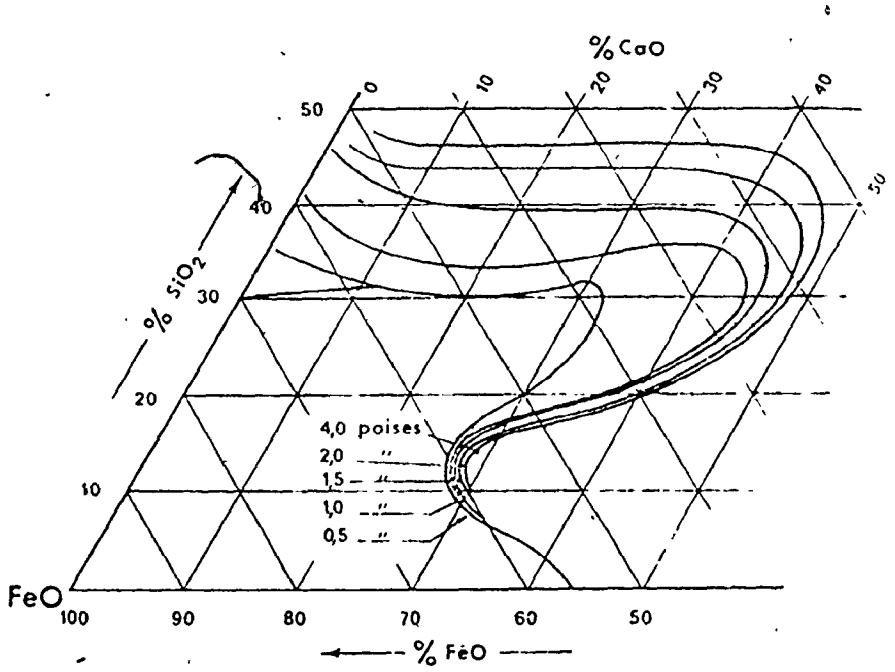

Fig. 11. Iso viscosity lines for the system FeO-CaO-SiO_2 at 1450°C. Compositions in mole percent; FeO in equilibrium with solid iron. (after Geiger (75)).

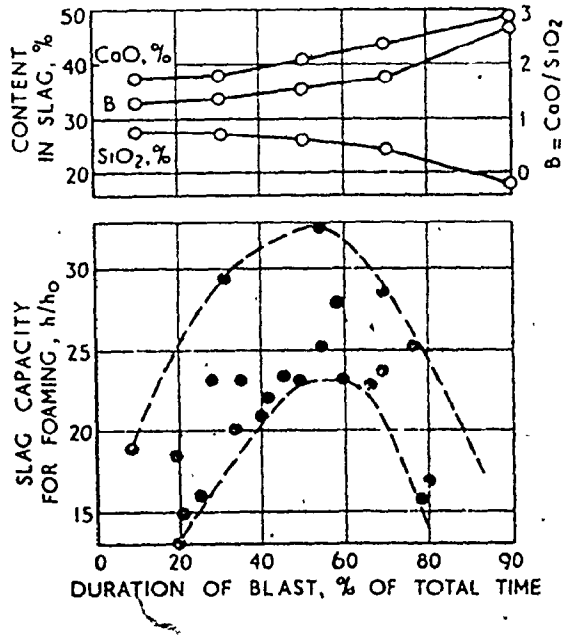

Fig. 12. Variation in slag composition and in the capacity of the slag for foaming during the process of a blow. (after Baptizmanskii (76)).

The highest values were reached in the middle of the blow with a slag basicity of 1.5 - 1.7, which is close to that of calcium orthosilicate. Emulsions can also be stabilized by the adsorption of certain solutes at the surface of the dispersion. SiO_2 and P_2O_5 are two such surface active components which lower the interfacial tension by forming monomolecular films of high viscosity around the droplet[51, 61]. Gas bubbling through an emulsion may also stabilize it by attaching itself to a metal droplet and thereby acting as an aerostat. In addition, the gas through its buoyancy effect supplies the mechanical force necessary to support a foaming emulsion. Rapid CO evolution would thus be amenable to emulsion formation. The metal droplets present in the emulsion are created by a variety of mechanisms (See Figure 13), but the predominant ones are considered to be shearing of the metal bath by the jet and metal being carried across the metal bath-slag interface as a coating on the rising CO bubbles[65].

Any condition that causes extremely fast decarburization rates to take place in the emulsion or at the slag-metal bath interface will increase the chances of slopping. Furthermore if such a situation materialises when the emulsion volume is large or the furnace is overcharged slopping will be further enhanced since the trajectory distance is shortened. This allows a greater proportion of the disturbed material in the furnace to escape without being collected on the inward sloping walls of the vessel cone. One condition that can precipitate rapid uncontrollable decarburization in the first half of the blow when slopping normally occurs is an overoxidized slag. Reported slag analyses indicate a slag Fe^{3+} to Fe^{2+} ratio lying in the 0.1 to 0.5 range[51,73] throughout the blow. The corresponding slag oxygen potential is about 10^{-5}atm., considerably above the equilibrium oxygen partial pressure of the metal droplet of 10^{-8} atm.[51; 52]. If the droplet carbon concentration is high, rapid CO

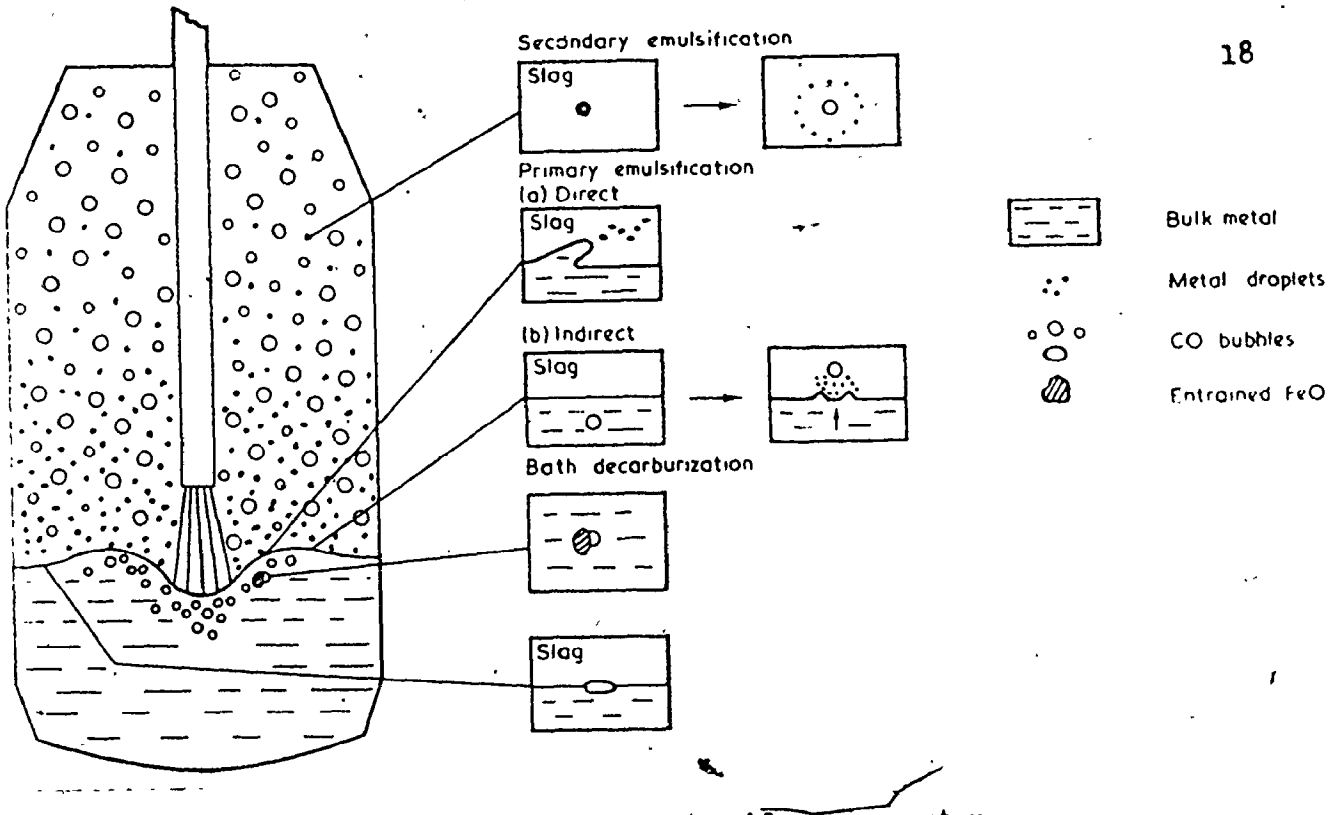

Fig. 13. Foam and emulsion formation in a top-blown converter. (after Walker (65)).

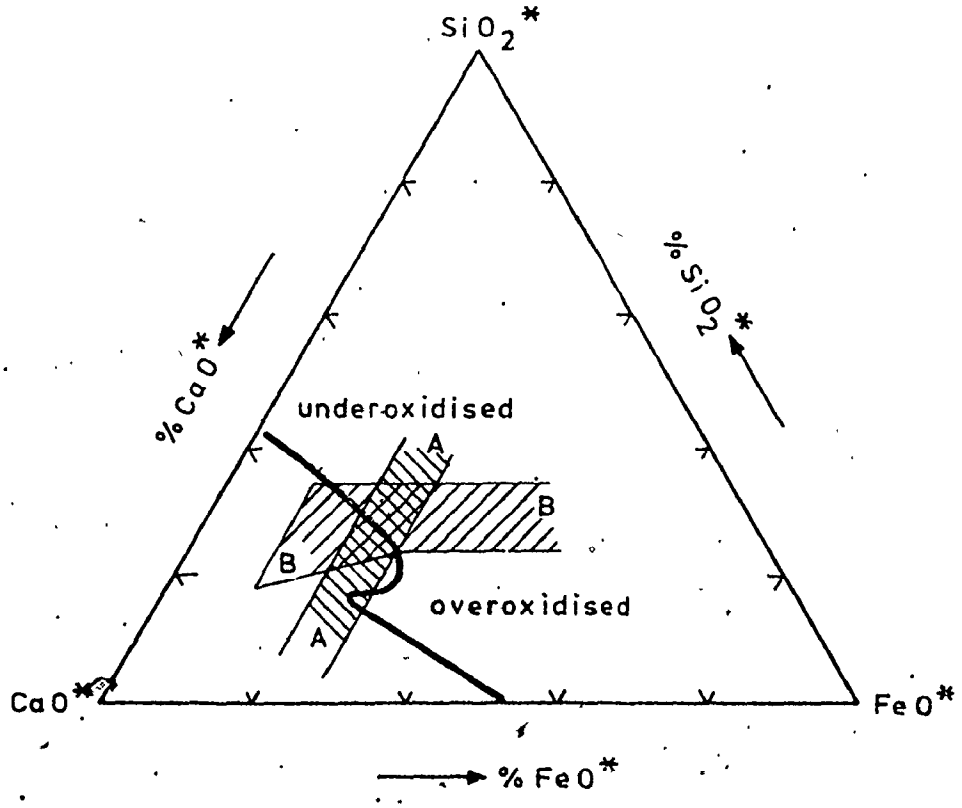

Fig. 14. Proposed slag paths by Nilles[40] (Path A) and Baker[39] (Path B) to prevent slopping. (after Van Hoorn (47)).

evolution usually results under these oxidizing conditions.

Two optimal slag paths have been suggested in literature to prevent slopping[39, 40]. One consists of maintaining a constant manageable slag iron oxide level during the entire blow (Path A) and the other recommends a continually decreasing iron oxide content as the blow proceeds (Path B), (See Figure 14). Both recognize the importance of preventing an overoxidized slag condition. Both slag paths terminate in the heterogeneous region so that a dry, lime saturated, unreactive slag is present at the end of the blow. In this way, endpoint metal specifications are more easily achieved by preventing any untimely slag-metal reactions. The main difference in the proposed paths is the importance ascribed to the presence of a slag-metal emulsion. Path A is supposed to form an early stable emulsion by passing through the precipitation region of calcium orthosilicate early in the blow. The stabilizing mechanism is the increase in the slag's apparent viscosity. Path B, though not neglecting the important refining contribution of emulsion, favors a path where the iron oxide level decreases in the critical period where the decarburization rate peaks so that the metal will be in contact with a less oxidizing slag. The emulsion can still be created in this latter operating condition through other stabilizing mechanisms. In order to force slag development along these courses, some method of dynamic control is necessary to monitor the partition of supplied oxygen between slag oxidation and the refining reactions. Adjustments could then be made in blowing practice to achieve one of these desired slag paths.

While these two recommendations differ in their efforts to control slopping, both emphasize the necessity to prevent an underoxidized slag. This situation is characterized by low iron oxide levels and high slag silica contents[39-44]. This type of slag is very viscous and dry and has poor lime

dissolution capabilities. It has a tendency to coagulate and is readily pushed aside by the oxygen jet towards the furnace walls[19, 46]. This condition is generally referred to as "slagless" blowing since the jet acts directly on the metal-bath. Metal ejection in the form of fine spray and splash occurs in this state due to the shearing action of the jet on the metal bath. It will persist as long as there is no slag cover. This slagless state can be detected using audiometric measurements of furnace noise[42, 86]. Through this means it has been determined that the total iron loss by ejection is proportional to the total time period that this state exists (See Figure 15). A fluid foaming slag richer in iron oxides can prevent this from occurring but must be controlled since excessive levels can enhance slopping.

Decarburization patterns that signal the presence of slopping in the early slag formation periods have been identified[80]. Figure 16 illustrates how erratic decarburization rate profiles, that exhibit plateaus where the imput oxygen accumulates in the slag, lead to heavy slopping conditions. The optimum path to avoid slopping is to have a smoothly increasing decarburization rate (Figures 16 and 17) after the silicon and manganese have been removed. This can again be achieved by controlling lance practice in conjunction with continuing monitoring instruments that measure the decarburization rate through off-gas analysis and flow measurement[78-88].

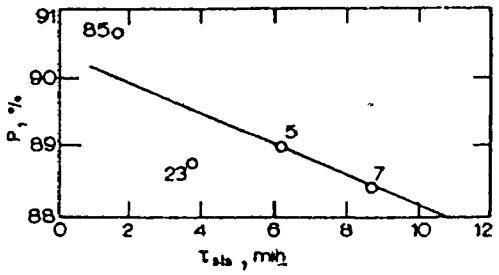

Fig. 15. Relationship between yield of good metal (P) and duration of period of slagless blow. (after Okhotskii (4)).

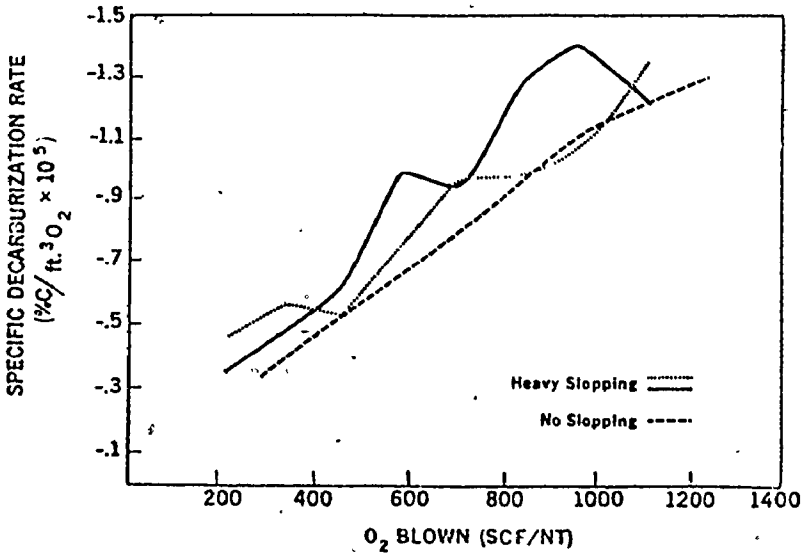

Fig. 16. Refining curves taken during critical slag formation period showing the pattern for slopping and non-slopping heats. (after Meyer (77)).

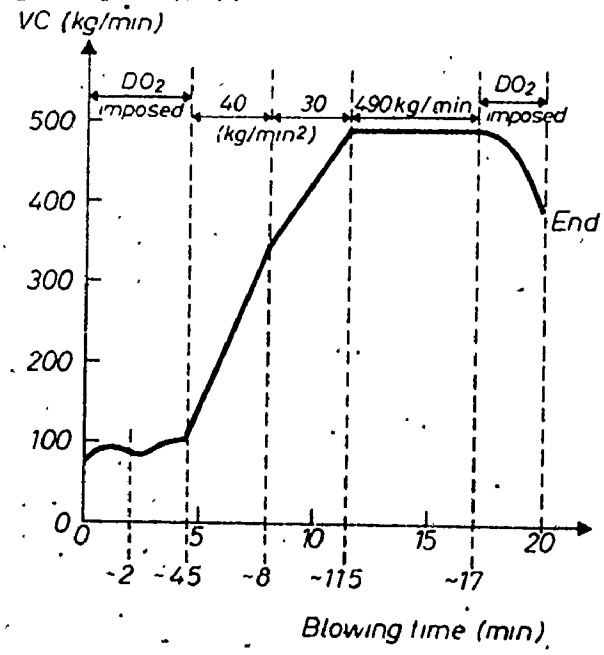

Fig. 17. Examination of set decarburization profile at Cockerill-Seraing to eliminate slopping. (after Nilles (40)).

2B. JET PROPERTIES AND INTERACTION WITH THE METAL BATH

Jet nozzles used in basic oxygen steelmaking operate primarily at supersonic velocities so discussion is limited to them[107-111].

A convergent-divergent nozzle (Figure 18) is employed to achieve supersonic velocities. In the convergent section, the gas velocity cannot exceed the speed of sound. In the second stage further acceleration is achieved through adiabatic, isentropic expansion. There is an optimum ratio of throat area to exit area that allows the gas to expand to a pressure at the exit section equal to the surrounding pressure[108]. Thus a nozzle is most efficiently operated at its designed flow rate. Underblowing or overblowing will result in decreased conversion of pressure energy to the kinetic form, with the excess going to shock wave formation. As the gas exits from the nozzle, it spreads in the surrounding atmosphere. This interaction is one of tangential shear such that the overall jet momentum is conserved. In the control core of the jet the supersonic velocity persists for a distance that is dependent on the exit velocity[109]. Very little spreading occurs up to this point. Once subsonic velocities are reached the jet decays at an included spreading angle of 18°. In BOF practice, since lance heights are usually in the range of 30 to 40 times the throat diameter, the jet will impinge on the metal at subsonic velocities. The slag also slows down the oxygen jet but it is presumed this effect is negligible[109]. Most lances presently used have three nozzles. In this case the individual gas jets will not interact with each other at any distance unless their mutual inclination angles are less than 10°[108].

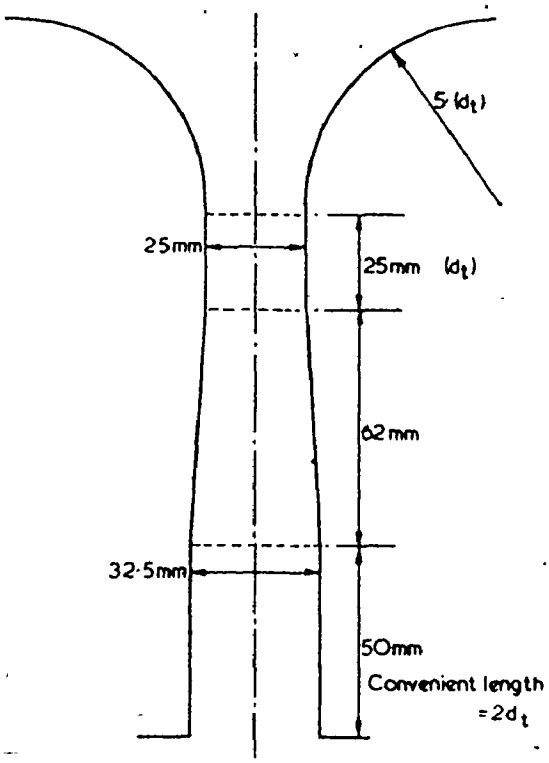

Fig. 18. Correctly designed Mach 2 nozzle with a 25mm throat diameter. (after Chatterjee (109)).

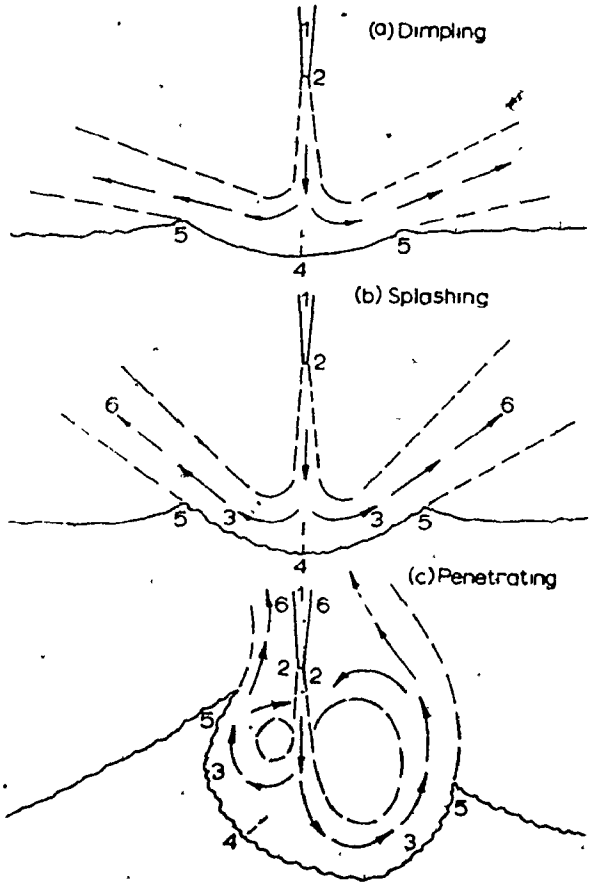

(1) nozzle body; (2) entrainment region of the original jet; (3) entrainment region of the wall jet across the phase interface; (4) stagnation point of the original jet; (5) separation point of the wall jet; (6) two-phase exit flow

Fig. 19. Comparative geometry of the three modes of jet impingement on a liquid.

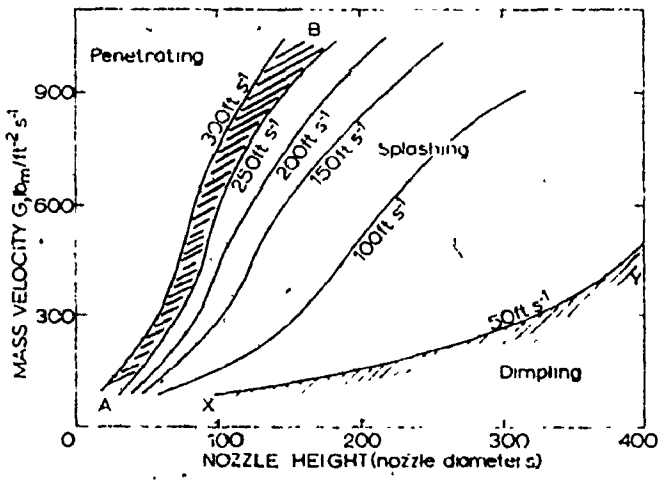

Fig. 20. Region of existence of the three flow modes as characterized by the jet impact velocity. (after Molloy (8)).

Since the most comprehensive studies[5-29] of jet liquid interaction have been conducted using aqueous media and mostly non-assimilable gases, it is best to review their findings before further discussion of systems under consideration. These are model studies and can provide a clue to the operation of steelmaking.

There are three main modes of jet impingement characterizable by the central impact velocity of the jet (See Figures 19 and 20). For impact velocities lower than 15m/sec a stable surface depression termed "dimpling" is formed[8]. This depression oscillates slightly in the vertical direction. As the jet momentum increases the indentation becomes deeper and at a certain critical dimension the cavity becomes unstable. At this point there is some entrainment of the liquid phase in the deflected gas stream leading to splashing. A small portion of this splashed material is captured in the incoming gas stream. Splashing is seen to occur by three randomly occurring, independent mechanisms that can be categorized according to their cavity motion (See Figure 21). In the stretching mode the cavity tapers in and out with splash-forming when there is an overhanging lip. In the bending and rotating modes, material is ejected from the protruding cavity edge. There is considerable energy absorption involved in maintaining these cavity motions.

The critical cavity depth at which splashing begins has been experimentally identified as being a function solely of the liquid properties[9, 14]. Using dimensional analysis in conjunction with the laboratory findings, the following relationship was developed[14]:

$$\frac{g\mu_L^4}{\rho_L \sigma_L^3} = 4.3 \times 10^{-22} \exp\left[4.34 \frac{(\Delta\rho_L)^{1/2}}{(\overline{\sigma_L})} \bar{n}_c\right] \qquad (2.1)$$

This equation has been experimentally verified over a wide range of media including some liquid metal baths. It presumably is applicable to steel

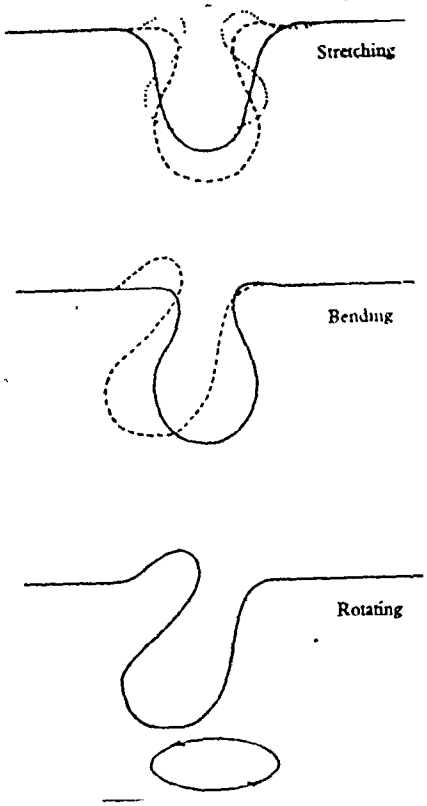

Fig. 21. Modes of indention instability leading to splashing (after Rosler (7)).

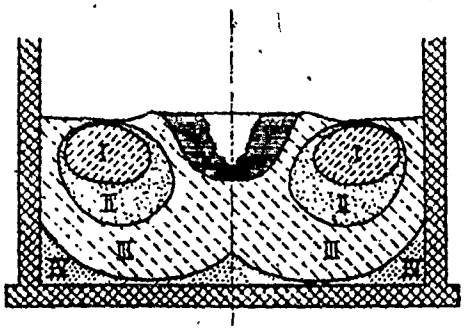

Fig. 22. Regions of fluid flow in a water bath for a single nozzle system. Regions I, II and III have decreasing velocities. Region IV is a dead zone. (after Mathieu (9)).

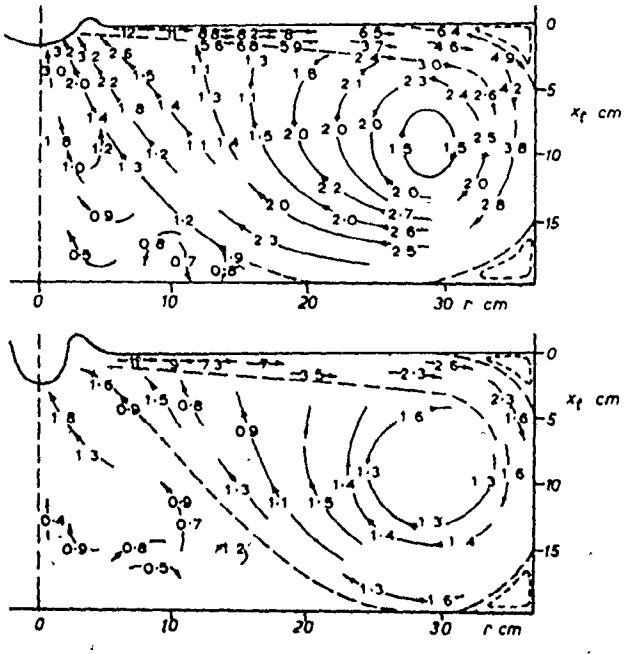

Fig. 23. Measured flow pattern in liquid caused by an impingement jet. Top figure, M = 14700 dyne, h = 17cm; bottom, M = 8650 dyne, h = 8 cm. Velocities in cm sec-1. (after Davenport (21)).

TABLE 1

PROPERTY VALUES OF STEEL AND A

BASIC SLAG AT 1550°C (CHATTERJEE[14])

Phase	Density ($gm\ cm^{-3}$)	Surface Tension ($ergs\ cm^{-2}$)	Viscosity ($gm\ cm^{-1}\ sec^{-1} \times 10^{-2}$)
Steel	7.20	1200	6.0
Basic Slag	3.0	500	50.0

and slag systems. Using the property values at 1550°C of steel and a basic slag (listed in Table 1), the critical cavity depths for splashing to commence are respectively 2 cm. for steel and 3 cm. for the slag. As will be shown later, cavity depths in BOF systems exceed these values by far.

With increasing jet impact velocities the amount of spray continually increases. Another critical point is reached at about 75 m/sec[8, 10], whereupon much deeper penetration of the bath takes place accompanied by a reduction in the amount of outwardly directed splash. In this mode (Figure 19C), the jet splits into two streams of unequal but interchanging magnitudes. The whole cavity again oscillates in the vertical direction and rotates about its central axis. Splashing occurs through the shearing of droplets at the cavity lip. However, because of the steeper profile of the cavity, more droplets are captured by the incoming gas stream. These droplets are impacted on the crater bottom and thus contribute to the vertical oscillation. This entrainment is also responsible for the reduced amount of splash in this "penetrating" mode. In determining the mode of jet-bath interaction, it was found[20-23] that different gases produce the same effects as long as the jet momentum is kept constant. Even assimilable gases, such as in the CO_2-water system, behave in the same manner as long as the impact area is not too large. The presence of a foam cover on the liquid leads to a distribution of larger and fewer droplets in the splashing mode when the jet impinges directly on the liquid[14, 25]. Thin foam covers offer very little resistance to the jet motion so the different modes of interaction can still be characterized by the same impact velocities.

The cavity depth in the splashing and non-splashing liquid ranges can be determined by balancing the hydrostatic force of the liquid with the central jet impact pressure. The equation that results has been experimentally verified for a number of cold model systems[21]:

$$\frac{\dot{Q}\,\dot{V}_j}{\rho_L g h^3} = \frac{\pi}{2k^2}\,\frac{n_o}{h}\left[1 + \frac{n_o}{h}\right]^2 \qquad (2.2)$$

A k value of 7.6 has been found to fit very well for a number of tested systems using different liquids and both assimilable and non-assimilable gases[21]. Besides forming a cavity the jet interaction also causes fluid motion in the bath since the deflected gas streams run along the side walls of the depression exerting a shear stress on the liquid. The resulting fluid motion is upwards at the centre and down at the walls.

Fluid flow in the bath is maximized when the jet interaction is in the splashing range. In the liquid bath there are four distinguishable regions of fluid flow for a single nozzle system (See Figure 22). Region I is an area of fast circular flow. In region II, flow is still rapid but somewhat elliptical. In region III the flow varies between being very fast in the top section and somewhat slower in the wider bottom section. Region IV is essentially a dead zone where very little mixing takes place. The exact dimensions of each zone are dependent on furnace geometry, blowing rate and lance height. Some actual measurements of the velocities encountered in these flow patterns with cold models are given in Figure 23. A note should be made on the flow pattern of thick foams above the liquid. For levels below the lance height, the exit gas stream forces the foam aside and through its frictional action it causes an upward motion in the centre (See Figure 24). For foam levels exceeding lance heights, the jet acts like a pump imparting a downward motion in the centre. The exit gas flow in the converter (Figure 25) is seen to be mainly uniform except in the region surrounding the lance where slight suction effects are present.

The nature of the impingement zone has also been studied[112-123] on hot metal in models of the BOF by using a transparent quartz medium to view the steelmaking bath under certain corresponding operating conditions. These results are discussed below. For soft blowing conditions, a parabolic

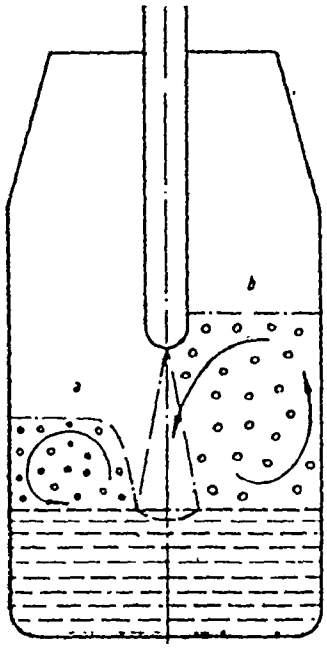

Fig. 24. Diagram showing the flow set up in a foaming slag by a gas jet, a) lance above and b) within the foam. (after Krainer (73)).

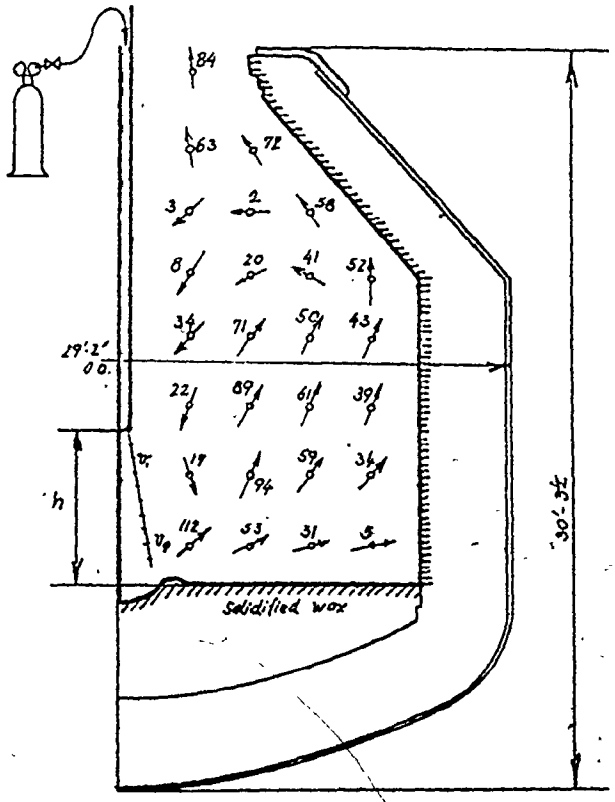

Fig. 25. Measured gas flow velocities above the bath in a BOF. (after Reichmayr (126)).

open crater is formed in the impingement area. Waves of metal appear at the surface of the cavity and move upwards with the deflected gas stream. When these waves reach the edge of the cavity, droplets of diameter between 0.5 to 1.0 mm. break away. These droplets are either ejected into the outer furnace regions or they are entrained in the incoming oxygen stream where they burn. At faster blowing rates the movement at the depression edge becomes more turbulent with more metal expulsion occurring randomly. Periodically, metal is expelled in the form of larger splash from the central impact area. This material is broken up by the jet into a stream of finer droplets, similar in dimension to those mentioned previously. At very high blowing rates a deeply sunken crater with a metal cap is formed. The rate of metal ejection to the exterior is then decreased. Under all blowing conditions there are some droplets entrained in the oxygen stream which burn to form iron oxides or if they still contain sufficient carbon, they will boil and explode to much finer fragments due to CO evolution. Thus it is seen that the behaviour of the metal bath is quite similar to that of aqueous systems when acted upon by a jet. The delineating central impact velocities which characterize the different modes of interaction are thought to apply to this system as well[8].

For all the different blowing conditions, a two-structured reaction zone is always observed (See Figure 26). In the high temperature primary reaction area (I), entrained droplets are combusted together with its components and carbon monoxide in the oxygen jet. In the cooler outer secondary zone (II), carbon and any other of the remaining impurities in the hot metal are oxidized by the products of the primary reaction zone. The CO liberated rises along the edge of zone I and reacts partially with the oxygen jet to form CO_2. For fast decarburization rates, an alternate hole (Figure 26a)

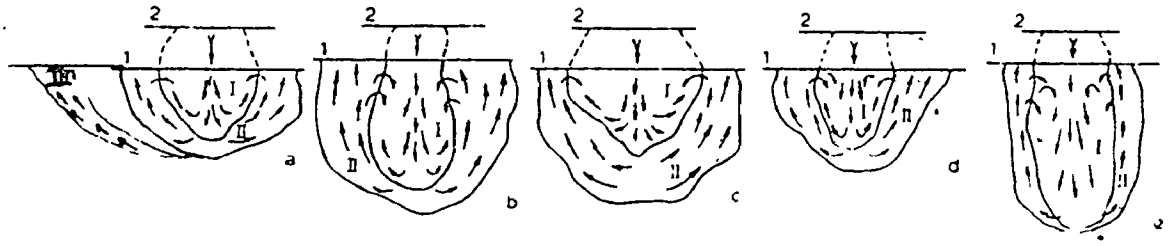

1, *level of metal in a quiescent state,* 2, *level of nozzle supplying oxygen*

Fig. 26. Diagram of reaction zone when injecting pig iron (a) and steel containing 2%C (b), 1%C (c), 0.5%C (d), and less than 0.1%C (e) with oxygen. I is the primary reaction zone and II is the outer secondary zone. III is an alternate gas hole that can form with fast decarburization rates. (after Okhotskii (112)).

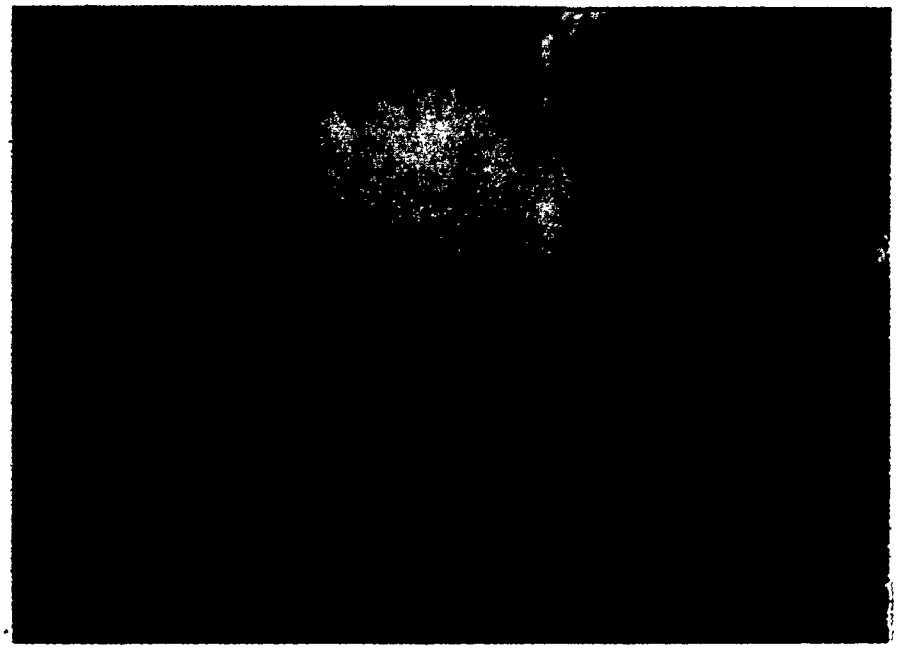

Fig. 27. Slag and metal ejection from the central cavity region in a small scale BOF. (after Yamada (46)).

through which gases and dust pass is formed beyond zone II. This gas hole moves randomly about the periphery of the cavity due to the instability of the main reaction zone. This is accompanied by further metal expulsion. The outgoing gases from both the centre region and the auxiliary gas hole can also cause slag ejection through their shearing action (See Figure 27). The depth of the overall reaction zone decreases marginally with an increase in the decarburization rate. This is caused by the counteracting force of the rising carbon monoxide gas, thereby reducing the effective oxygen driving pressure.

The cavity depth under different blowing conditions has been measured experimentally in a hot model BOF using a single hole lance[32]. The equation for jet penetration obtained based on empirical studies of the data is:

$$n_o = 5.741 \times 10^{-2} \sqrt{\frac{\dot{Q}V_j}{h}} + 5.81 \qquad (2.3)$$

Using appropriate values of blowing rates and lance heights (See Table 2), it can be shown that the cavity depth as predicted by this equation is roughly twice that using the hydrostatic pressure balance as in equation 2.2. The increase can be explained by the marked expansion of the oxygen jet as a result of combustion and by the added impingement onto the cavity bottom by those droplets entrained in the gas stream. However, similar[119] and even contradictory evidence[113] where the cavity depth was measured in comparison to that predicted by equation 2.2 has been presented for hot model systems. The question of cavity depth in BOF's therefore still remains in doubt.

The liberated gases impart a shear force on the metal bath along the surface of the cavity creating a fluid motion similar to that described previously. Bulk metal moves up in the centre where the impurities react and then flows down the wall area. Evidence of this occurring in metal baths has

TABLE 2

COMPARISON OF CAVITY DEPTHS
FOR HOT AND COLD MODEL STUDIES

Q (gm sec^{-1})	h (cm)	n_o - Hot Model (cm)	n_o - Cold Model (cm)
2600	80	62.4	33.6
	120	51.6	21.6
	160	45.2	14.3
	200	40.8	9.9
5200	80	86.6	50.7
	120	71.4	35.7
	160	62.4	25.2
	200	56.2	18.2

been gathered in a variety of ways: actual mechanical measurement[32], concentration and temperature gradient measurements[102], and visual observation[112, 113]. No velocity profiles have been established but the motion should be similar to that depicted in figures 21 and 22.

2C. EFFECTS OF LANCE OPERATION ON REFINING PATH AND MATERIALS LOSS

The general purpose of controlling lance operation is to produce a jet penetrating sufficiently to get good refining, but not enough to cause refractory wear. The lance practice must also be amenable to slag development. The slag should foam sufficiently to obtain good metalloid removal through reactions in the emulsion and to reduce the ejection of metal from the vessel. The two lance parameters which the furnace operator controls are the oxygen flow rate and the blowing height. Adjustments of these parameters during the blow will seriously affect the refining path.

Under very soft blowing conditions attainable with small flow rates or high lance heights, the jet will not penetrate deeply or possibly not at all into the metal bath if the slag cover is too thick. The supplied oxygen in this case serves primarily to oxidize the metal bath, thereby increasing the iron oxide content in the slag to very high levels (greater than 30%). Any unabsorbed oxygen burns CO to CO_2 above the bath. The overoxidized slag can react violently with the emulsion droplets to cause slopping. Similarly, a hard blowing operation with high flow rates and low lance heights may not supply sufficient iron oxide to the slag, causing it to become dry and viscous. In this condition the slag can be pushed aside by the jet, thereby allowing metal splash to escape from the impingement area. The efficiency of oxygen utilization in this case is high since decarburization will be the primary reaction in the impact zone. However, material losses may be too great to be acceptable. A balance between decarburization efficiency and slag development must be achieved by compromising the blowing practice in order to get fast

refining and high metal yield. The optimum slag paths previously mentioned are obtainable by using a soft blowing practice in the early segments of the blow to produce a well conditioned slag and later switching to a harder blowing practice so that rapid, controlled decarburization occurs.

Examinations into lance parameters, critical in determining the amount of metal splash when a slagless state exists, have been carried out with water models[5-29]. Single hole cylindrical nozzles were used to blow gases on water baths contained in vessels that were scale models of BOF's. Material loss rates were measured by collecting the ejected water splash. Some results from these studies are given in Figures 28 and 29. Figure 28 shows that as the gas flow rate increases for any particular lance height, the material loss rate increases to a maximum and then subsides. For constant flow rates, an increase in lance height causes more material loss up to a peak level after which there is a steady decline. The maxima all occur when the central jet impact velocity is around 70 m/sec. This was previously described as being the demarcation between "splashing" and "penetrating" modes of interaction between a jet and a liquid bath. Thus the maxima are the boundaries between these two modes. It would be best then to have a lance operation far removed from this impact condition. For increasing lance diameters, the maximum quantity of ejections remained the same but higher flow rates were required to achieve this maximum[10]. Ejection rates in hot model BOF's also displayed a similar tendency to attain a maximum (See Figure 30) at certain blowing heights[10].

Experiments of a similar nature were carried out with different types of lance nozzles to determine the effect of lance height on splashing rates[15]. The results are given in Figure 31. The gas flow rate through each nozzle was kept constant and the lance heights were always such that the jet inter-

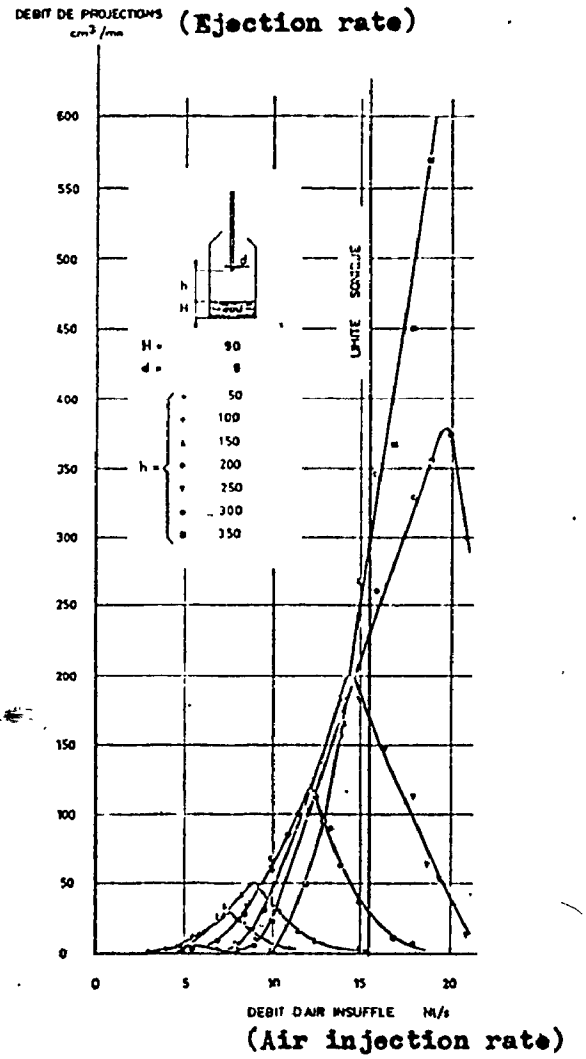

Fig. 28. Influence of the gas flow rate on the quantity of ejections in a water model. (after Chedaille (10)).

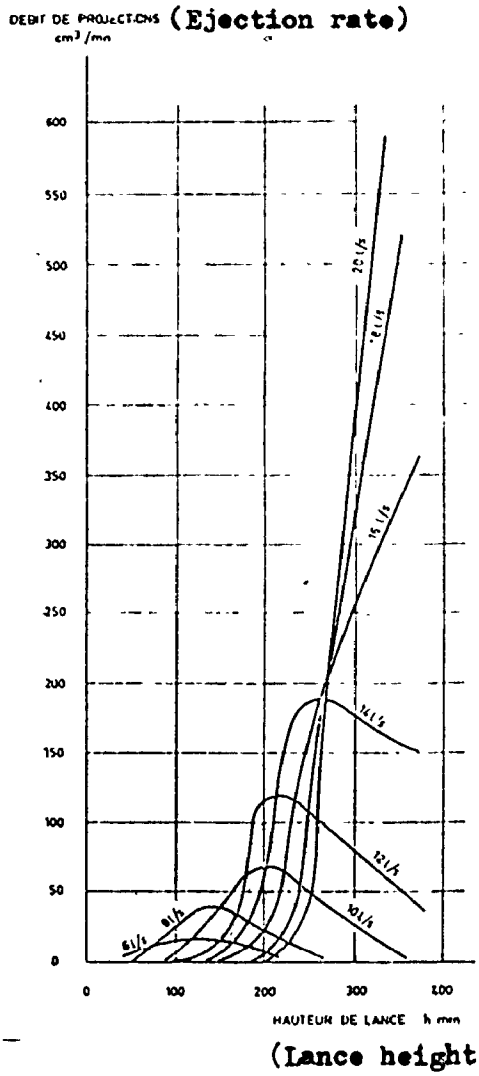

Fig. 29. Influence of the lance height on the quantity of ejections in a water model. (after Chedaille (10)).

(Quantity of ejections per minute)

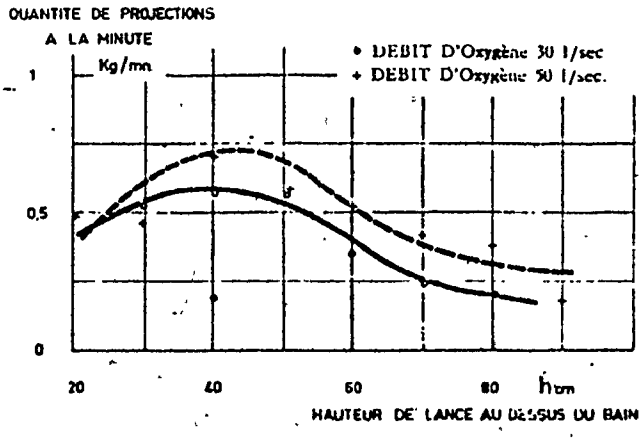

(Oxygen Flow rate)

(Lance height)

Fig. 30. Variations in the ejection rate as a function of the lance height above the bath for a 300 Kg pig iron bath. (after Chedaille (10)).

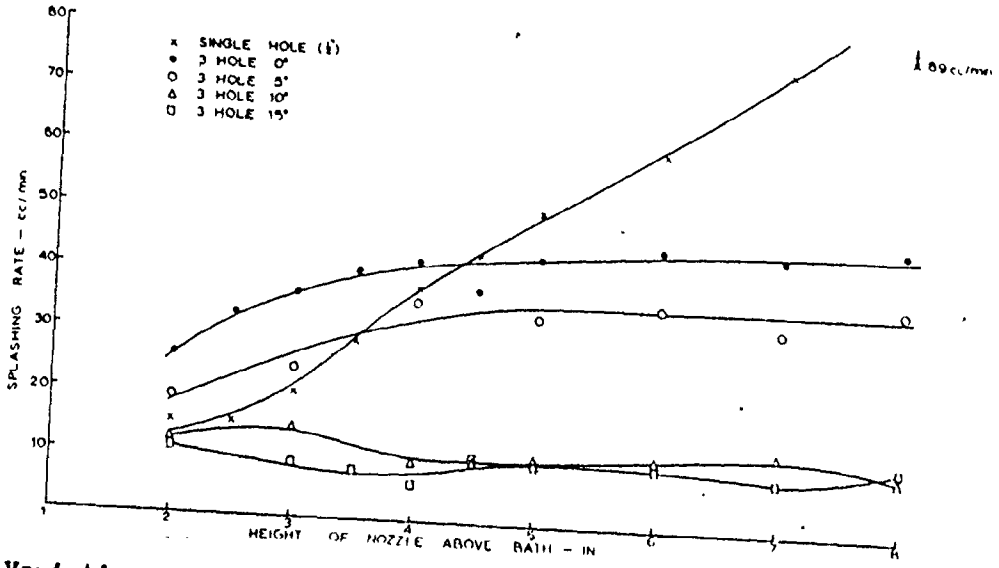

Fig. 31. Variations of splashing rates of various nozzles in a water model study with a constant air flow rate. (after Jervais (6)).

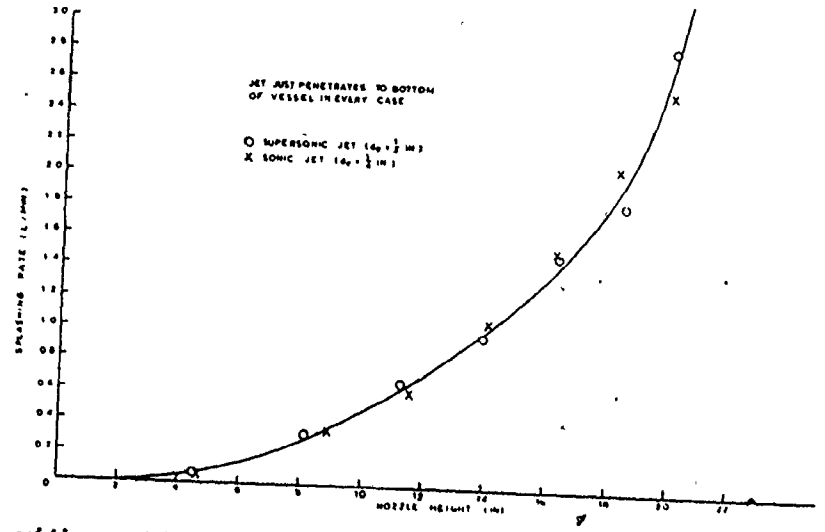

Fig. 32. Tests with sonic and supersonic nozzles blown at the same flow rate showing no variation in splashing rates in a water model. (after Jervais (6)).

action was of a penetrating mode. As can be seen the three hole nozzles with a divergence of 10° or greater behave differently, having substantially smaller rates of material loss. The reason for this is that these nozzles produce non-interacting jets, thereby avoiding a high central impact velocity. Also more spray is directed towards the vessel walls rather than straight upwards where it can escape. Tests with supersonic and sonic jets operated at the same flow rate (Figure 32) showed there was no variation in splashing between the two. The jet impact on the bath must therefore have been quite similar.

For the case of bath circulation under different blowing conditions, it has been observed in studies with water that mixing is optimized when splashing just commences[9]. This is due to a maximum in the translation of shear energy to bath motion in place of any dissipitation by droplet formation or cavity motion.

2D. EFFECTS OF VESSEL CONFIGURATION AND SIZE ON MATERIALS LOSS

Furnace volume plays an important role not only in determining the limits of vessel charge but it also influences the occurrence of slopping. Present BOF's have a productivity, expressed in the inverse form, ranging from 0.6 to 1.1 m^3t^{-1}[124]. The metal itself, with an average density of 7.2 $gm.cm^{-3}$, will occupy 0.14 m^3t^{-1}. The remainder of the furnace volume is available for slag and gas containment. A survey[124] of existing BOF operations where the occurrence of slopping is infrequent has shown that the top blowing rate is limited by the speed of removal of the gases formed. The data used to substantiate this finding is presented in Table 3. It was assumed that all the supplied oxygen goes to decarburization and the off gas is entirely CO at a temperature of 1500°C and a pressure of 1.5 atm. Based entirely on free volume considerations the minimum calculated gas residence time before slopping occurs is 1.3 seconds[124]. Shorter residence times indicate faster throughput of the gas. The free volume in which the gas circulates can be thought of as a collection chamber for any sprayed material. If the gas flows quickly it can naturally entrain more sprayed material causing an undue amount of slag and metal to be ejected. Any condition in which the slag foams excessively will also decrease the available gas residence time making it easier for slag ejection.

The vessel configuration will determine the diameter to depth ratio of the metal bath. For circulation considerations, a certain bath depth (1.6 to 1.7m)[125] must not be exceeded if irregular and incomplete refining

TABLE 3

RESIDENCE TIME OF OFF GASES IN THE BOF (KREYGER[124])

	Converter	Steel Capacity (t)	Specific Volume ($m^3 t^{-1}$)	Converter Height: Diameter Ratio	Converter Height (m)	Free Volume for Gas, Vg (m^3)	Waste Gas Flow Rate, Wg^1 ($m^3 h^{-1}$)	Gas Residence Time[2] (sec)
1	(Benelux)	105	0.77	1.96	7.75	57	25000	0.95
2	(Japan)	160	0.77	1.52	7.50	92	30000	1.27
3	(Japan)	175	0.94	1.48	8.00	133	30000	1.84
4	(Benelux)	180	0.97	1.72	9.00	140	36000	1.62
5	(Australia)	208	0.65	1.74	8.80	109	34000	1.33
6	(Benelux)	244	0.74	1.72	9.70	132	42000	1.31
7	(Benelux)	280	0.77	1.62	9.80	160	45000	1.48
8	(Benelux) expanded	280	0.77	1.62	9.80	160	57000	1.17
9	(Japan)	300	1.0	1.48	10.1	243	70000	1.44
	(Japan) expanded	300	1.0	1.48	10.1	243	88000	1.15
1	(Japan)	310	1.06	1.83	11.6	271	80000	1.41
	(Japan) expanded	330	1.0	1.83	11.6	267	100000	1.11
	(Germany)	385	0.63	1.48	9.54	167	60000	1.16

[1] Expressed as total O_2 flow rate.

[2] Gas Residence Time $= \frac{Vg}{Wg} \times \frac{1}{2} \times \frac{273}{1773} \times \frac{1.5}{1} \times 3600.$

due to large dead zones is to be avoided. Thus as vessel size increases this ratio must become higher. Cold model investigations[10] where the bath to mouth height remains constant have been conducted to determine the effect of bath depth on splashing rates. These results are given in Figure 33. With increasing bath depth the splash rate also increases but asymptotically. This asymptotic behaviour is due to the combined action of cavity formation and bath circulation. With increasing bath depth past a certain point, bath circulation will not change; only the size of the bottom dead zone will increase. For industrial practice where the bath level increases through larger metal charges, the bath to mouth height decreases allowing more material to escape because of the shorter trajectory and because of the faster gas velocities which can entrain more splash. The base profile of the BOF can also influence the ejection rates. In water model studies, it was determined that a dished shaped base produces less splash when compared with a round base profile (See Figure 34). The increase arose from periodic oscillations causing splashing of the bath in the latter vessel[6].

The furnace mouth diameter is governed by metal and slag splashing and by the exit gas velocity. If the hole is made too large, too much material will be ejected from the furnace. Likewise, if the mouth is too small the waste gas velocity will be high enough to drag droplets of slag and steel into the cleaning system. With higher gas velocities, larger steel particles can be carried in the gas stream by drag forces, possibly leading to erosion problems of the furnace cone. Metal yields also decrease under these circumstances.

A furnace lining should gradually erode during a campaign. As it does, the interior volume increases thereby reducing slopping and splashing rates since the metal bath is shallower and the gas residence time is longer.

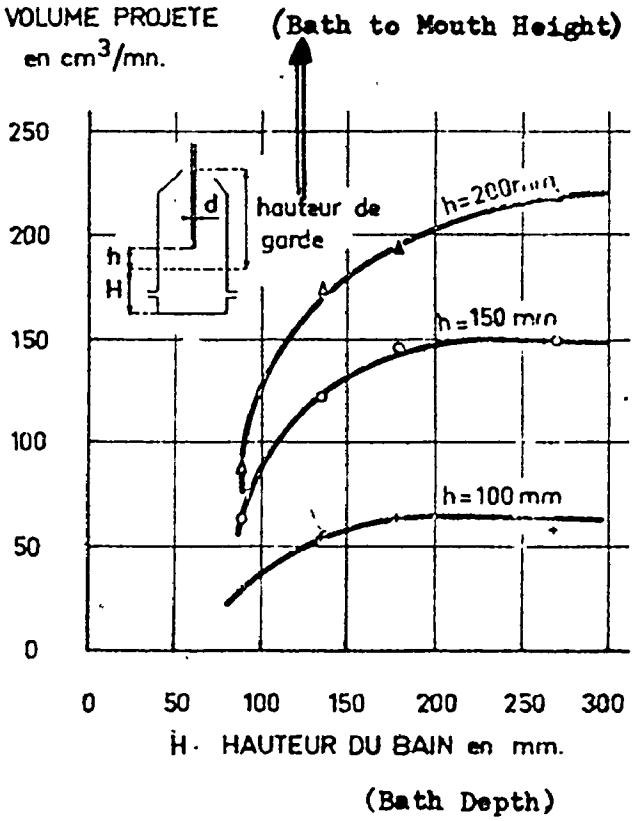

Fig. 33. Variation in the ejection rate as a function of bath depth for different lance heights in a water model study with a constant bath-to-mouth height. (after Chedaille (10)).

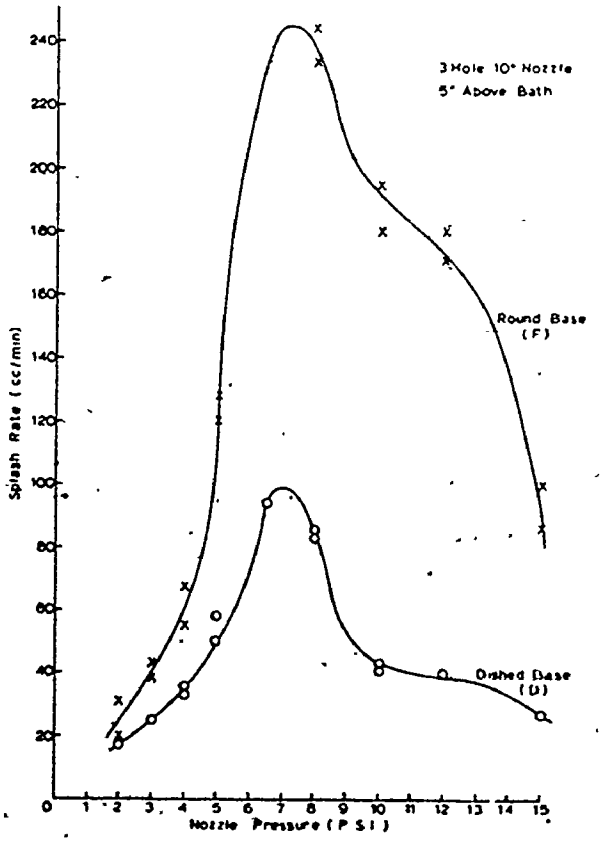

Fig. 34. Comparison of ejection rates by round and dished base profiles in a water model

2E. EFFECTS OF SLAG DEVELOPMENT ON MATERIALS LOSS

The BOF metallic charge generally consists of 70 to 80% hot metal with the remainder comprising of iron ore pellets, cold pig iron and various types of scrap. The silicon and manganese levels in the hot metal will vary depending on blast furnace operating practice and the type of ores used. A generally quoted[127] ideal composition is 0.7 - 0.8% silicon and similarly for manganese. Changes in the hot metal composition alter the chemistry of the slag and its physical properties if there are no flux changes. The slag viscosity as well as the emulsion stability vary with the slag composition. Higher silicon levels lead to a greater slag mass (about 5 kg. per ton steel per 0.1% Si maintaining same basicity) with an increased chance of slopping since the foam level at its peak will be higher. Correspondingly higher manganese levels also increase slag volume (about 1 $kg.t^{-1}$ steel per 0.1% Mn). MnO in the slag acts in a similar manner to FeO increasing the slag's fluidity. For high hot metal manganese concentrations an overoxidized slag condition may result[3]. In such a state the slag can react erratically with the bath and droplet carbon generating large amounts of CO. Slopping may thus occur.

Lime is added to the furnace charge to form the necessary basic slags. Its physical and chemical properties must be such that it dissolves as rapidly as possible. Otherwise a heterogeneous slag more amendable to slopping will result[128-129]. Burned dolomite additions are generally made to cut down on brick erosion by supplying MgO to the slag. The proper quantities must be

used to avoid MgO precipitation in the slag in the form of periclase. If this occurs the slag viscosity increases becoming unsuitable for fast refining.

Slag conditioners such as fluorospar and pellets are employed to prevent slag coagulation which can be accompanied by the formation of metal splash. If spar is added to early slags it is not too effective[95]. It will only make the dry slags that form later in the blow less viscous. Pellets can be added if a dry slag low in iron oxides is present. The oxides supplied will partly dissolve in the slag with the remaining fraction reacting with the bath carbon. If the pellet addition is made when the slag iron oxide level is adequate, rapid decarburization due to the large amount of available oxygen will result. This may thereby lead to slopping.

All the different flux additions will influence the course of slag development. In this manner, they also affect bath circulation since the slag condition will partly determine the mode of jet-liquid interaction. Bath circulation, however, is more directly influenced by the type of scrap addition. Light scrap will result in greater bath chilling with a consequently slower bath motion[130-133]. Heavy scrap will not dissolve as rapidly and may thereby interfere physically with bath circulation.

3. THE DESIGN AND EVALUATION OF SAMPLERS

Recognizing the need for further study in the area of material ejections from basic oxygen furnaces, it was felt that the best course of action would be to conduct the work with actual production equipment. Sampling under regular operation conditions was carried out at the melt shop of Dominion Foundries and Steel Ltd., Hamilton, Ontario.

In order to measure ejection rates from the BOF during the blow a sampling technique had to be developed. In order to prove the worth of this method, many tests were carried out just to measure the efficiency of sampling for ejections. The course followed in the design of the sampler and its evaluation is given in this section. In order to study the process in greater depth, auxiliary equipment was devised to obtain slag and metal samples throughout the blow. The construction and evaluation of this sampler for slag and metal is also reviewed. The chemical analysis methods used to study all these different materials are also given.

In order to provide a complete picture of this investigation, a brief outline of Dofasco's blowing practice is first given.

3A. DOFASCO BLOWING PRACTICE

Dofasco's melt shop includes three vessels originally designed for 80-95 ton* steel heats. The current vessels have an internal volume of 77m^3 with a new lining and produce 147 tons steel on the average. This corresponds to a working volume of only 0.52 $m^3 t^{-1}$. The blowing rate is typically 21000$m^3 h^{-1}$ and the quantity of slag generated is around 150 kg t^{-1} steel. The gas residence time can be calculated for these conditions as was in Table 3 for other operations. The slag density is taken from Table 1 to be 3.0gm cm^{-3}. The computed gas residence time is 0.97 seconds which is considerably smaller than the recommended 1.3 seconds[124]. In this overcharged condition the furnaces are more susceptible to slopping and metal ejection. Indeed this is the case since slopping is observed in every heat with normal operating practice. Metal ejection also usually occurs but at a different time period in the blow. The extent of these material losses varies from heat to heat.

Scrap is charged first into the furnace and then topped with the hot metal. The average metallic charge is 165 - 170 tons. A three nozzle lance is then lowered to 3 meters above the bath whereupon the oxygen is delivered at around 17000 $m^3 h^{-1}$. As soon as ignition is achieved the lime and dolomite addition is started. Lime consumption is around 50 - 60 kg per ton steel and the calcined dolomite used is roughly half this value. The exact rate is dependent on hot metal chemistry and the aim MgO content of the slag at turn-down. These flux additions are made continually over the first 7 minutes of

* One ton = 1000 kg., oxygen flow given at STP

the blow. Fluorospar is also added with these fluxes when a fluid slag is required, at a rate of 1 - 1.5 kg t^{-1}. The oxygen flow rate is gradually built up to 21000 m^3h^{-1} during the first few minutes of the blow. During this time the lance is lowered at a controlled rate of 0.3 m. min^{-1} until it is 1.4 m above the metal bath (based on the initial static bath). It is left at this height for the remainder of the blow. The oxygen flow rate is kept constant at 21000 m^3h^{-1} throughout the blow except when slopping occurs. Slopping typically occurs between the seventh and fifteenth minute of the blow. An adjustment is made to cut back the flow rate to 17000 m^3h^{-1} during this interval. Metal splashing generally takes place after the slopping period. The steels produced in the melt shop are blown to less than 0.2%C. The average blowing time is 24.5 minutes. A schematic of the blowing practice for a typical heat is given in Figure 35.

A diagram showing the dimensions and configuration of the furnaces in the melt shop is given in Figure 36. Because of the slanted cone design of the vessel, slopping and metal ejection material normally falls behind the furnace into the slag pit. Only the finer particles are carried along by the waste gas. The gas velocity increases in the furnace cone because of area constriction. The waste gas consists basically of CO, but there is a small fraction of CO_2. Immediately above the furnace mouth this gas burns in the surrounding air to produce temperatures exceeding 1600°C. These product gases and a certain amount of air are sucked into the gas cleaning system through a water cooled hood located 2 meters directly above the vessel mouth.

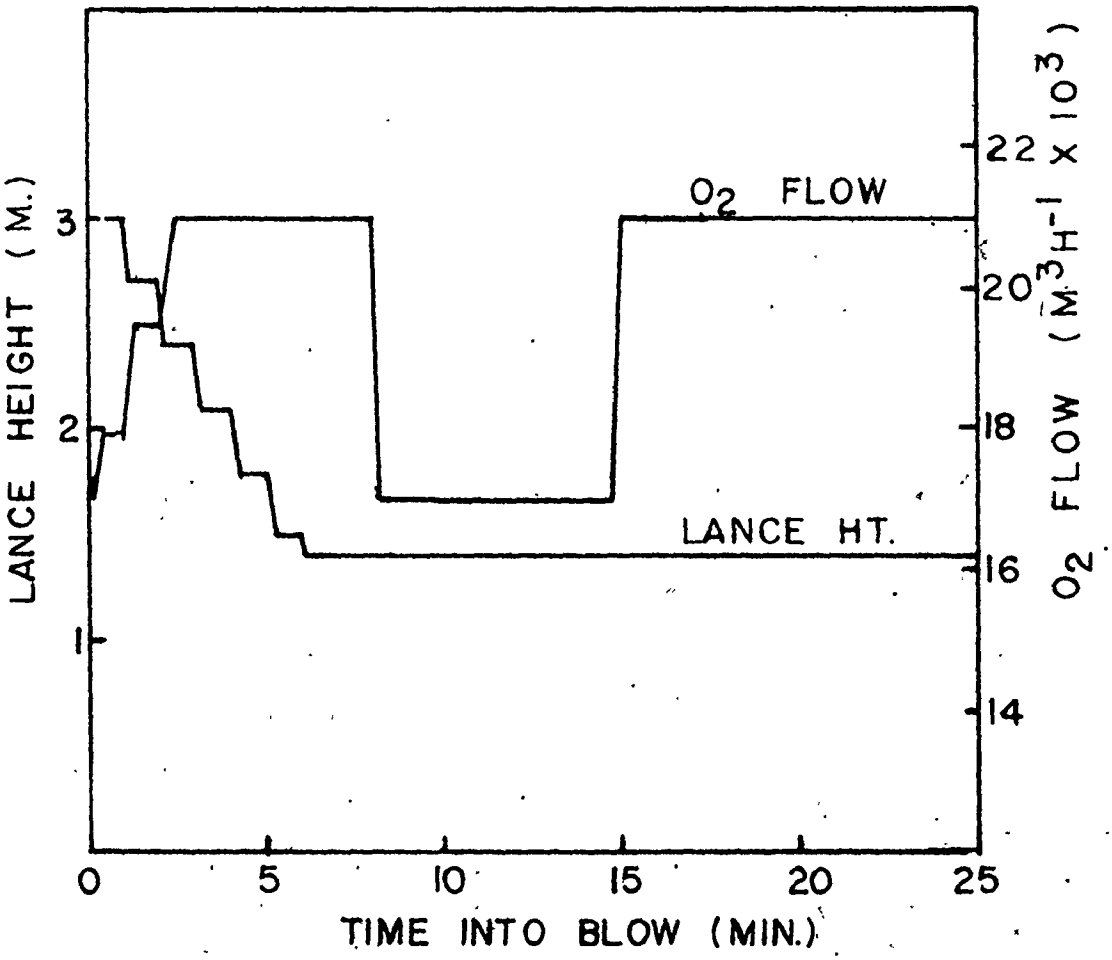

Fig. 35. Blowing practice for a typical heat at Dofasco.

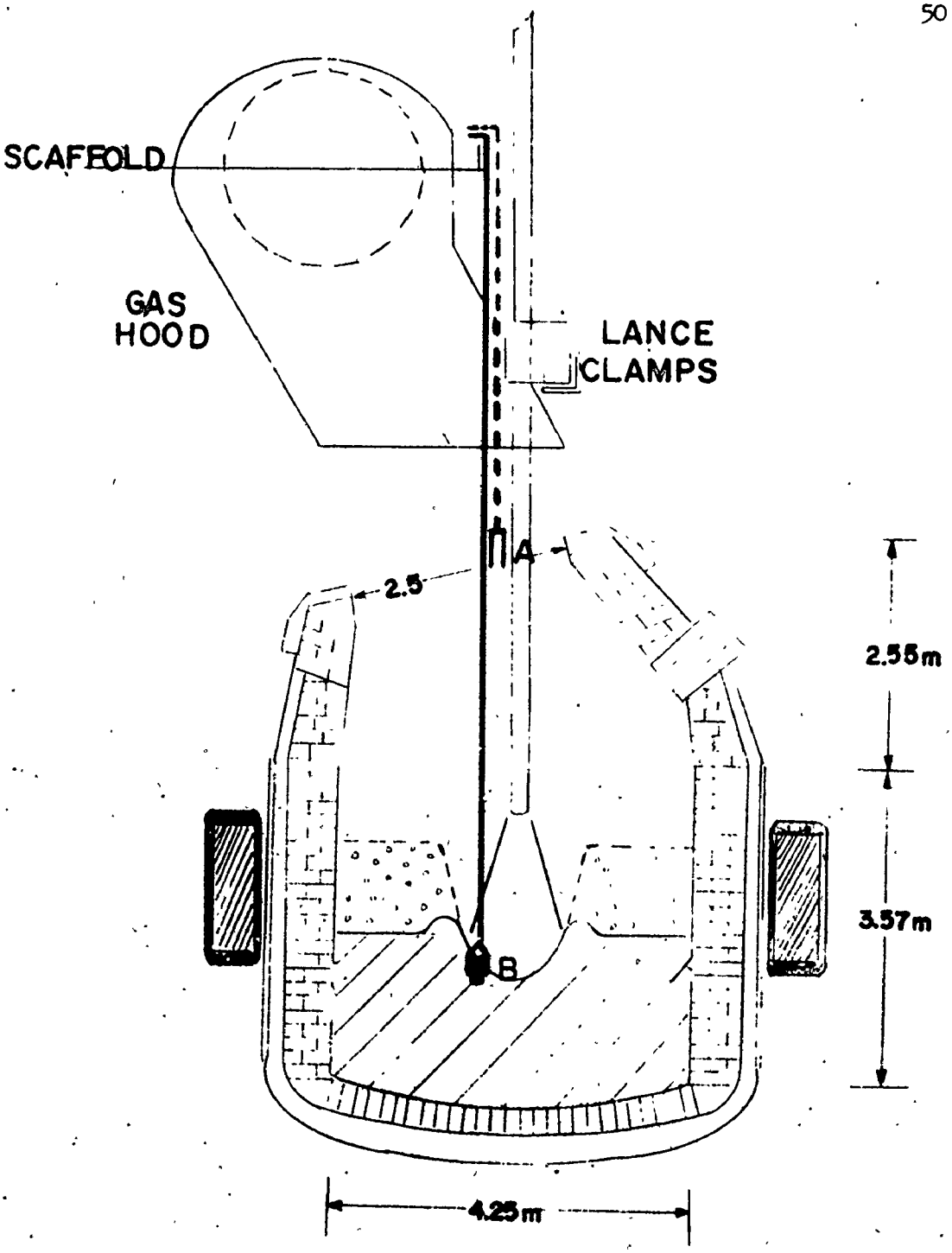

Fig. 36. BOF configuration and dimensions with (A) ejection sampler and (B) slag and metal sampler.

3B. SAMPLING LOCATION AND CABLE CONSTRUCTION

The furnace mouth represents the source point for any material ejection. Anything exiting from here may be entrained in the waste gases or may fall behind the furnace. Occasionally if the size and trajectory of the ejected material is suitable, it may return into the furnace. In order to sample the full stream all tests were conducted at the tip of the furnace mouth. It could be accessed in two directions, vertical or horizontal. The horizontal point of entry was the gap between the furnace mouth and the hood. A swing arm mechanism would have to be employed to sample through this route. However this would not be convenient since it would cause too much interference with the movement of production equipment in the plant. Only one vertical point of entry was available, this being the unoccupied portion of the lance hole in the furnace hood. This area is roughly annular with a width of about 0.2 m (See Figure 37). It can be reached by standing on the scaffolding surrounding the gas cleaning system and suspending the sampling device on a cable. The distance between this position and the lance opening is roughly 10 m. and can be reached using a steel cable. Whenever sampling was carried out, the lance clamps had to be opened to allow easy access.

To support a device at the furnace mouth, a second cable had to pass through the 3 meter section where the waste gases are combusted. In this area the temperatures are at times during the blow high enough to melt steel. Since sampling times of about one minute were anticipated, supporting cables capable of lasting a few minutes were felt necessary. 8 mm diameter steel strand cables were originally tested but could only withstand these temperatures for

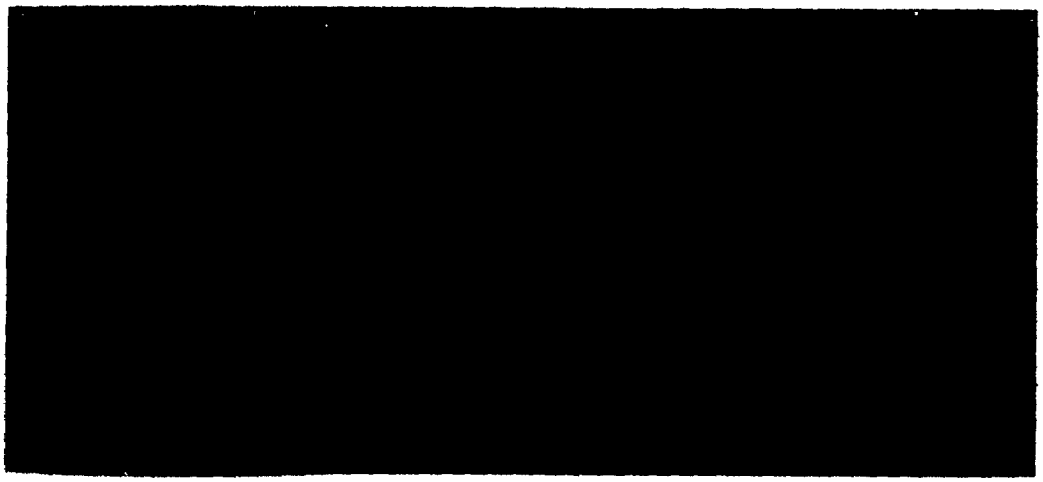

Fig. 37. Lance hole opening for entry of ejection, and slag and metal samplers.

periods generally less than one minute. Steel bar sections of 13 mm diameter lasted for around two minutes. However this proved to be too cumbersome to work since the bar was withdrawn from the furnace at red hot temperatures.

An insulated cable was constructed using asbestos tape, coarse MgO powder and 8 mm diameter steel strand cable. Its construction is depicted in Figure 38. The different layers were applied in the form of tape by rotating the steel cable at one end using a pipe threading machine. The cable was kept taut by applying a force at the other end using a freely rotating supply crane. Insulation was applied to a 3m section of cable measuring 4 m. in total length. The inside asbestos cover only served to isolate the steel cable from the MgO powder. This powder was applied dry by supplying it with the exterior asbestos tape (4 cm wide) layer. The MgO powder was an industrial ramming mixture (Permanente 165 Periclase) on non-uniform sizing having particles up to several millimeters in diameter. Several trials testing this cable's durability in the atmosphere above the furnace mouth were carried out. Deadweights of 5 kg mass were attached to the bottom end to keep the cables motionless in the rapid waste gas stream. The results are given in Table 4. The shorter endurance time between the 10 to 20 minute mark is due to the higher gas temperatures arising from peak CO evolution rates. The cables always failed by melting about 1 m above the furnace mouth, indicating this is the hottest point in the combustion zone. If suspended in the furnace for one minute periods the cables could be safely used twice, thereafter the asbestos flaked off exposing free steel surface.

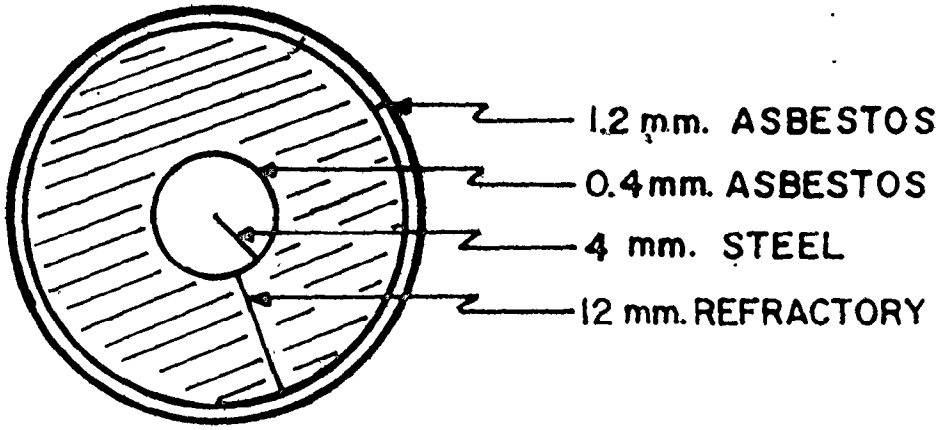

Fig. 38. Schematic of the insulated cable used for supporting the ejection sampler in the off gas stream.

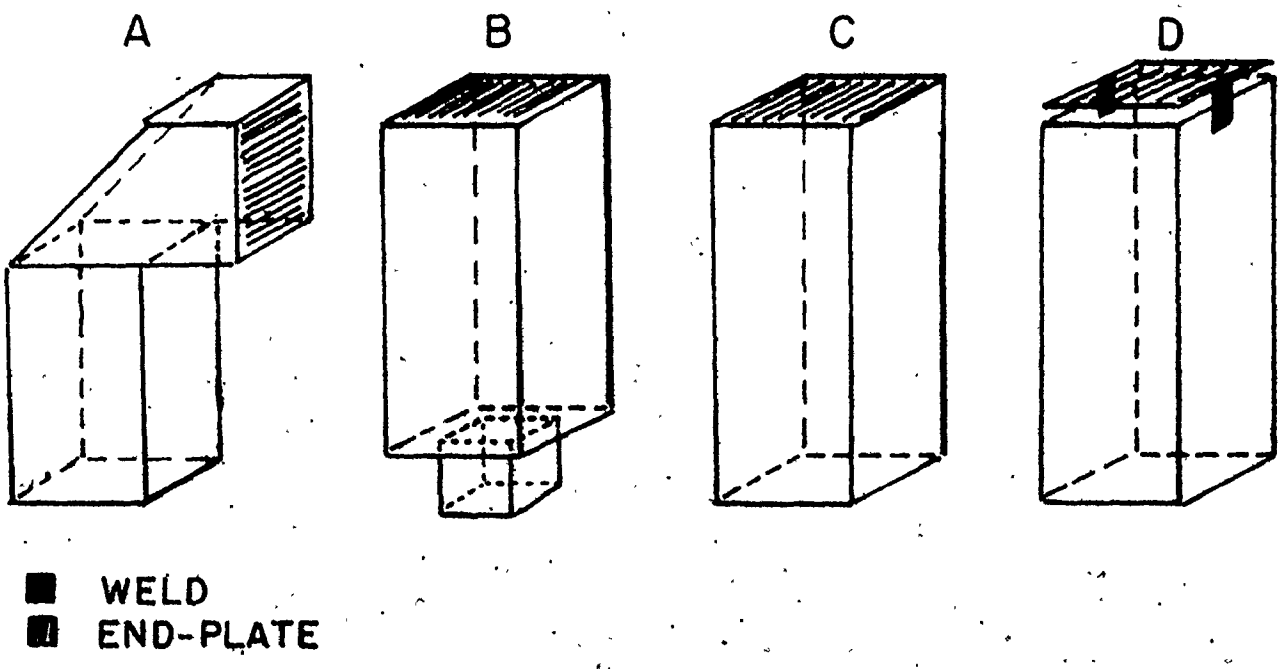

Fig. 39. Schematic of the different devices tried in ejection sampling. Material entered through the bottom opening.

TABLE 4

TESTS ON DURABILITY OF INSULATED CABLE

Time into Blow (min)	Number of Cables Tested	Time Before Failure (min)
0 - 5	3	> 5
5 - 10	3	> 5
10 - 15	4	2 - 3
15 - 20	2	2 - 3
20 - 25	2	> 4

3C. SAMPLING DEVICES

In order to measure ejection rates, the sampling device had to have a controlled entry area and all the material coming into this area would have to be collected by some means. A variety of sampling devices were examined by suspending them at the furnace mouth before a suitable one was found. The different devices are presented in Figure 39. All the samplers were constructed of 3.2 mm thick low carbon steel.

The basic concept behind sampler A was to deflect the ejected particles on the inclined plate into the horizontal collection chamber. Tests with this device showed no deflection at all. Slop material and metal droplets were collected on the vertical surfaces and on the deflection plate by welding and adhesion but none was carried over to the horizontal chamber. Modifications in this sampler's dimensions and the provision of openings for gas escape through the end plate also produced the same results. The idea behind device B was to have an entry port with a larger collection chamber for the settling out of any ejected material. Some material was collected on the inside walls of the entry chamber, again by welding and adhesion, but very little actually entered the main collection chamber. Modifications in the sampler's dimensions similarly produced negative results.

The results from testing with the two previous devices indicated that metal ejections were still molten upon reaching the furnace mouth and could be collected on vertical surfaces by welding. Similarly liquid slop material would stick by surface adhesion as it was quenched by the cooler sampler walls. If the vertical surface area is substantially larger than the entry area,

most of the particles should be collected since the probability of not contacting a surface on which they can freeze is very small. Material also stuck to the outside walls but as this did not pass through a controlled area its quantitative significance would be difficult to assess. Tube samplers depicted in Figure 39-C and D were found to give good ejection samples. The open ended device (D) allowed the waste gas to pass through, thereby causing less disturbance in the waste gas flow. Various tube lengths of each type were tried, but material was generally collected only on the first 25 cm length of the inside surface for the size of openings used. A tube length of 38 cm was found to be adequate for efficient sample collection. The exterior sample walls were normally coated with slag or metallics along the whole length. Photos of two such samples are given in Figure 40. Further evaluation of the two tube samplers, open ended and closed, was conducted and will be discussed later (Section 3F).

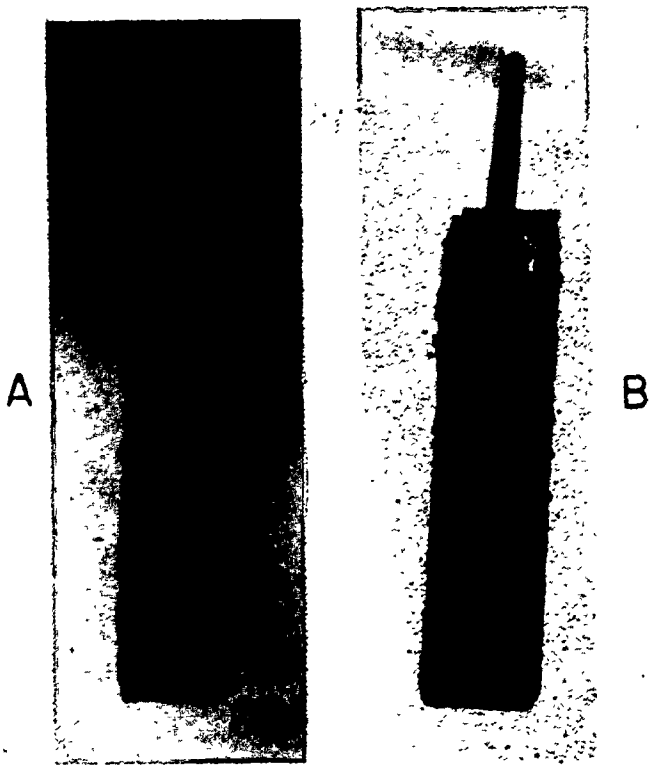

Fig. 40. Appearance of sampler D after 1 minute sampling period: (A) slop at 7 minute mark in blow, (B) metal ejection at 18 minute mark.

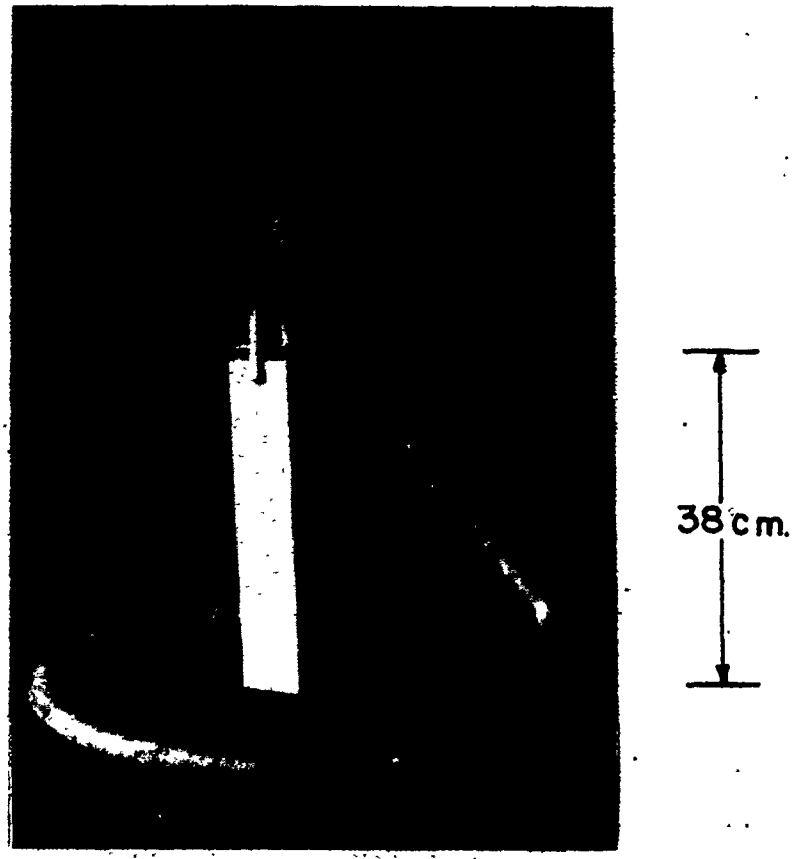

Fig. 41. Complete sampling assembly with open ended tube device (Sampler D).

3D. SAMPLER PAINTING

The tests with the tube samplers indicated that metal ejections could be collected by welding onto the steel surface. However this made their removal very difficult. To avoid this sticking problem an insulating paint of Ca CO_3 was applied to the sampler walls. A suspension was prepared by dissolving finely ground industrial lime in water. Lime was added until a thick colloidal mixture of $Ca(OH)_2$ particles in water resulted. This paint was applied on the tube samplers which were first heated in a natural gas flame and then dipped into the colloidal solution. The samplers were then dried by reheating in the flame for half an hour. All the excess water evaporated off and the $Ca(OH)_2$ combined with the CO_2 in the oxidizing flame to form $CaCO_3$. A firebrick furnace (1m x 1m x 1m) equipped with a natural gas burner could heat simultaneously sixteen samplers.

Since it was the intention to strip the tube's interior completely after sampling to get a representative sample weight, the inside coating weight had to be known to avoid any further chemical treatment to dissolve out the paint. The weight of the total coating was determined by weighing the samplers before and after application of the paint. The uniformity of the coating between the inside and outside tube walls was checked by stripping ten samplers separately on both sides. The two weights were then compared. The results are given in Table 5. The average ratio of inside weight to outside weight was 1.01 which clearly demonstrates the evenness of the coating. The standard deviation of this ratio was 0.175. This was rather high since for an outside coating weight of 50 gm, one would have 95% confidence limits of 50 ± 17.5 gm on the inside coating weight. However, as will be demonstrated

TABLE 5

TESTS ON COATING EVENNESS
WITH OPEN ENDED TUBE SAMPLER

Test Number	Inside Coating Weight (gm)	Outside Coating Weight (gm)	Ratio Inside : Outside
1	80	75	1.07
2	43	68	0.63
3	57	48	1.19
4	62	55	1.13
5	61	68	0.90
6	63	58	1.09
7	70	62	1.13
8	76	66	1.15
9	56	57	0.98
10	45	54	0.83

mean ratio = 1.01

standard deviation = 0.175

later, this error can be accounted for in another manner (Section 3F). This method allowed the inside coating weight to be taken as one half the total paint weight.

The coating weight could be varied by two methods. The tube sampler could be heated up to a higher temperature before dipping or the paint could be thickened with lime addition in order to increase the coating weight. When taking slop samples only thin coatings were required since the material stuck by adhesion and could easily be removed. For metal ejection samples thicker coatings were required to prevent excessive surface welding. Generally, samplers with inside coating weights of 30 - 50 gm were used for slop and those of 70 - 100 gm for metal ejection.

3E. TUBE SAMPLER EVALUATION

In testing the open ended and closed tube devices a standard length of 38 cm was used. The open ended device was constructed with a top plate spacing of 1.7 cm. This plate prevented any slop material from entering the sampler by falling into it on a downward trajectory. Some excess material could still come in through the vertical opening but this is considered to be negligible. The top plate also served to collect any material that may have passed through the whole tube length without sticking to the side walls. This is possible if the particle is minute and fully entrained in the gas stream. The closed tube device was completely shut off at the top with a welded plate. Both devices were supported by 1.3 cm diameter rod fixtures welded to the tube walls. For both devices the ratio of vertical collection area to horizontal entry area was 22. For the open ended device the ratio of exit area to entry area was roughly 0.9. A photo of the complete assembly with the open ended device is given in Figure 41. A U-bolt clamp was used to attach the samplers to the 4m insulated cable. This was further attached via the second loop to a 10m steel strand cable used to manually lower the device into place above the furnace. Markers on this cable allowed the devices to be accurately positioned ($\pm$ 0.3m) at the tip of the furnace mouth.

As stated before, these two types of tube devices gave good ejection samples. As a method of comparison, the two painted tube devices were simultaneously lowered on separate cables into the furnace mouth for a one minute period. Altogether 25 comparison tests were conducted with the two samplers at different times during the blow. The samplers were stripped on the inside

and the ejection sample weights were determined by subtracting the coating weight. Depending on the time period of the blow during which the sample was taken, a different type of ejection material was normally collected. All the results of the comparison tests are given in Table 6. Only in 5 of the 25 cases did the closed device collect more material than the open ended sampler. For those instances (Tests 10, 17 and 24) where there was an extremely large deviation between the two sample weights, it was observed that the samplers were not placed correctly at the furnace mouth. This problem was eliminated by taking extra care in positioning the sampler.

This data in Table 6 was tested statistically for its goodness of fit. According to the Central Limit Theorem, any natural process that is measurable will have a spread in the data that comes from errors in data gathering. If the error is the sum of many component errors which may not necessarily be normal, then their sum will tend towards a normal or Gauss distribution. A statistical test determining the degree to which the sample data represents the total population (level of significance) can be carried out using the Chi-Square method. This method is illustrated in Appendix I. Normally a minimum of 20 data points is necessary. For industrial data, a 30% level of significance is generally acceptable. Low significance levels indicate the presence of some exterior interfering factor. This data analysis method is used extensively in this thesis since it gives a good indication of whether a natural process is being accurately measured. The data distribution of the % weight difference for the comparison studies and the accompanying X^2 test is given in Table 7. The three excess points (Tests 10, 17 and 24) were ignored. The mean weight difference was 28.7% in favor of the open ended device with a standard deviation of 40.5%. The level of significance at >30% was acceptable.

TABLE 6

COMPARISON STUDIES OF OPEN ENDED AND CLOSED TUBE SAMPLERS

Test Number	Time Into Blow (min)	Type of Sample[1]	Open Sample Weight (gm)	Closed Sample Weight (gm)	% Difference[2]
1	1:30	M	20	12	67
2	4:30	M	22	19	33
3	18:30	M	114	62	84
4	16:00	M	132	68	94
5	18:00	M	181	109	66
6	0:30	S+M	41	58	-29
7	3:00	S+M	59	59	0
8	5:30	S	38	54	-30
9	8:30	S	86	90	-4
10	0:30	S+M	198	66	200
11	5:30	M	25	25	0
12	8:00	S	383	232	65
13	1:30	S+M	66	100	-34
14	6:00	S	35	31	13
15	8:30	S	518	392	32
16	1:00	S+M	47	37	27
17	1:00	S+M	66	10	560
18	1:00	S+M	101	61	66
19	1:00	S+M	87	65	34
20	1:00	S+M	46	41	12
21	1:00	S+M	66	80	-18
22	1:00	S+M	87	79	10
23	1:00	S+M	132	90	47
24	1:00	S+M	79	15	433
25	1:00	S+M	73	37	97

[1] S = slag
M = metallics

[2] $\% \text{ Diff.} = \frac{(\text{Open Wt} - \text{Closed Wt})}{\text{Closed Wt}} \times 100\%$

TABLE 7

COMPARISON STUDY DISTRIBUTION

AND X^2 TEST

Range of % Difference	Number of Observations
-40 to 0	6
0 to 40	8
40 to 80	5
80 to 120	3

$N = 22$

$\bar{x} = 28.727$

$s = 40.490$

X^2 Test

Range	fi	U	Pc	Pi	NPi	X^2
-40 - 0	6	-0.7095	0.2391	0.2391	5.260	0.104
0 - 40	8	0.2784	0.6097	0.3706	8.153	0.003
40 - 80	5	1.2663	0.8973	0.2876	6.327	0.278
80 - 120	3	2.2542	0.9879	0.0906	1.993	0.509
				0.9879	21.733	0.894

Degrees of freedom = 4 - 3 = 1

Level of significance $\geq$ 30%

It was evident from these studies that the open ended device was much more efficient in collecting ejection samples. The explanation for this behaviour is as follows. The closed device was completely sealed with no possible place for gas exit other than the actual entry point. Any particles coming into the device first had to overcome this gas back pressure. Not all the material succeeded in doing so. Proof of the existence of back pressure was given by the observation that no material reached the end plate of the closed device whereas moderate amounts of both slop and metal ejection were found on the open ended device's end plate. With the open ended device there was no such interference force so it collected a representative sample.

The presence of some material on the end plate of the open ended device suggested the possibility that some material escaped through the vertical gap. Random particle trajectories make it possible for some material to pass through the device without sticking to the walls. To determine how much material escaped, a double tube device was constructed. A diagram of this device is given in Figure 42. Any material not collected in the first chamber should be accumulated in the second tube. To facilitate sample weight measurement in both tubes, only the first chamber was coated. 15 tests in which this device was suspended at the furnace mouth for one minute were conducted. The result of these trials is given in Table 8. Photos looking down into the second chamber after samples were taken are given in Figure 43. The amount of material collected in the second chamber varied from as little as 0.4% to a maximum of 4.0% based on the total sample weight. No material was collected on the second end plate indicating very little further material loss from the device. The average sample loss that could be expected from a one chamber device was 1.8%. This was acceptable considering the sampler's simplicity.

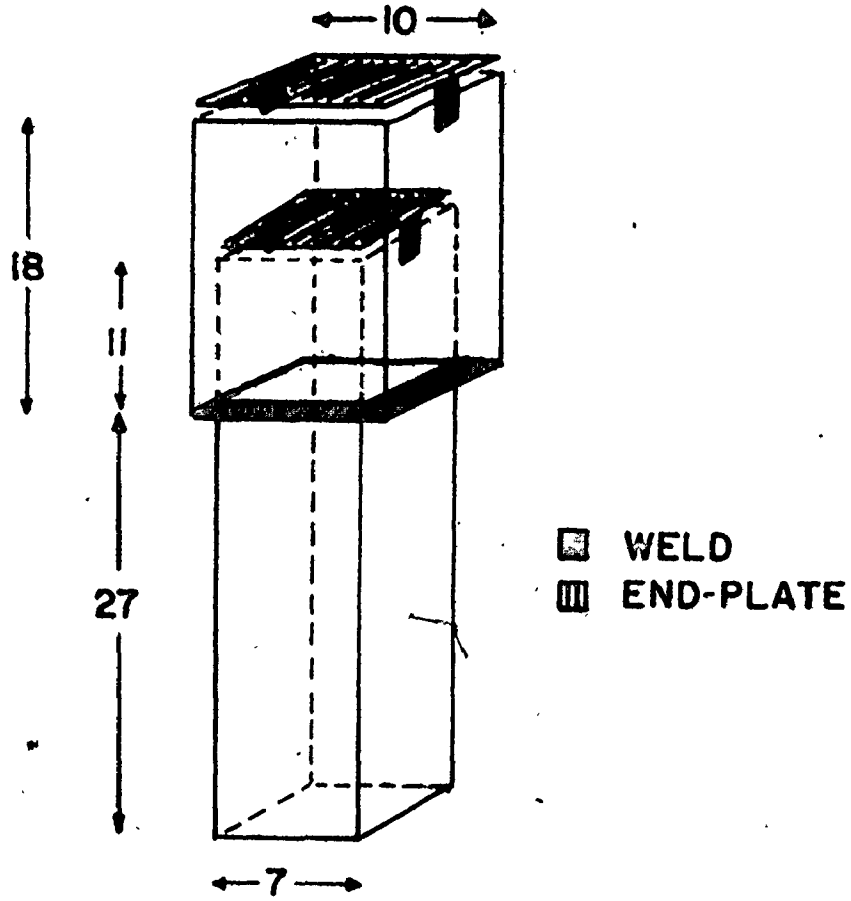

Fig. 42. Schematic of double tube device used to measure material loss through the top opening. All measurements are in cm.

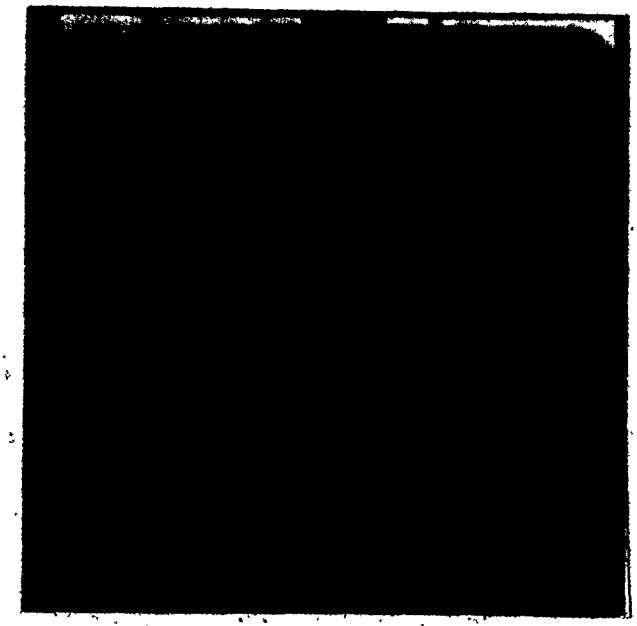

Fig. 43. Second chamber appearance after sampling showing the small amount of material loss.

TABLE 8

TESTS ON LOSS OF MATERIAL
FROM THE OPEN ENDED TUBE SAMPLER

Test Number	Time into Blow (min)	Type[1] of Sample	1st Chamber Sample Weight	2nd Chamber Sample Weight	% loss[2]
1	1:00	M	30	0.6	1.96
2	7:00	S	31	0.9	2.94
3	1:00	S+M	238	2.5	1.04
4	12:00	S	145	2.0	1.36
5	12:00	S	274	4.5	1.62
6	18:00	M	625	18.5	2.87
7	7:00	S	282	2.4	0.84
8	1:00	S+M	228	4.9	2.10
9	7:00	S	112	2.6	2.27
10	12:00	S	219	1.7	0.77
11	18:00	M	202	1.4	0.69
12	18:00	M	134	2.8	2.05
13	7:00	S	290	1.2	0.41
14	12:00	S	168	4.6	2.67
15	1:00	M	17	0.7	3.96

[1] S = slag
M = metallics

[2] $\% \text{ Loss} = \left(\frac{\text{2nd Chamber Wt.}}{\text{(1st Chamber Wt. + 2nd Chamber Wt.)}}\right) \times 100\%$

The question of whether any material was lost by falling out the entry port could not be adequately answered. However, since the sampling location was at the tip of the furnace cone, the off gas velocity would be at its highest. Any material trying to exit through the entry area would have to pass through a positive velocity gradient. This is unlikely since the material reaches the sampler with the assistance of the gas stream. Further work dealing with this subject is presented later (Section 3F).

Based on the favorable comparison and material loss studies, the one chamber open ended device was chosen for further testing of sampler reliability.

3F. TUBE SAMPLER RELIABILITY

To test how reliable the sampler and sampling procedures were, two identical tube devices (coated) were simultaneously suspended at the furnace mouth on separate cables for one minute intervals. The height deviation during sampling between the two devices was about ± 0.1m. The distance separating the two devices was at most 0.4m. Both samplers were manually lowered and raised to their position simultaneously with time differences of less than 3 seconds. Since the sampling conditions were nearly identical, only small differences in the sample weight would be expected. This testing was carried out only at two time intervals in the blow, the first being the 7 min. mark and the second at 18 min. These periods were chosen because examination of the previous studies (Tables 6 and 8) showed that slopping always occurred at about 7 min. whereas only metal ejection occurred at about the 18 min. mark. In this manner, separate checks on sampling reliability for slop and metal ejection could be obtained.

Altogether 31 such tests were carried out at the 7 min. mark and 30 tests at 18 min. The results of these studies are given in Tables 9 and 10. Since the sample weights vary quite substantially, the variance for any test is expressed as an absolute percent difference based on the average test weight of the two samples. If it is assumed that the discrepancy was caused by randomised behaviour in the furnace and in sampling, the error variations empirically expressed as percent difference should pattern themselves to follow a normal distribution. Chi-Square tests on these data sets are given in Tables 11 and 12. For slopping material, the sampling accuracy was ± 9.3% with a standard deviation of 5.9%. The level of significance is acceptable

TABLE 9

SAMPLING RELIABILITY FOR SLOP MATERIAL

Test Number	Weight Sample 1 (gm)	Weight Sample 2 (gm)	% Difference[1] on Mean
1	305	307	0.33
2	73	89	9.88
3	55	75	15.38
4	450	535	8.63
5	510	615	9.33
6	75	97	12.79
7	98	137	16.60
8	168	201	8.94
9	58	63	4.13
10	255	290	6.42
11	28	41	18.84
12	496	620	11.11
13	324	361	5.40
14	583	587	0.34
15	287	311	4.01
16	287	432	20.17
17	57	88	21.37
18	151	155	1.31
19	395	508	12.51
20	80	105	13.51
21	113	142	11.37
22	186	208	5.58
23	318	391	10.30
24	257	328	12.14
25	289	322	5.40
26	522	592	6.28
27	74	80	3.90
28	204	226	5.17
29	235	238	0.63
30	173	246	17.42
31	44	54	10.20

[1] $\% \text{ Difference on Mean} = \frac{(\text{Wt.2} - \text{Wt.1})}{(\text{Wt.2} + \text{Wt.1})} \times 100\%$

TABLE 10

SAMPLING RELIABILITY FOR METAL EJECTION MATERIAL

Test Number	Weight Sample 1 (gm)	Weight Sample 2 (gm)	% Difference[1] on Mean
1	565	568	0.26
2	350	450	12.50
3	89	91	1.11
4	131	138	2.60
5	85	106	11.00
6	103	116	5.94
7	141	177	11.32
8	60	67	5.51
9	25	29	7.41
10	134	193	18.04
11	139	156	5.76
12	168	201	8.94
13	208	226	4.15
14	155	183	8.28
15	112	124	5.08
16	215	224	2.05
17	218	269	10.47
18	320	351	4.62
19	248	284	6.77
20	94	104	5.05
21	421	534	11.95
22	27	31	6.90
23	34	42	10.53
24	65	78	9.09
25	281	330	8.02
26	194	201	1.77
27	105	138	13.58
28	32	40	11.11
29	131	170	12.96
30	84	92	4.55

[1] $\%\ \text{Difference on Mean} = \frac{(\text{Wt.2} - \text{Wt.1})}{(\text{Wt.2} + \text{Wt.1})} \times 100\%.$

TABLE 11

X^2 TEST ON DISTRIBUTION OF SAMPLING ACCURACY FOR SLOP

Range	fi	u	Pc	Pi	NPi	X^2
0-4	5	-0.9097	0.1815	0.1815	5.627	0.070
4-8	8	-0.2277	0.4099	0.2284	7.080	0.119
8-12	8	0.4544	0.6752	0.2653	8.224	0.006
12-16	5	1.1364	0.8721	0.1969	6.104	0.200
16-20	3	1.8184	0.9655	0.0934	2.895	0.004
20-24	2	2.5004	0.9938	0.0283	0.877	1.437
				0.9938	30.807	1.836

Degrees of freedom = 6 - 3 = 3

Level of significance $\geq$ 50%.

N = 31

$\bar{x}$ = 9.335

s = 5.865

TABLE 12

X^2 TEST ON DISTRIBUTION OF SAMPLING ACCURACY FOR METAL EJECTION

Range	fi	u	Pc	Pi	NPi	X^2
0-4	5	-0.8480	0.1983	0.1983	5.949	0.151
4-8	11	0.1002	0.5399	0.3416	10.248	0.055
8-12	10	1.0484	0.8527	0.3128	9.384	0.040
12-16	3	1.9967	0.9771	0.1244	3.732	0.144
16-20	1	2.9449	0.9984	0.0213	0.639	0.204
				0.9984	29.952	0.594

Degrees of freedom = 5 - 3 = 2

Level of significance $\geq$ 70%

N = 30

$\bar{x}$ = 7.577

s = 4.218

at >50%. For metal ejection material, the sampling accuracy was ± 7.6% with a standard deviation of 4.2%. The level of significance of the data distribution is >70%. The sampling errors were rather high for both cases but are tolerable since the experiments were being conducted on an industrial process where all the parameters are not controllable.

There was a slightly greater sampling inaccuracy for slop samples because of the lower density of this material. The slop could constrict the entry area to a larger degree than the metal ejection, thereby creating a source of sampling error. Included in these discrepancy tests was any variance in the coating evenness on one sampler or between two samplers since the inside paint weight has already been shown to be, to certain extent, an uncontrollable variable.

The most easily accessible vertical entry port for sampling was the lance hole opening. This area represented only a small portion of the furnace mouth. The samples obtained from this area may not have been representative of what was being ejected from the entire furnace mouth. Tests were therefore conducted at two different sampling positions. This was made possible by partitioning the two water cooled panels of the gas cleaning systems whose junction was at the lance opening (See Figure 37). A 30 cm wide gap thereby ran along the whole furnace diameter. Two samplers were simultaneously suspended at the tip of the furnace mouth for one minute intervals; one sampler was located at the furnace centre through the lance hole and the other was positioned 1m away, near the edge of the mouth. The separation of the devices was kept within limits of ± 0.2m. All sampling was again carried out at two periods in the blow, at 7 min. for slop and at 18 min. for metal ejection. Time permitted only 25 such tests to be conducted, 13 for slop and 12 for metal ejection. The results of these studies are given in Table 13. The weight

TABLE 13

TESTS ON REPRESENTATIVITY OF SAMPLING

Test Number	Time into Blow (min)	Sample Weight at Mouth Centre (gm)	Sample Weight at Mouth Edge (gm)	% Difference[1]
1	7:00	339	292	-13.9
2	7:00	259	253	- 2.3
3	7:00	117	121	+ 3.4
4	7:00	37	55	+48.7
5	7:00	236	197	-16.5
6	7:00	359	470	+30.9
7	7:00	387	316	-18.4
8	7:00	450	269	-40.2
9	7:00	17	10	-44.5
10	7:00	66	123	+86.4
11	7:00	65	110	+69.2
12	7:00	409	304	-25.7
13	7:00	395	235	-40.5
14	18:00	218	206	- 5.5
15	18:00	340	370	+ 8.8
16	18:00	584	434	-25.7
17	18:00	378	292	-22.8
18	18:00	290	321	+10.7
19	18:00	205	145	-29.3
20	18:00	433	538	+24.3
21	18:00	172	343	+99.4
22	18:00	88	103	+17.1
23	18:00	85	33	-61.2
24	18:00	91	88	- 3.8
25	18:00	14	23	+64.3

[1] $\% \text{ Difference} = \frac{(\text{Wt. Edge} - \text{Wt. Centre})}{\text{Wt. Centre}} \times 100\%$

TABLE 14

X^2 TEST ON DISTRIBUTION OF SAMPLING REPRESENTATIVITY

Range	fi	u	Pc	Pi	NPi	X^2
-75 : -25	7	-0.7005	0.2418	0.2418	6.045	0.151
-25 : 25	12	0.4852	0.6862	0.4444	11.110	0.071
25 : 75	4	1.6708	0.9526	0.2664	6.660	1.062
75 : 125	2	2.8565	0.9979	0.0453	1.133	0.664
				0.9979	24.948	1.948

Degrees of freedom = 4 - 3 = 1

Level of significance $\geq$ 15%

N = 25

$\bar{x}$ = 4.541

s = 42.170

difference is expressed as a percentage based on the centre sample weight.

The slop samples obtained from the two positions appeared quite similar and were not tested for differences in chemistry since their source point, the slag-metal-gas emulsion, was relatively homogeneous as will be shown later (Section 3H). Likewise, the metal ejections at both locations were the same, being composed almost entirely of iron as will be demonstrated later (Section 4C.5). The weight differences between the centre and outside positions were quite variable ranging from -61% to 99%. The data can be analyzed separately for both types of material. The mean weight difference for slop was 2.82% with a standard deviation of 43.00%. Similarly for metal ejection the mean was 6.4% with a standard deviation of 43.08%. A t-test of these values shows they are statistically similar at a 99% significance level and so the data can be treated together. The X^2 test on the data distribution given in Table 14 shows a >15% level of significance. This is a rather low value but could possibly have been improved had further testing been carried out. All in all, this study showed that slopping and metal ejection were generally uniform over the furnace mouth but large deviations were possible. This variation could be explained by the fact that the off gas flow was not uniform over the whole furnace mouth area. There was a certain amount of air intake around the edges which disturbs the flow. The cone constriction could also cause gas velocities to vary across the furnace mouth. The asymmetry of the cone could also have an effect.

A rough measure of the efficiency of sample collection could be made. The influence of such exterior variables as sampler dimension, loss of material through the entry port, effectiveness of deposition, and sequential layer buildup of ejected material could be noted. To test the sampling efficiency two open ended probes, depicted in Figure 44, of different entry areas were

inserted simultaneously into the furnace mouth through the lance hole for one minute periods. The ratio of the entry areas between the two devices was 1.85. Under ideal sampling conditions the ratio of the material collected in the two devices should be directly proportional to the ratio of the entry areas. For non ideal conditions the rate of deposition should be higher in the larger sampler. Altogether 11 runs with both devices were made. The tests were conducted randomly during the 7 to 20 min. mark of the blow. The results are presented in Table 15. In Table 15, the coefficient R marks the deviation between actually observed sample weight ratios and the theoretically predicted value based on the area ratio. R should approach unity under ideal conditions. In the tests conducted an average R value of 1.25 was obtained. If the one excessively large value from test 5 is eliminated, the average is 1.17. The cause for R value being greater than unity is considered due to the diminished accuracy of measurement with the smaller tube. Here sampling was more easily interfered with by such factors as the reduction in entry area due to material deposition and the greater disturbance of the waste gas flow creating more back pressure and causing the deflection of incoming material. Though the larger sampler proved to be more efficient, it was considerably bulkier and could not be handled as easily. For this reason, the smaller sampler was employed in the investigation of commercial heats.

The sampling error of the open ended tube device was shown to be between 7 and 9% on the average. The central sampling location also proved to be roughly representative of the whole furnace mouth. The sampling time of one minute had thus far been found to be adequate in getting representative samples and was employed in all further experimental work. The tube probe after sampling could be manually changed in two minutes so ejection samples could be taken, if necessary, at every three minute interval in the blow.

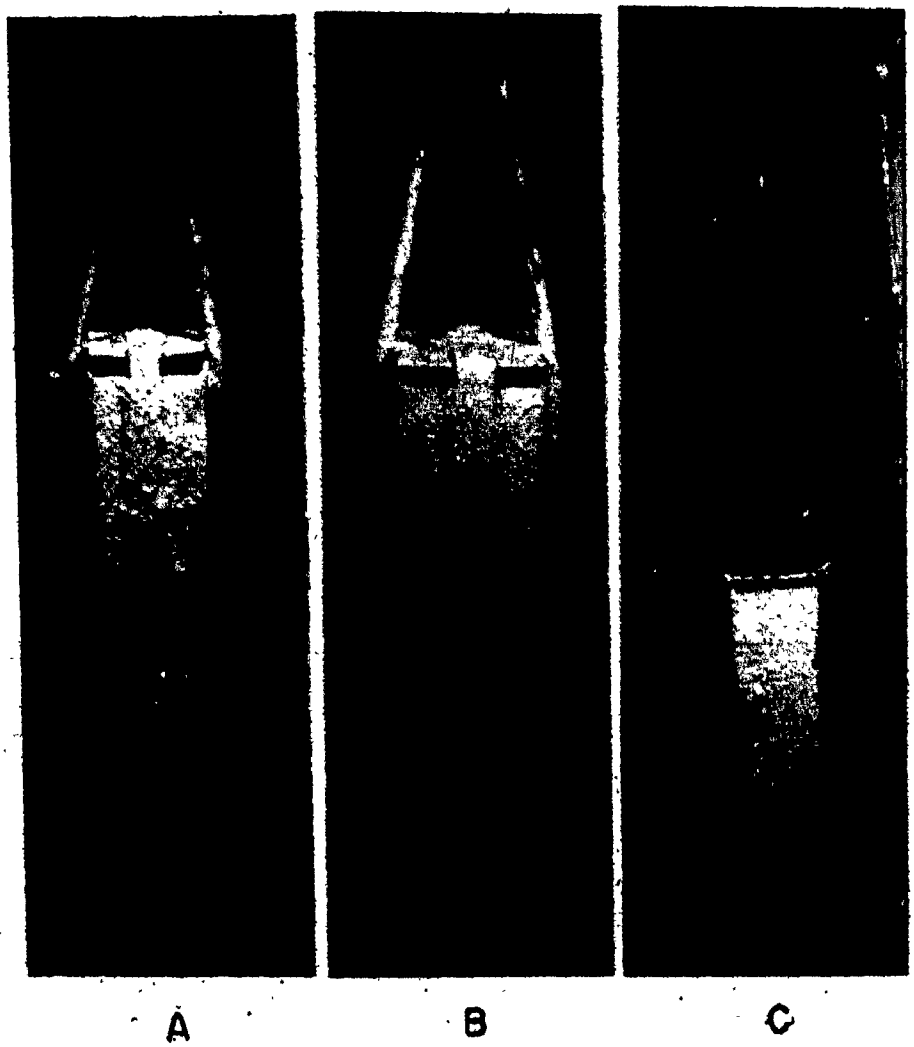

Fig. 44. Coated ejection samplers used in the sampler evaluation study.
(A) Regular open ended device
(B) Larger entry area for efficiency studies
(C) Double tube device for material loss studies.

TABLE 15

TESTS ON SAMPLING EFFICIENCY

Test Number	Time into Blow (min)	Sample Weight of Large Tube (gm)	Sample Weight of Small Tube (gm)	R^1
1	7:00	462	212	1.18
2	10:00	520	319	0.88
3	13:00	126	106	0.64
4	7:00	583	254	1.24
5	13:00	695	183	2.05
6	7:00	304	117	1.40
7	17:00	513	235	1.19
8	19:00	1171	504	1.26
9	7:00	98	61	0.87
10	11:00	520	176	1.60
11	15:00	235	87	1.50

$$^1 R = \frac{\text{(Wt. Large Tube)}}{\text{(Wt. Small Tube)}} \div 1.85$$

Entry area ratio = 1.85

3G. CORRECTIONS IN SLOP SAMPLING

Because of the low density of BOF slop, continual slag accumulation in the probe during the one minute sampling period could substantially reduce the entry area. Slop samples greater than 300 gm could effectively block off one third the area. Therefore the measured slag ejection rate was a low estimate of the true slopping rate. To account for this area change a model was set up. Several assumptions were made: first, that the slopping rate was constant during the one minute sampling period, second, that only material entering through the free area would be collected, and third, that there existed a linear relationship between the final sample weight and its thickness. The first two assumptions were simplifications that could not be verified. The third assumption was checked out by measuring some average slag thicknesses and correlating them to the sample weights. Altogether 24 such data points were accumulated. The regression coefficient between the slop weight and its average thickness was 0.826, giving strong evidence that a linear relationship was present. The data is plotted in Figure 45 along with the least squares regression line of the form $h = b \times W$, where W is the weight and h is the thickness. The calculated b value was 4.382×10^{-3} cm gm^{-1}. The mathematical model devised in Appendix 2 combines this relationship along with the previous assumptions to produce an incremental analogy of the collecting process. Using differential calculus, it was possible to predict the corrected slopping rate on the basis of the final sample weight by using it as the integration limit. The relationship developed is given by the equation:

$$E = \frac{1597 \times W_f}{1597 - 2 \times W_f} \qquad (3.1)$$

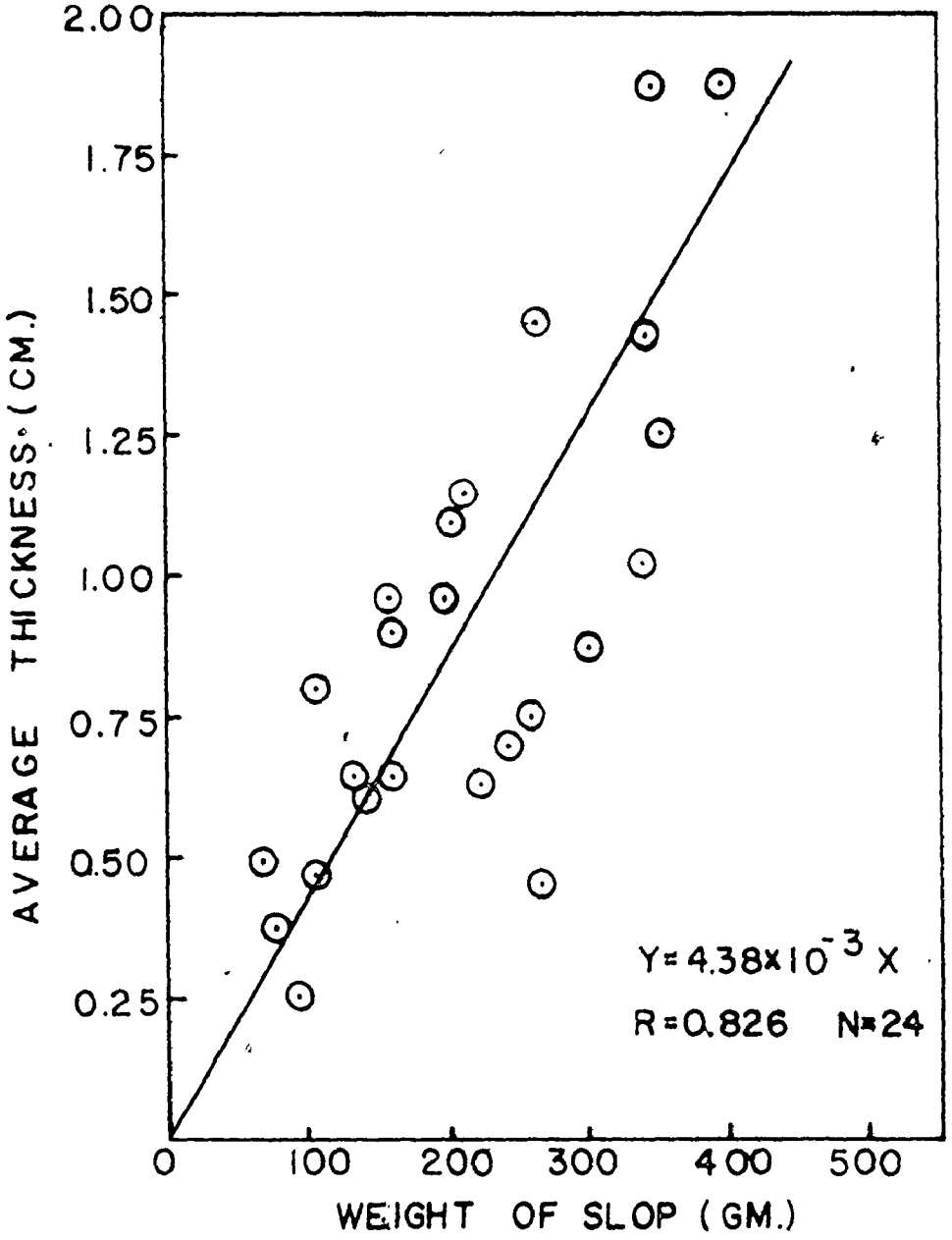

Fig. 45. Relationship between slop sample weight and sample thickness.

where E is the corrected ejection weight in grams and W_f is the final slop sample weight expressed in units of grams. All the measured slop weights were normalized using this equation.

The metal ejection samples also accumulated in successive layers on the tube walls but their overall thickness, due to the higher density, was generally less than 0.2 cm. Any errors due to this small area reduction were neglected.

3H. SLAG AND METAL SAMPLER

To get further information about the processes giving rise to ejections, a method was developed to simultaneously obtain slag and metal samples while the ejection probe was in position. Chemical analysis of all this material would hopefully serve to point out any deviations or causes for ejection. There was no interruption of the blowing process during sampling. The slag and metal sampler could only be dropped into the BOF from the same scaffold location used for the ejection probe. Passage through the gas cleaning system was again via the lance hole opening. Preliminary tests with simple steel pots, weighted down so that they could pass through the slag layer, showed that a 15 second time period was sufficient to drop and retrieve the sampler from the BOF. Steel strand cables were originally used to suspend the device but they proved to be undependable. They frequently burned off when coming in contact with the oxygen jet. Rubber cables, taken from sinker thermocouples used for BOF end-point control, were found to be more durable in the very oxidizing furnace atmosphere. The rubber burnt more slowly and was not sheared by direct oxygen jet impingement.

The weighted steel pot was adequate in obtaining slag and metal samples. It would sink through the slag layer and penetrate into the metal bath sufficient enough to obtain a sample. On withdrawing the device, slag would fill the empty portion of the pot and also coat the outside walls. The metal contained in the pot had a tendency to weld onto the surface and thereby was difficult to remove. This problem was eliminated by coating the sampler completely with the lime paint used for the ejection sampler. The coating was applied by dipping the heated pot in the colloidal solution and

drying it in the gas fired furnace. The metal specimens were quite porous because of the high oxygen content of the molten metal bath. Aluminum was therefore added to the pot to deoxidize the metal. The aluminum was contained in two square, coated, steel tubes wedged into the pot. The pot and the tubes were sealed with masking tape to prevent the aluminum from falling out before immersion. The smaller metal specimens obtained from these tubes were more easily cut for analysis. A photo of the completed assembly is given in Figure 46.

The sampling pot weighed around 4 kg with the attached weight. Metal specimens obtained with this device generally weighed between 1 and 2 kg. The 10 gm of aluminum added would be sufficient to kill this material. Slag samples of around 0.5 kg were normally secured. However at times, particularly in the last stages of the blow, only a metal sample was obtained. The reasons for this behaviour are given later. Only large chunks of slag free of any paint coating were selected for analysis.

When immersed in the metal bath, the sampling pot was in the vicinity of the oxygen jet. Questions were raised as to whether the oxygen jet might refine the metal sample while it was being taken during the blow. To check for this possibility, metal samples were taken simultaneously at two different positions in the furnace. This was carried out when the panels surrounding the lance were opened. A regular sample was taken through the lance hole and another was obtained at a distance 1m away. This second position was roughly half the distance between the lance and the furnace walls.

One heat was sampled at these positions at different times during the blow. One further test was carried out during another heat. The results of the chemical analysis of these metal specimens are given in Table 16. These compositions essentially represent the top layers of the metal bath. With

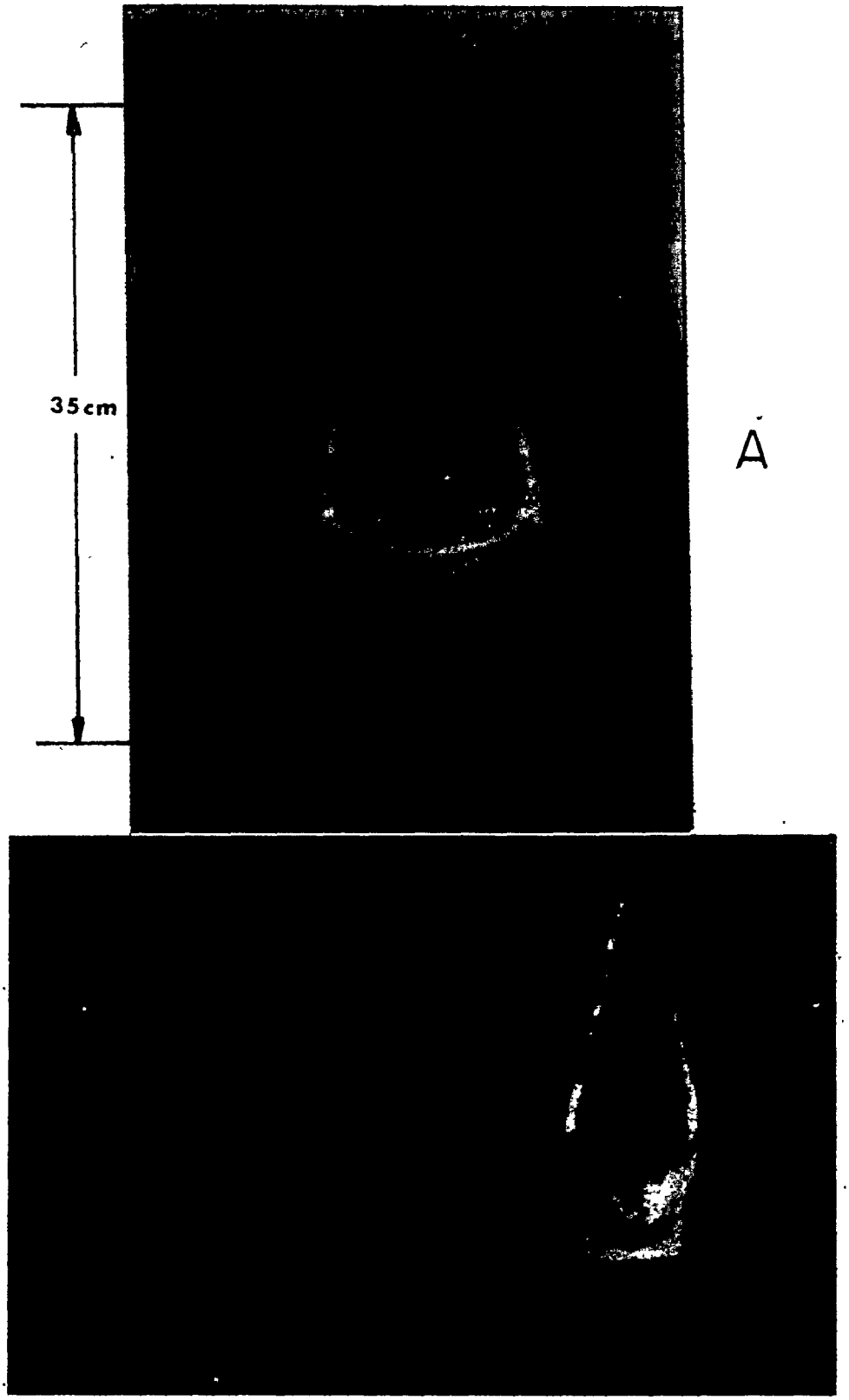

Fig. 46. Coated slag and metal sampler with (A) aluminum inserted in tubes, and (B) attached to rubber cable, ready for sampling.

TABLE 16

STEEL COMPOSITION IN DIFFERENT AREAS OF THE BATH

Sample Time into Blow (min)	%C		%Si		%Mn	
	Centre	Outside	Centre	Outside	Centre	Outside
4	3.60	3.36	.187	.053	.41	.20
7	2.94	2.81	.010	.004	.14	.16
10	-	2.30	-	<.001	-	.16
13	1.67	1.64	<.001	.002	.27	.29
16	1.23	1.14	<.001	.001	.30	.32
19	0.41	-	<.001	-	.33	-
4	3.70	3.42	.042	.011	.13	.08

respect to carbon analysis, the outside region consistently had a lower value. Silicon followed a similar path while it was still present in the metal bath. For manganese, the early blowing periods had higher levels in the centre but this reversed itself later in the blow. The differences in the various elemental compositions gave no indication of enhanced refining in the sampling pot around the oxygen jet region. Rather, the higher central concentrations gave clear evidence of metal circulation in the molten bath. Bulk metal of higher impurity concentration was delivered by a central upward flow to the jet region. In the impingement area and in the course of the outward metal flow, direct and indirect refining reactions reduced the impurity concentrations. The case of manganese was unique in the later stages of the blow. The slightly higher concentrations in the outer regions were due to the manganese reversion as the metal contacted the slag. The slag rejected manganese into the bath for a number of reasons[65], i.e. increased basicity and decreased iron oxide concentration. The composition differences between the two locations were small enough to ignore, but as demonstrated, they can serve to give further information on circulation patterns. The metal sample could be taken to represent the overall bath concentration.

Since slag could only be readily sampled around the lance region, questions regarding slag homogeneity had to be answered. Previous studies[134] had been conducted at Dofasco in this area, so these results are quoted. The method of testing was to sample the furnace slag about the lance by the familiar pot method, then quickly turn down the furnace and rotate it to a different position so that a slag sample could be taken from the vessel edge. The major inaccuracy of such a sampling method was that the slag immediately began to subside when the oxygen flow was stopped. Chemical reactions between slag and metal did not stop and the emulsion droplets began to settle out. Some of the

results are presented in Table 17. As can be seen, there were no great variations in CaO, SiO_2, MnO and metallic Fe analysis between the two locations. On the other hand there was a greater relative variance in divalent and trivalent iron concentrations. However this is due mainly to their extremely low ranges and to difficulties in actual chemical analysis. These errors will be discussed further in the next section.

TABLE 17

TESTS ON SLAG HOMOGENEITY

Heat Number	Sampling Location[1]	Time into Blow (min)	CaO	SiO_2	MnO	Fe^{o}	Fe^{2+}	Fe^{3+}
1	C	5	28.9	18.2	9.8	27.5	4.1	1.7
	E	5	30.6	17.4	9.4	27.4	3.0	0.0
2	C	10	30.7	18.0	9.5	22.8	5.7	-
	E	10	32.0	17.8	9.2	20.1	3.9	0.2
3	C	15	33.7	19.8	9.2	22.6	2.8	0.6
	E	15	31.5	18.1	8.5	29.4	1.5	-

[1] C = furnace centre
E = furnace edge

3I. SLAG SAMPLE PREPARATION AND CHEMICAL ANALYSIS

The presence of metal droplets in the sample presents problems in slag analysis. These droplets cannot be discounted for they form an integral part of the slag-metal emulsion. An often encountered problem is that these droplets are analyzed for as ferrous iron, leading to dubious slag analyses in which the iron oxide levels are quoted to be very high. A method to circumvent this problem and to actually measure metallic iron concentrations in the slag has been developed at Dofasco. The methods of sample preparation and analysis are briefly reviewed as follows.

SAMPLE PREPARATION

A general outline of the procedure is given in Figure 47. This method will produce a fine -35 mesh powder free of most extraneous metal and unreacted CaO.

Material foreign to the slag such as irregular shaped iron and lumps of unreacted lime are removed by hand. Particle size is reduced first by a jaw crusher and plate grinder, then with a disc mill assisted by screening. Slag samples of 250 - 500 grams are generally prepared to insure homogeneity. Analysis of several + 35 mesh portions, generally a small fraction of the total sample weight, has shown it to be consistently greater than 90% metallic iron. It is therefore accounted for in the slag analysis as pure iron.

EXTRACTION OF UNREACTED CaO

Since free lime is not an actual component, it must be removed before analysis proceeds. The -35 mesh material obtained after sample preparation is used in this extraction.

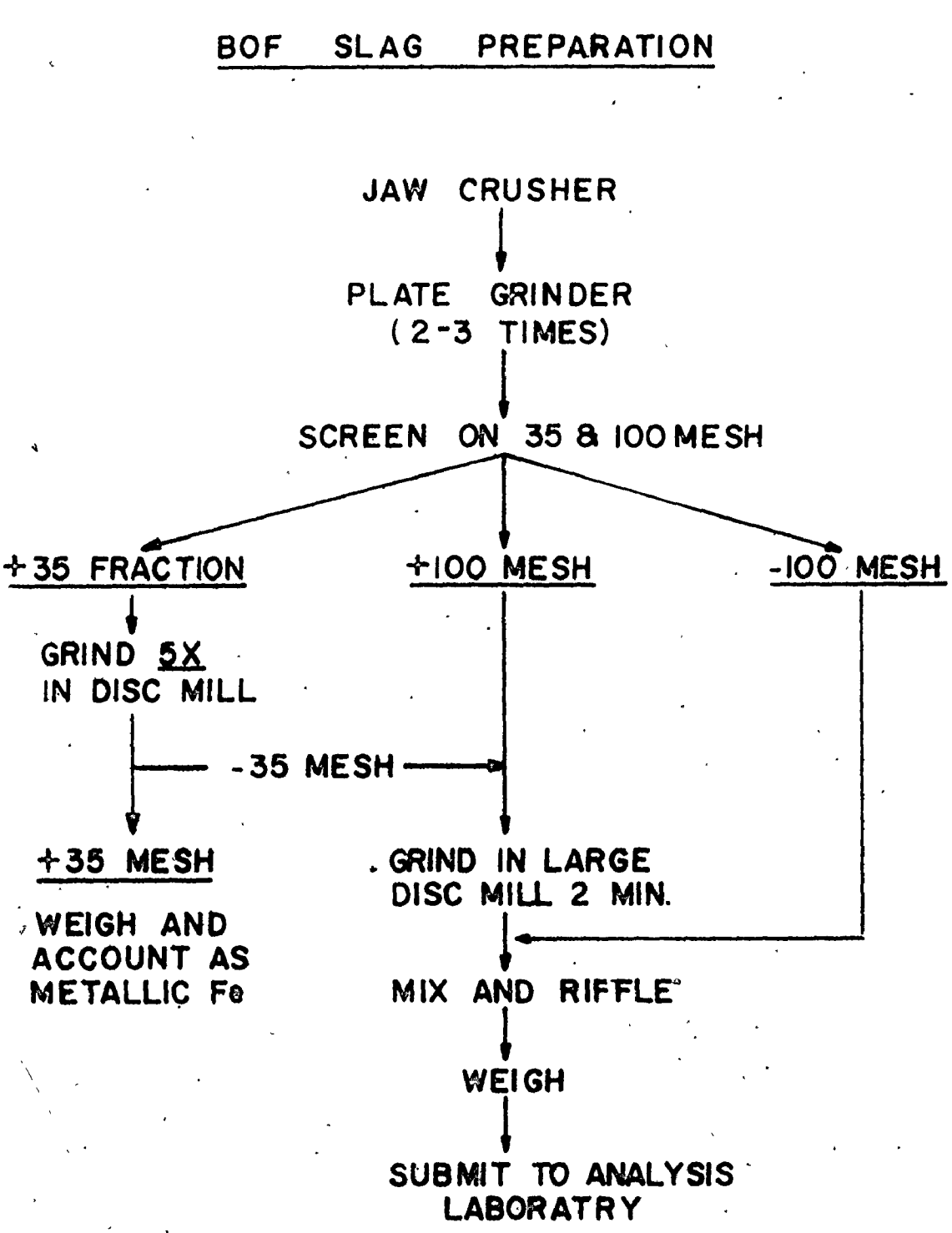

Fig. 47. Slag (as emulsion) preparation techniques employed in this study.

A 20 gram riffled sample is mixed with hot ethylene glycol (70°C), stirred for a 30 minute time interval and filtered. The sample is washed free of glycol with isopropyl alcohol and dried. The dry material is crushed and mixed to produce a fine, homogeneous sample containing no unreacted lime. Generally the free lime content of the slag is less than 15%.

SiO_2 ANALYSIS

A 0.5 gm portion of ground sample obtained after free lime extraction is used for this analysis. All the major slag components other than silica are leached out using hot hydrochloric acid. The residue is collected by filtering. This is transferred with the filter paper to a previously ignited and tared platinum crucible. This crucible is heated slowly in a muffle furnace to 900°C. When ignition is complete, it is removed from the furnace and cooled in a dessicator. The crucible together with its contents is weighed. Silica is then dissolved by adding a HF - H_2SO_4 solution. The liquid is evaporated on a hot plate until heavy fuming starts. The previous furnace procedure is then repeated. On reweighing the cooled crucible, the loss in weight marks the slag's silica content.

CaO, MgO, MnO AND TOTAL IRON ANALYSIS

The filtrate from the hydrochloric acid leach used in SiO_2 analysis is employed to measure these major slag components. Additional hydrochloric acid is poured into the filtrate to ensure that all the material is dissolved. Dilutions with water in the proper quantities allow elemental analysis for the metal ions to be carried out using atomic absorption methods. By taking into account the dilution factors, the corresponding oxide and total iron concentrations can be determined.

METALLIC IRON ANALYSIS

Another 0.5 gm sample of ground material, already leached to remove any free lime, is used for this analysis. A bromine-methanol solution is

added to dissolve the metallic iron. Once dissolution is complete, the mixture is filtered to separate out the residue which contains the ferrous and ferric iron. Hydrochloric acid is then added to the solution, followed by drying to evaporate off the bromine and methanol. Further acid addition ensures complete iron dissolution. Stannus chloride is used to reduce all the iron to the ferrous state. Mercurous chloride is also added to tie up any excess tin. The solution is finally titrated with potassium dichromate to analyze for iron content. This represents the metallic iron content of the ground sample. It is added to the +35 mesh portion to get the total slag metallic iron content.

FERROUS IRON ANALYSIS

The residue from the bromine-methanol leach is used for ferrous iron analysis. To prevent any oxidation of this material, the chemical analysis is carried out in a nitrogen atmosphere. Hydrochloric acid is added to the residue to dissolve the ferrous iron. The resulting solution is topped off with distilled water and mercurous chloride solution. Mercurous chloride is added to replicate the same conditions for redox titration. Potassium dichromate is again used in this titration.

FERRIC IRON CONTENT

Ferric iron can be analyzed for using a wet chemical method but the procedure is time consuming. For this reason the ferric iron content is obtained directly by subtracting the ferrous and metallic iron portion from the total iron. Though this method is quite inexact, it does provide some useful information.

ACCURACY OF ANALYSIS

To measure the experimental error in slag analysis, a standard slag sample was routinely analyzed for some of its components. The standard

deviations for the major slag components obtained in this manner are given in Table 18. The experimental error for ferrous and metallic iron analyses was measured by doing duplicate analyses on several samples. The standard deviation for ferric iron was determined by combining the variances of the total, ferrous and metallic irons. For the major slag components, the standard deviations were relatively low. However for the different iron constituents, these values were considerably higher because of problems with sample oxidation. To minimize this interference as much as possible the slag samples were stored in a freezer in sealed plastic envelopes.

TABLE 18

ACCURACY OF SLAG ANALYSIS

Component	Standard Deviation
CaO^{1}	0.16
MgO^{1}	0.10
$SiO_2{}^{1}$	0.10
Total Fe^{1}	0.12
MnO^{1}	0.07
Metallic Fe^{2}	0.50
$Fe^{2+}{}^{2}$	0.30
$Fe^{3+}{}^{3}$	0.60

[1] obtained from analysis of standard

[2] obtained from duplicate analyses

[3] obtained from calculation

3J. METAL SAMPLE PREPARATION AND CHEMICAL ANALYSIS

Bulk metal samples were obtained in the sampling pot. The metal specimen was first rough cut to expose an inner surface. Grinding was then carried out on a lathe. The clean surface was then analyzed for Mn and Si using optical emission spectroscopy. The specimen was then drilled to get finer material for carbon analysis on a Leco® analyzer. The standard errors of analysis were obtained by repeated testing of steel standards. These standard deviations are given in Table 19.

TABLE 19

ACCURACY OF METAL ANALYSIS

Component	Standard Deviation
Mn	0.0125
Si	0.0125
C	0.005 for levels < 0.2%C 1% of measurement for levels > 0.2%C

3K. FURNACE SAMPLING

Random heats were selected for sampling. In each heat eight ejection samples were taken. The sampler for ejected materials was suspended in the BOF for one minute intervals starting at the one minute mark of the blow. Thereafter, with new samplers, sampling proceeded after every three minute interval. Slag and metal bath samples were simultaneously obtained starting at the 4 minute mark. A slag and steel sample was also taken at the first vessel turndown. The blowing practice was recorded throughout the heat. Altogether 30 heats were sampled. The physical condition of the furnace varied during the sampling period. In recording these changes only measurements of the furnace bottom depth could be taken. Bottom buildup or erosion could be noted. Erosion along the side walls could not be measured. Changes in the furnace mouth area were evident but again could not be measured.

After sampling, the interior of the sampler for ejected materials was stripped completely and the sample weight was obtained by subtracting the recorded coating weight from the measured weight. The physical appearance of each ejection sample was noted. Ejection sampling was successful in all but a few cases where the cable was burned through. In sampling the slag and metal, the rubber cable used was not as sturdy, leading to a success rate of about 80%. Frequently no slag sample was obtained in the later stages of the blow. For these two reasons and also because of the lengthy period required for slag analysis, only four or five slags (always including the turndown slag) were analyzed per heat. Generally those samples from the 4, 10, 16 minute and first turndown period were used. All the metal samples taken were analyzed.

4. EXPERIMENTAL RESULTS

4A. SAMPLING PERIOD

Sampling was conducted over the course of one and a half furnace campaigns. As the service time of the lining increased, there was a gradual accumulation of permanent buildup on the vessel bottom. This accumulation was measured using an instrument available at the plant. The buildup resulted because of the practice of making viscous turndown slags high in MgO content for extended lining life. Combined with other factors such as slow tapping rates and large slag volumes, this allowed gradual slag buildup on the vessel bottom and on the lower furnace sidewalls. Buildups as great as 1m were noted. In the region of active slag and metal contact, the refractory lining eroded substantially along both sides of the trunion area. The region between the trunions had less erosion because of slag coating during tapping and slag dumping. The cone area accumulated material much more rapidly due to the buildup of slop and metal ejections. However this buildup was cleared regularly so an essentially constant mouth area was maintained. Of the 30 sampled heats, 23 were taken during one entire furnace campaign: 8 in the first third of the campaign, 8 in the second third and 7 in the last period. Sampling days were evenly spaced with two back to back heats always being tested. Two of these heats had special scrap charges (about 40% of metallic charge) and were blown under different conditions. They will be discussed later (Section 4F). The remaining 7 heats were sampled in the latter third of another campaign on the same furnace.

There was no standardization of blowing practice in the heats which were investigated. Most operators followed a similar course to that outlined in Figure 35, but the actual time period of reduced oxygen flow, during slopping, varied considerably. A maximum time length of 11 minutes of reduced oxygen flow was observed. On a few occasions no reduction was applied because slopping was very light.

4B. QUALITATIVE PRESENTATION OF EXPERIMENTAL RESULTS

All of the 28 regular heats sampled exhibited a similar ejection pattern. Various stages of material ejection could be categorized according to the sample's visual characteristics. A photograph of the exterior appearance of the samplers at different times during the blow is given in Figure 48. The appearance of the interior of the sampler was the same as that shown in the picture but could not be readily photographed. Close up shots of the various sample material from two typical heats are given in Figures 49 and 50. The BOF blowing period could be roughly categorized according to the types of ejection samples obtained. They were as follows: 0-6 minutes, fume and fine slag and metal ejections; 6-15 minutes, slop; 15-21 minutes, metal ejection; 21 minutes - turndown, metal ejection or light fume.

(i) 0-6 MINUTES

In the early stages of blowing most of the samples comprised of various shades of reddish powder sometimes combined with varying quantities of ejected slag and metallics. The red powder was fumes (Fe_2O_3) that had collected on the device's paint coating. The sample's colour intensity depended mainly on the relative weights of fumes and paint. The quantities of powder collected were generally less than 20 gm, representing an overall evolution rate of 20 kg of fumes per minute across the furnace mouth. This evolution rate was too low to account for all the fume losses from the furnace. Approximately 0.8 tons of fumes are generated in the first 6 minute period. This figure is based on the quantity of fumes collected in the dust cleaning system. Most of the fumes were therefore not collected in the sampler.

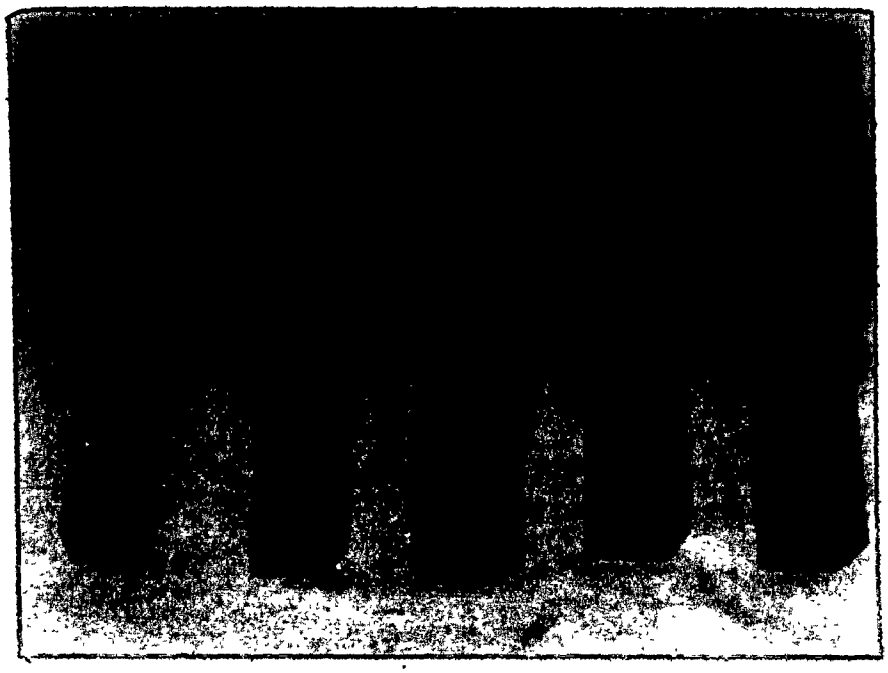

Fig. 48. Exterior appearance of samplers at different times during the blow.

A) 1 Min. - Fume and fine metal ejections.
B) 7 Min. - Fume and light slop.
C) 10 Min. - Heavy slop.
D) 16 Min. - Metal ejection.
E) 22 Min. - Negligible material. Dark appearance because of burnt coating.

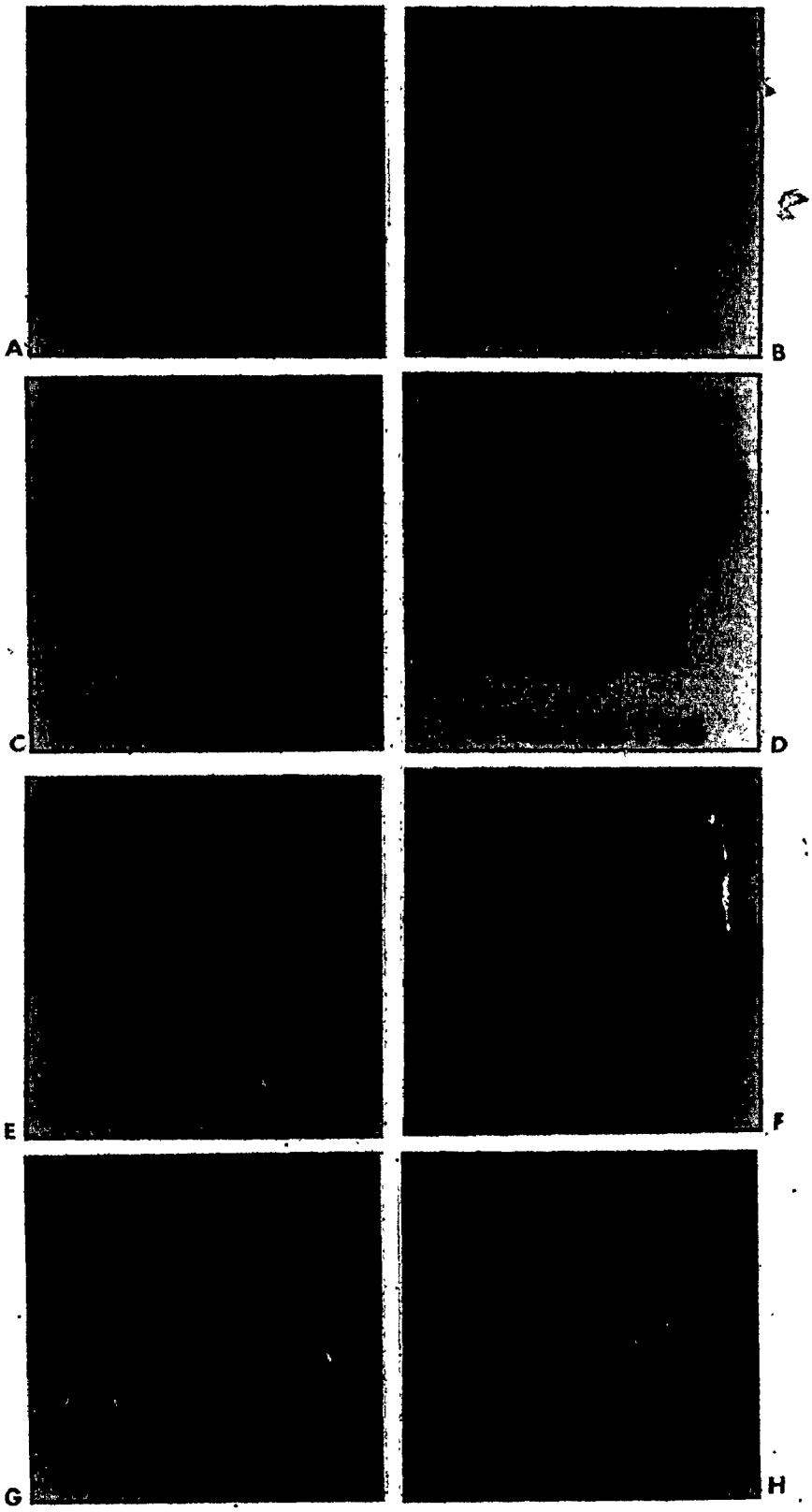

Fig. 49. Ejection material from heat 17 at ½ magnification.

i) 1, 4, 7 min. - fume and fine metal and slag ejections.
ii) 10, 13 min. - slop.
iii) 16, 19 min. - metal ejection.
iv) 22 min. - fume and fine metal ejections.

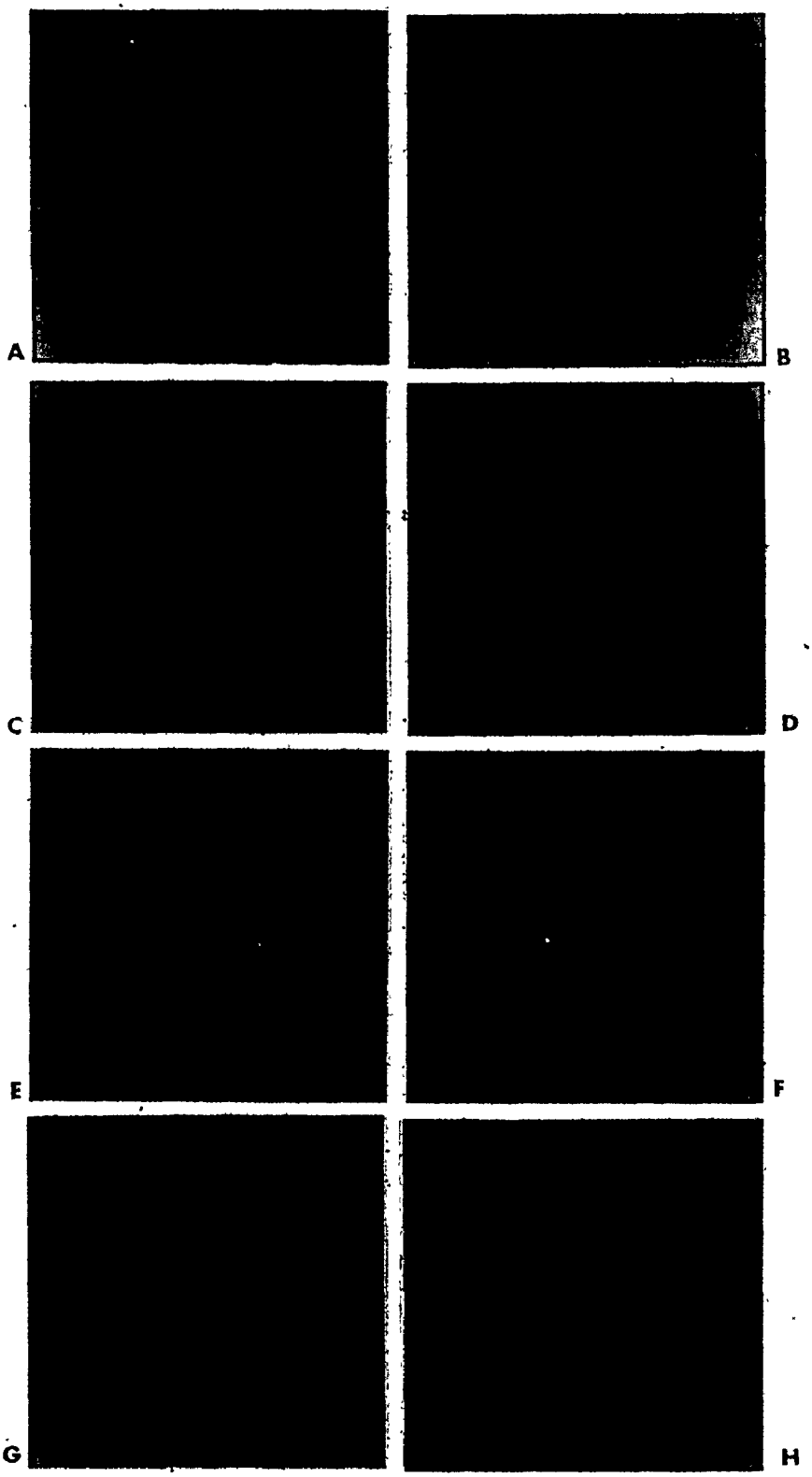

Fig. 50. Ejection material from heat 30 at ½ magnification.

i) 1, 4 min. - fume and fine metal and slag ejections.
ii) 7, 10 min. - slop.
iii) 13, 16, 19 min. - metal ejection.
iv) 22 min. - fume and fine metal ejections.

This discrepancy will be discussed later. The sample obtained at the one minute mark often contained an abundance of ejected slag and metallics (between 50 to 200 gm) so that the fume weight could essentially be discounted.

(ii) 6-15 MINUTES

Slop was often present at the 7 minute mark, always at the 10 minute point, and most times at 13 minutes. Rarely was there any slop at the 16 minute mark. The sample's appearance was generally dark and glassy with gas holes, and weighed between 50 to 500 gm. Frequently, abundant quantities of metal droplets of various sizes (Figures 49d and e) and free lime (Figure 50d) were present in the slop. Sometimes only fine metal droplets occurred (Figure 50c) and in other cases they weren't even visible by naked eye (Figure 50d). All the slop material was easily friable because of its slag matrix. Trace amounts of fumes were collected in the top sections of the sampler where there was no slop coating. This quantity was insignificant in comparison to the slop weight.

(iii) 15-21 MINUTES

Metal ejection samples were normally obtained at the 16 and 19 minute sampling of the blow, but occasionally, such type of material was collected at the 13 and 22 minute sampling. This material could be identified visually by its greyish colour. The samples varied in thickness ranging from about 0.1 to 1.0 cm. Only the thin material could be fractured by hand. The metallics present varied in appearance from accumulations of fine droplets in the light samples (100gm, e.g. Figure 49g) to combinations of large splash material (diameter less than 1cm) and finer droplets for the heavier samples (Figures 50f and g). The splash portion did not retain a spherical appearance,

indicating that the material was molten when it struck the sampler's surface. The diameter of this splash material could be roughly estimated from its width perpendicular to the direction that it originally struck. Transverse fractures of several samples exposed a bright shiny metal surface composed of layers of droplets and splash. Only the exterior surface had a greyish appearance, presumably due to surface oxidation. The metal ejection samples varied in weight from 50 to 1500 gm, indicating the possibility of enormous metal loss rates of 1500 kg. per minute. However for the most part the sample weights were less than 500 gm. In other cases small fume samples, present as surface layers of reddish powder on the paint coating (Figures 49h and 50h), or negligible quantities of ejection material were found at 22 minutes. In some cases blowing was terminated before this point so no sample was obtained. Some samplers were suspended in the period of carbon reblow. The material collected was always of the fume or red powder variety but again only as a surface layer over the paint coating.

(iv) RESULTS OBTAINED FOR SIMILAR HEATS

Two consecutive heats were normally sampled on one furnace. Since this involved the same operator, the blowing practice would normally be uniform in the two heats. The hot metal chemistry and other operational parameters could differ, but in most cases these were quite similar. The measured ejection weights and blowing practice of two very similar heats are given in Figure 51. It is evident that the rates of slopping and metal ejection were quite different. This behaviour is typical. This discrepancy indicated that ejection rates could not be pinpointed as being functions of certain variables, but rather, they were determined by a complex interplay of parameters that could not be readily observed. The BOF process is essentially metastable with

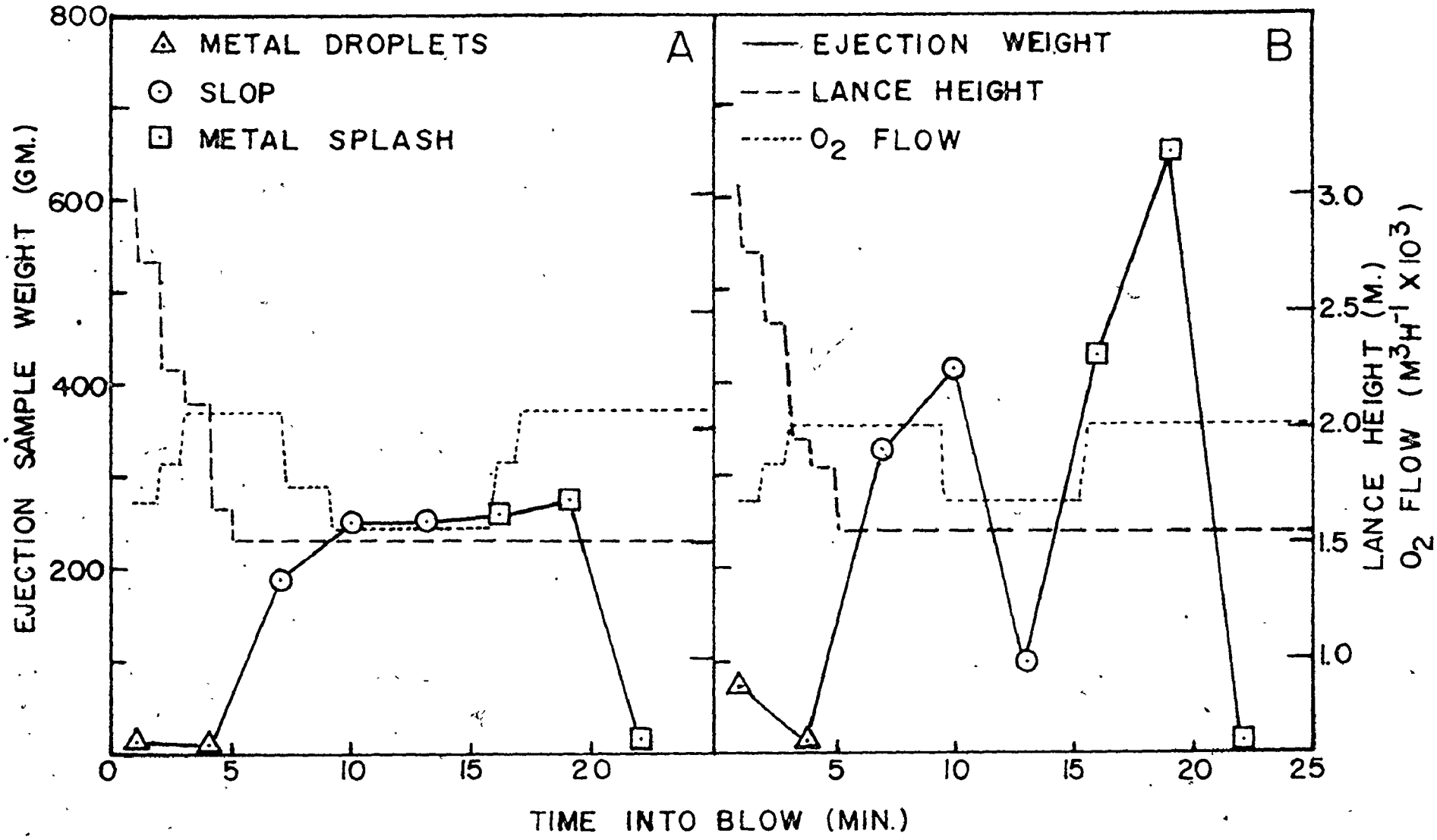

Fig. 51. Blowing practice and ejection weights for two consecutive heats with similar charge conditions. (A) Heat 6, (B) Heat 7.

small differences in chemistry or blowing performance leading to major variations in ejection rates and paths of refining. Though such deviations were seen to occur, it should be possible to characterize the ejection rates at any one time period on the basis of a Gaussian distribution if the parameters and errors involved were random. This is explored in subsequent sections.

4C. QUANTITATIVE PRESENTATION OF RESULTS

The different types of ejection material collected were examined both chemically and microscopically in an effort to classify the material more concretely than just by its physical appearance. These examinations and the resulting insights into BOF furnace behaviour are presented in the following sections. Each class of material previously described is treated separately.

4C1. SAMPLES AT ONE MINUTE MARK

There were two classes of material obtained at the one minute mark with certain similarities. Both types of sample contained metal droplets and red fumes but the one with slag was much higher in ejection rate. However all the metal droplets had relatively low concentrations of carbon. The droplet size distributions of these two classes were quite different, the slagless one having a mean of 31μ and the other a mean of 99μ. The quantity of fumes present varied as indicated by the different shades of colour. The fumes were not the prime object of this study and it has been already shown that the fumes were not being collected representatively. They were of small amount in most cases (less than 10% of total ejection weight).

(i) METAL EJECTIONS WITH SLAG

Of the 28 regular heats sampled, 16 (or 57%) had abundant fine ejections consisting of slag and metal droplets combined with varying quantities of red fume powder. These samples typically had a weight greater than 30 gm. The fine ejections are shown in Figure 52a. This is similar to that material on top of the powder in Figures 49a and 50a. A close examination of this material in a scanning electron microscope exposed them to be accretions of fine droplets (Figure 52b) and stringers (Figure 53). The surface layer was broken on a few droplets, exposing a bright inner sphere. These spheres were identified as being mainly iron through metallographic examination (Figure 53). The surface coating was therefore partly an iron oxide layer of 3μ to 15μ thickness that formed while the device was stationed in the furnace mouth or when the hot sampler was exposed to the air after

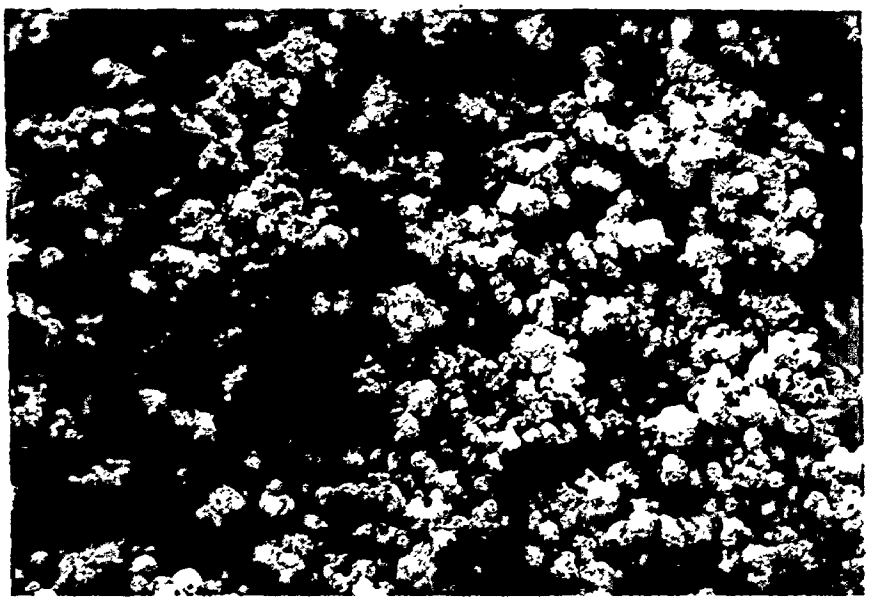

(A) X 20

(B) X 110

Fig. 52. Metal droplet ejections with slag from 1 minute mark of blowing period.

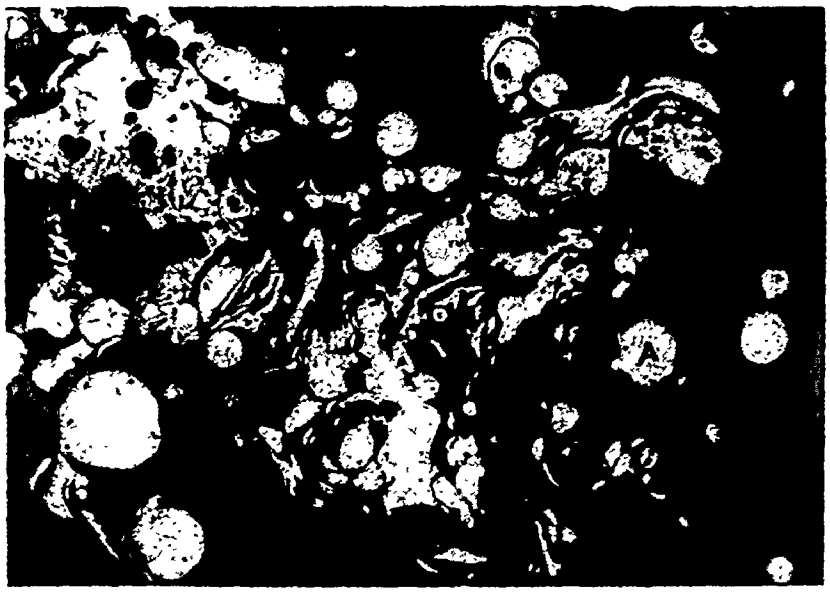

X200

Fig. 53. Metallographic examination of (A) metal droplet ejections with (B) slag from 1 minute mark.

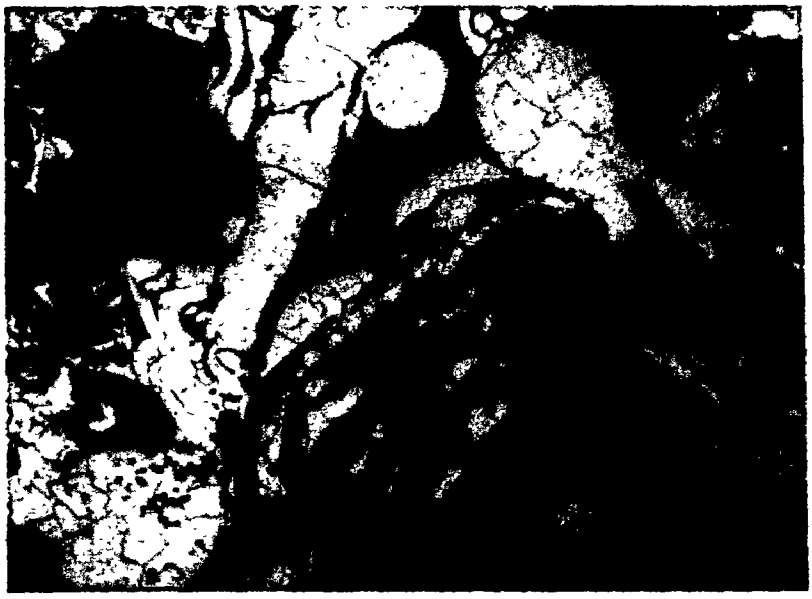

X 200

Fig. 54. Etched material from 1 minute mark showing ferrite structure with grain boundaries. (Etched in 2% nital solution).

withdrawal. This oxidation could not be avoided. Etching of mounted specimens with 2% nital solution revealed that the metal had very little carbon since the structure was either ferrite (Figure 54) or ferrite with small amounts of pearlite.

As is evident from the metallographic photos, there is some sort of slag matrix encompassing the metal droplets. This material was examined by making some X-ray maps of a polished surface using an electron probe analyzer. The elements considered were Ca, Fe, Si, Mg, Mn and Al which are the main components of steelmaking slag. These maps are presented along with an outline of the studied area in Figure 55. The Fe map indicated a rather even distribution throughout the whole matrix. This component is presumably present as both ferrous and ferric oxides. The Ca and Si levels were generally uniform except for localized regions of high concentrations. These areas indicated that the slag composition was not uniform. Though the metal droplets appear to contain some silicon, this would be highly unlikely because of the very low carbon levels in the metal. Silicon is preferentially oxidized so its concentration levels would be even lower. The silicon most probably arose from metal surface contamination during grinding of the very porous material. The Mn and Mg concentrations were essentially constant along the whole matrix. Some contamination of the metal surface by these components was also observed. The Al map showed isolated regions of high concentration in areas different from those of other peak levels. Certain aluminum based compounds could be present in these areas. Because of the fragmented nature of the slag matrix, the peak concentrations of the components cannot be attributed to segregation occurring on freezing. Rather, the slag matrix formed through rapid quenching of various bits of heterogeneous components along with the metal droplets. This slag matrix was almost continuous in

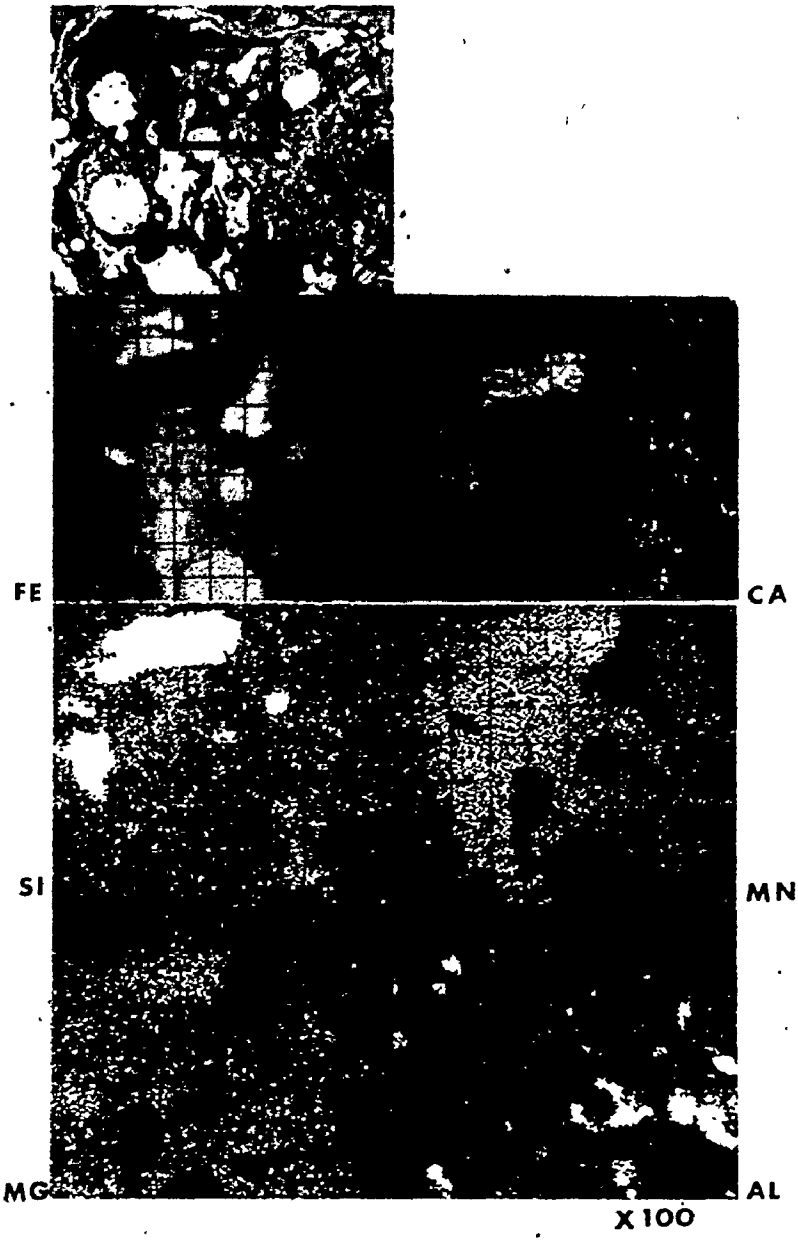

Fig. 55. Electron probe studies of metal droplet ejections with slag taken at 1 minute mark of blow.

the inner sections of the layered ejection material except for the void regions. On the exposed sampler surface (Figure 52), these slag components could only coat the metal droplets or fill any empty voids. This made it possible to do a size distribution of the metal droplets.

(ia) METAL DROPLET SIZE

Because of the fine size of the metal droplets, generally less than 200μ, any method of grinding used to separate the droplets would alter the size distribution of the sample because of unavoidable comminution. This problem was overcome by employing microscopy methods, combined with manual sizing using a Zeiss Particle Sizer instrument. Scanning electron microscope photos were taken of the ejection material at a magnification of 20. The metal droplets were then manually counted and sized using the Zeiss instrument. This machine could separate the particle sizes into 45 different ranges. It involved lining up each particle with a circular light beam, upon which a switch was depressed, and the particle size was recorded on a counter. About a thousand counts were made for each sample. The final number of particles in each size range was used in determining the number distribution. The mean size and weight distribution were further obtained from this number distribution by taking into account the proper geometric factors. The percentage standard error of the mean size in a number distribution is $100/\sqrt{n}$, where n is the number of particles sized[135]. In the case of a 1000 counts the error is quite acceptable at 3.2%.

A histogram of one number distribution and the corresponding weight distribution is given in Figure 56. The number distribution was typically skewed in the positive direction but the calculated weight distribution normally followed a Gaussian curve. Altogether five separate size counts

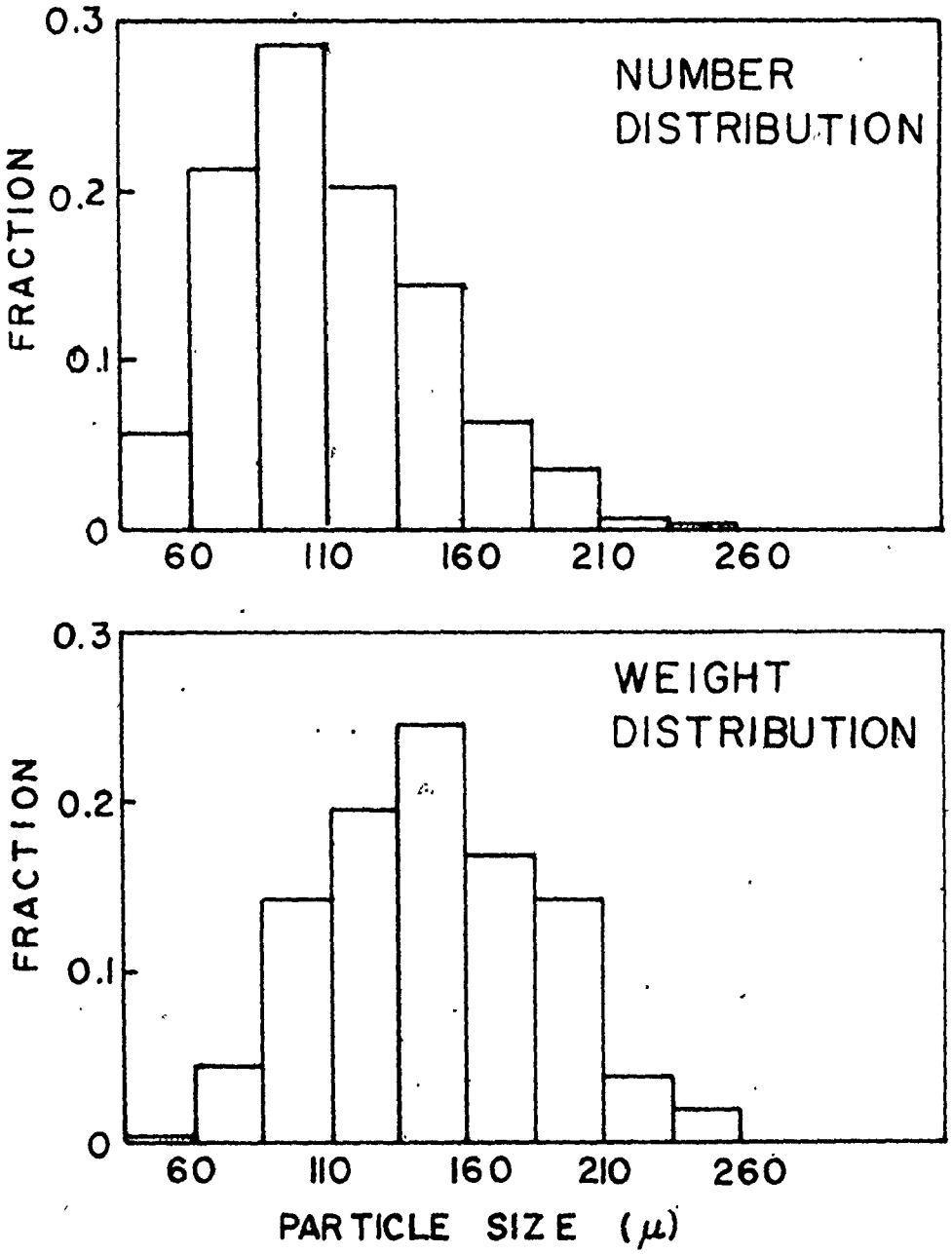

Fig. 56. Number and weight distributions of metal droplet ejections (with slag) from 1 minute mark of heat 17.

were performed on the ejection material obtained at the one minute mark from different heats. The results are presented in typical fashion in Figures 57 and 58 as cumulative percent passing vs. size plots. Both the number and weight distributions are presented. As can be seen, there was little variation with the different samples. Certain pairs of samples (14-19 and 17-18) of similar heats were almost identical in the number distribution for the lower size ranges. All the droplets were less than 300μ in diameter, with the mean size varying from 75 to 115μ for the five different distributions. The largest proportion of the droplets (between 60-80%) in each number distribution lay between 60 and 130μ. The weight distribution followed a different pattern because of the cubic scale up term used to calculate these values from the number distribution with an assumption of constant density. In determining all these size distributions, the surface layer of the metal was ignored and the particle size was taken to be that visually observed. Because of the thickness of this layer (less than 15μ) the expected error is small.

(ib) RATE OF EJECTION

The 16 heat samples had a mean weight of 83.6gm with a standard deviation of 54.0gm. These were combined with 15 other samples taken at the one minute mark during the previous stages of sampler testing. This distribution is presented in Table 20. The mean was 89.5 gm with a standard deviation of 59.9 gm. This distribution had an exterior interference at the high ranges. It was due to the excessively long ignition times in those three cases. A X^2 test, performed on the data in the first four ranges, (Table 20), indicated a greater than 40% level of significance. Thus these ejection weights were relatively predictable. These 16 heat samples were also

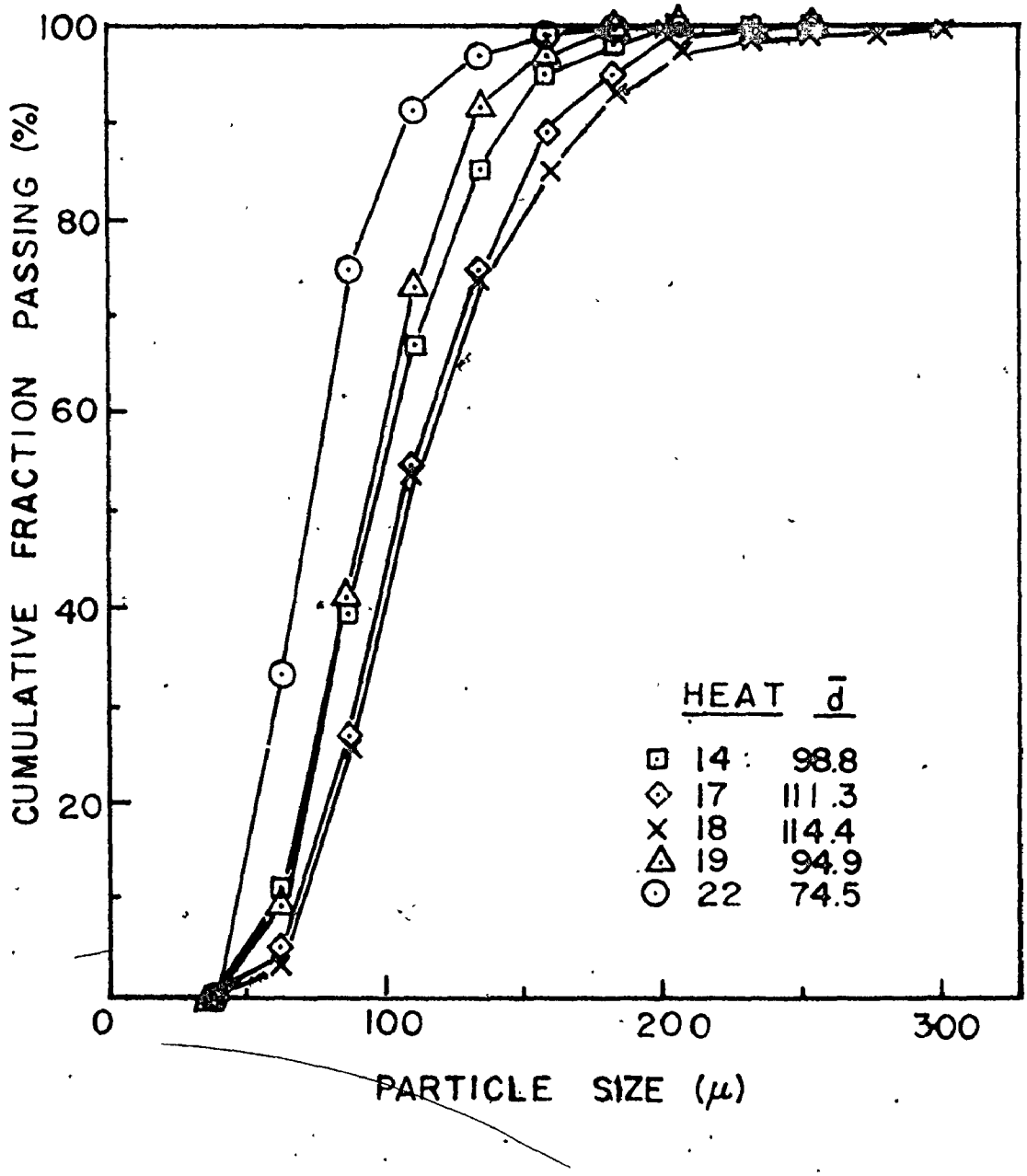

Fig. 57. Size distribution of metal droplet (with slag) ejections from 1 minute mark based on the number distribution.

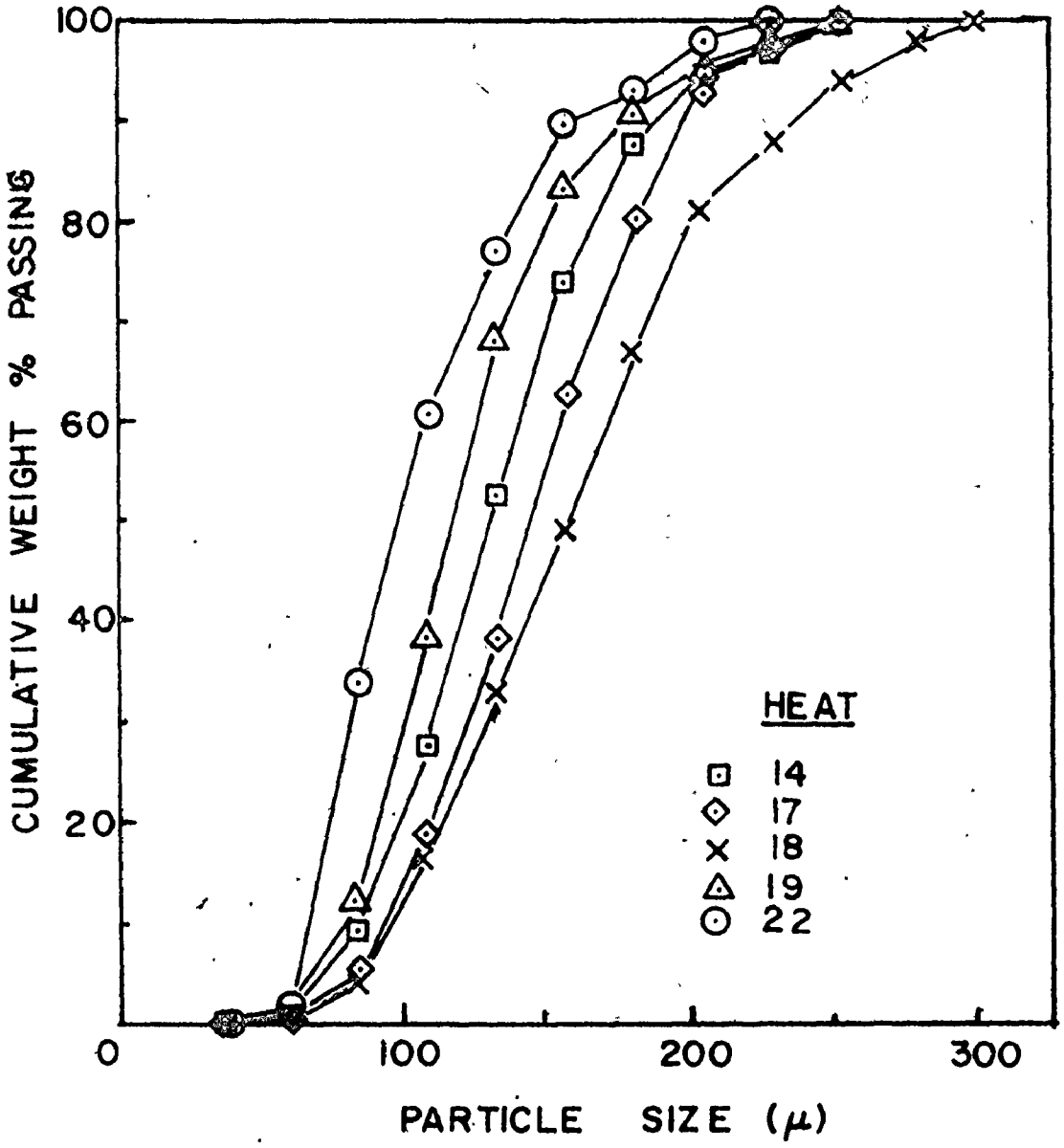

Fig. 58. Size distribution by weight of metal droplet (with slag) ejections from 1 minute mark.

TABLE 20

FINE EJECTION WEIGHT DISTRIBUTION
AT 1 MINUTE MARK

Weight Range (gm)	Number of Observations
0 - 50	7
50 - 100	15
100 - 150	5
150 - 200	1
200 - 250	3

$N = 31$

$\bar{x} = 89.483$

$s = 59.908$

X^2 TEST

Range	fi	u	P_c	Pi	NPi	X^2
0-50	7	-0.6310	0.2640	0.2640	7.392	0.021
50-100	15	0.6758	0.7504	0.4864	13.619	0.140
100-150	5	1.9827	0.9763	0.2259	6.325	0.278
150-200	1	3.2895	0.9995	0.0232	0.650	0.189
				0.9995	27.986	0.628

Degrees of freedom = 4 - 3 = 1

Level of significance $\geq$ 40%

analyzed for their metallic iron content using the standard method of slag analysis. The average metallic iron weight was 41.4 gm with a standard deviation of 25.7 gm. Therefore roughly half the ejection material was iron droplets. The remainder consisted of the slag metrix.

(ii) METAL EJECTIONS FREE OF SLAG

In the remaining 12 regular heats investigated, the one minute mark sample consisted of red powder with no visible ejection material. The colour intensities of this material varied from dull to bright red. The nature of this material was not readily apparent from direct visual observation. Examination under a stereoscope exposed the presence of fine droplets of material in conjunction with the fume. These droplets were found to be magnetic and were separated using a wet Davis Tube arrangement. A photo of this concentrated droplet material is given in Figure 59. As in the case of the previous ejection material, many of the droplets were attached to one another. Presumably this occurred because the droplets were molten prior to being quenched on the sampler's surface. All the droplets were essentially spherical, with no stringers, indicating instantaneous solidification on contact. These droplets also appeared to have a surface layer of some material as indicated by their faceted, porous appearance. Metallographic examination of these droplets indicated that they were predominantly composed of iron (Figure 60). The thin surface layers, less than 5μ, presumably consisted mainly of iron oxide. Some of the finer droplets were composed entirely of oxides. A nital etch of these specimens generally revealed a ferritic structure combined with varying amounts of pearlite (Figure 60). A low carbon level is thereby indicated. The levels of Mn and Si in the metal were not examined but they would be very low since these elements are more easily oxidized than carbon. The oxides of these elements could be present in the surface coating of the droplets.

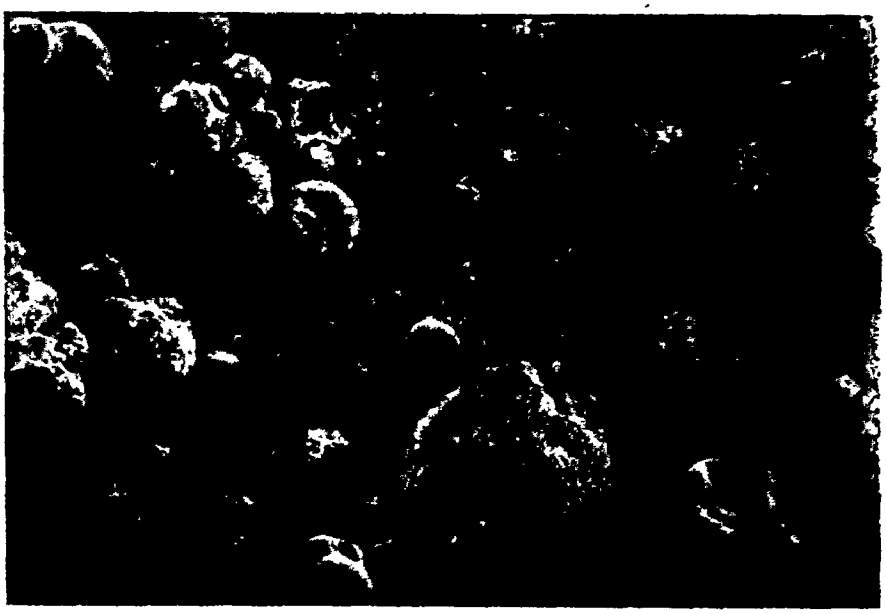

X200

Fig. 59. SEM photo of metal droplet (free of slag) ejections obtained with fume at 1 minute mark.

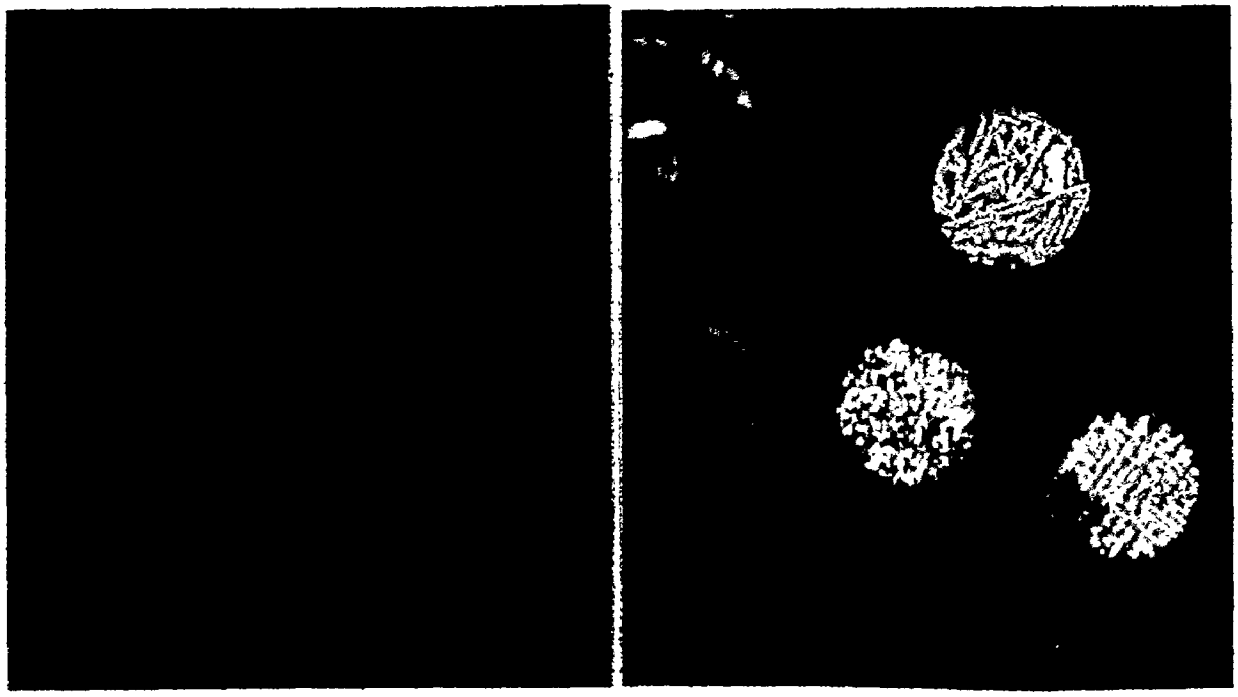

X1000

Fig. 60. Metallographic examination of metal droplets (free of slag) from 1 minute mark showing a ferrite with pearlite structure. (Etched in 2% nital solution).

(iia) METAL DROPLET SIZE

These iron droplets were photographed and counted using the Zeiss instrument in order to get the size distribution. Three samples were examined. The number and weight distributions are presented in Figures 61 and 62 in the form of cumulative percent passing versus particle size. The size distributions of these three samples were very similar. The largest fraction of droplets lay between 15 and 45μ. The largest observed particle diameter was 100μ. The mean particle sizes obtained from the number distributions were 29.7, 29.8 and 32.9μ. It was evident from this that this material was quite similar in all these heats. The expected standard error of the mean particle size was again based on a 1000 counts, giving a value of 3.2%.

(iib) RATE OF EJECTION

In the samples free of slag taken from 12 heats the actual sample weights could not be easily measured. As mentioned previously, the weight of the coating on the sampler was assumed to be one half the total paint weight. This could deviate from the real weight by about 20 gm. Since the ejection sample normally weighed less than 20 gm itself, the sample weights determined by subtracting the coating weight were not very accurate. The fume present in the powder was a contaminant that could not supply any information for our purpose. For these reasons, the samples together with the paint were chemically analyzed for metallic iron. The total quantity of fine metallic droplets ejected could thus be accurately determined. For the 12 cases, the mean weight of metallics was 4.0 gm with a standard deviation of 2.6 gm. These values are roughly one tenth those recorded for the other class of material obtained at the one minute mark.

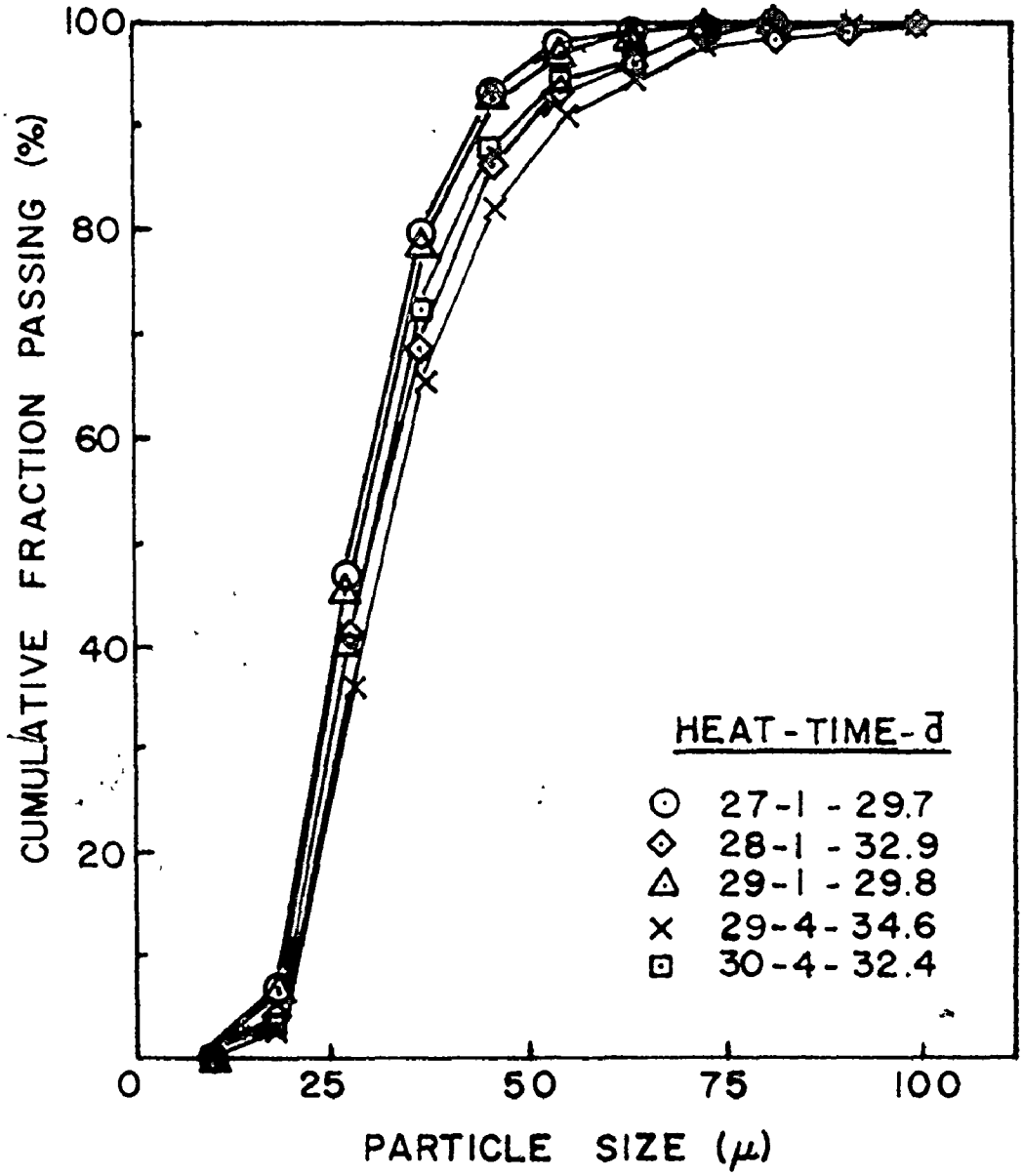

Fig. 61. Size distribution of metal droplet (free of slag) ejections from 1 and 4 minute marks based on the number distribution.

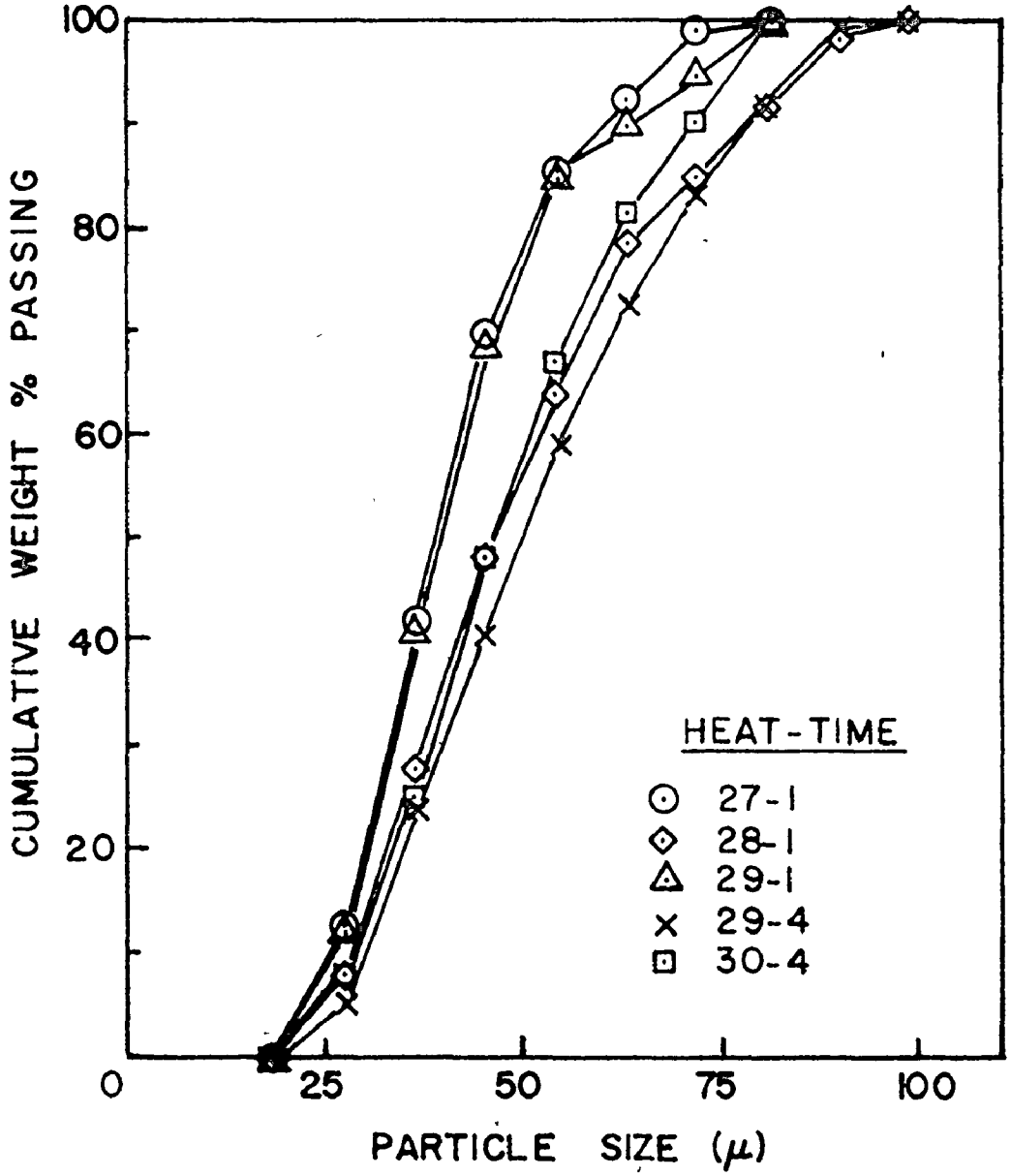

Fig. 62. Size distribution by weight of metal droplet (free of slag) ejections from 1 and 4 minute marks.

(iii) STEELMAKING PRACTICE AND DIFFERENCES IN EJECTION AT ONE MINUTE

In an attempt to determine what parameter differences cause these two classes of material to exist at the one minute mark, all the measurable BOF process variables were examined. These included hot metal chemistry and temperature, blowing rates, furnace bottom buildup, lance heights, flux addition times and scrap charge. There was no noticeable correlation between the patterns of ejection and any of the above mentioned variables. Thus the differences might have arisen from certain variations which cannot be characterized in the present work such as blast furnace slag carry-over, scrap positioning, bath chilling, slag development, etc.

4C2. SAMPLES AT 4 MINUTE MARK

In all but a few cases, the material collected at the 4 minute point in the blow consisted almost entirely of red powder and metal droplets. Various shades of material were found because of the differing quantities of fume present. Stereoscopic examination of this material at higher magnification again indicated the presence of fine droplets together with the fume. These droplets were isolated using a Davis Tube magnetic separator. Metallographic examination revealed that the droplets were iron with thin surface oxide films. The finer droplets were sometimes completely oxidized. Etching of these specimens again indicated a low carbon content because of the presence of ferrite and small quantities of pearlite.

Two samples of magnetically separated droplets were examined, using the previously described techniques, to obtain their size distribution. The results of these counts are given in Figures 61 and 62 in combination with the size distributions of the similar droplet material from the one minute mark. The size distributions of the different samples were quite similar. The mean particle sizes calculated from the number distributions were 32.4 and 34.6μ. This was very close to the mean size of the droplet material found at the one minute mark when the ejected material was free of slag. Because of the physical and chemical similarities of these two classes of droplets, the same mechanism of formation could be thought to exist in these two moments of sampling.

The fume present with the fine metallic droplets again did not merit sufficient cause for study because of its presence on the sampler as a contaminant only. To determine the quantities of metallic iron present in the ejection samples accurately the material was chemically analyzed as in

the previous case. Altogether, 23 such samples were examined. The mean weight of metallic iron present in these powder samples was 6.8 gm with a standard deviation of 5.4 gm. The distribution showed no signs of normality as the level of significance was less than 1%. The operating practice at the 4 minute mark was quite similar in all these heats, so there was no obvious explanation for this lack of normality.

In the other 5 heats of the 28 sampled, the material collected at the 4 minute mark consisted of heavy accumulations of slag and metallics. The weights of these samples varied from 50 to 300 gm. Chemical analysis of these materials showed that they consisted of roughly 50% metallic iron, the remainder being slag. The cause for these heavy ejections was found to be a surge in the oxygen flow. Normally the oxygen flow rate was increased gradually over a 3 minute period from an initial 17000 m^3h^{-1} to an operating level of 21000 m^3h^{-1}. However, in 4 of these 5 special cases, the flow rate was increased in one quick step (less than 15 seconds) at the 3 minute mark. In the one other case, the main difference was that the lime addition was started late, around the 5 minute mark. The slag in this heat was therefore much lower in CaO content in the first two time periods of ejection sampling (1 and 4 minutes). Both samples taken in this heat consisted of fine ejections of slag and metallics.

4C3. SAMPLES AT 7 MINUTE MARK

At this time there were again two classes of material collected, i.e. metal ejection without slag and slop ejection.

(i) METAL EJECTION

In 9 of the 28 heats, samples of red powder and metal droplets were obtained. These metallic iron droplets were similar to the droplets free of slag previously described. The droplets appeared to have a similar size distribution so this was not determined. The droplets again contained little carbon as indicated by their metallographic structure. The 9 samples were analyzed chemically for their metallic iron content in order to get an accurate sample weight since the previously described problems of paint coating weight and fume contamination were again present. The mean weight of metallic iron was 5.3 gm with a standard deviation of 2.6 gm.

(ii) SLOP EJECTIONS

In the other 19 cases, the materials collected were slop together with trace quantities of fume. The weight of slop varied from 40 to 550 gm. The mean sample weight was 225.0 gm with a standard deviation of 145.3 gm. In all the previous cases during sampler-testing, there were 49 additional slop samples taken at the 7 minute mark. Combination of the two groups of data was justified because the additional group (with a mean value of 246.9 gm. and a standard deviation of 161.7 gm) was statistically similar to the original data as indicated by a t-test. The enlarged group with 68 samples had a mean slop weight of 240.8 gm and a standard deviation of 155.4 gm. The data distribution is presented in Table 21. There appeared to be a large negative skewness in this distribution, but this was found to be caused by a

TABLE 21

SLOP WEIGHT DISTRIBUTION
AT 7 MINUTE MARK

Weight Range (gm)	Number of Observations
0 - 100	19
100 - 200	10
200 - 300	16
300 - 400	13
400 - 500	5
500 - 600	5

$N = 68$

$\bar{x} = 240.8$

$s = 155.4$

TABLE 22

SLOP WEIGHT DISTRIBUTION
AT 7 MINUTE MARK FOR
SAMPLE WEIGHTS LESS THAN 100 gm

Weight Range (gm)	Number of Observations
20 - 40	3
40 - 60	4
60 - 80	8
80 - 100	4

$N = 19$

$\bar{x} = 63.2$

$s = 19.1$

bimodal behaviour. The 19 data points in the first weight range (0-100 gm) could themselves be broken down to form another Gaussian type distribution as seen in Table 22. The measured slop weights, and not those obtained using the normalizing equation developed in the experimental section (Equ. 3.1), were used in formulating these data distributions. Though the normalized values would give a better approximation of the true slopping rates, they would not fit a Gaussian distribution because the equation automatically skews the data to the positive range. By examining the slopping rates in their raw state, the degree to which the sample data represented the total population could be measured.

The data in Table 21, minus the first grouping, and in Table 22 were tested by the X^2 method using appropriate mean and standard deviation values. This is presented in Tables 23 and 24. The first mode (mean = 63.2 gm, standard deviation = 19.1) had a low level of significance ($\geq$20%) while the second mode (mean = 309.7 gm, standard deviation = 129.5) was just slightly better with a $\geq$30% level of significance. There was only some degree of predictability then in the slop weight at the 7 minute mark.

In predicting an average slop weight at the 7 minute mark, the normalized values could be used since they eliminate certain previously described errors. For the first mode, the average slopping rate was not changed substantially from the measured mean since the low slopping rates could not effectively reduce the sampler's entry area. The new normalized mean for the first mode was 69.1 gm with a standard deviation of 22.4 gm. For the second mode of data (> 100 gm measured slop weight), the average slop weight changed drastically to 628.8 gm with a corresponding standard deviation of 506.4 gm. The data in this range was more clearly affected by the normalizing equation.

TABLE 23

X^2 TEST ON DISTRIBUTION OF SLOP WEIGHT AT 7 MINUTE MARK (FIRST MODE)

Range	fi	u	P_c	Pi	NPi	X^2
20-40	3	-1.2179	0.1116	0.1116	2.120	0.365
40-60	4	-0.1685	0.4331	0.3215	6.109	0.728
60-80	8	0.8810	0.8109	0.3778	7.178	0.094
80-100	4	1.9306	0.9732	0.1623	3.084	0.272
				0.9732	18.491	1.459

N = 19

$\bar{x}$ = 63.21

σ = 19.057

Degree of freedom = 4 - 3 = 1

Level of Significance $\geq$ 20%

TABLE 24

X^2 TEST ON DISTRIBUTION OF SLOP WEIGHT AT 7 MINUTE MARK (SECOND MODE)

Range	fi	u	P_c	Pi	NPi	X^2
100-225	13	-0.6539	0.2566	0.2566	12.573	0.014
225-350	18	0.3117	0.6223	0.3657	17.919	0.000
350-475]	12	1.2773	0.8992	0.2769	13.568	0.181
475-600	6	2.2429	0.9876	0.0884	4.332	0.643
				0.9876	48.392	0.838

N = 49

$\bar{x}$ = 309.65

s = 129.450

Degrees of freedom = 4 - 3 = 1

Level of Significance $\geq$ 30%

The distinction of these two modes was seen to be statistically acceptable because of the ability to represent the data by two Gaussian curves. This indicated that there must have been some sort of distinguishing marks that could characterize the data into these two groupings. All the known operating variables were examined. No identifiable cause for such differences between the two classes could be established. The differences would therefore have to be some parameters inherent to the operation but not readily observable under the conditions of the present work.

Actually three different classes were present if the samples with only red powder and droplets are considered. These red powder containing samples accounted for 9 of the 28 cases (32%); the light slop of the first mode represented another 19%, with the heavy slop of the second mode accounting for the remaining 49%. There were no observable differentiating points in BOF operations which resulted in three different patterns in materials ejection.

(iia) SLOP COMPOSITION

Of the slop samples taken during 19 heats, only 2 proved unsuitable for chemical analysis because of their small sample weights. The slop material was separated from the granular paint coating by using a fine wire mesh screen. This slop was then prepared for analysis by the method described in Figure 47 with one basic difference. The flat pieces of metal were not discarded since they composed part of the sample. They were not extraneous material as in the case of slag samples where only metal droplets were acceptable. The flat metal pieces were combined with the +35 mesh fraction. The already verified assumption that this material was iron was again made. The method

of chemical analysis was identical to that described for slag samples. Free lime extraction was carried out, followed by analysis for CaO, SiO_2 and iron in different oxidation states. The +35 mesh fraction was combined with the metallic iron analysis to give the total elemental content. The mean values, standard deviations and ranges of all these components are given in Table 25. By eliminating the metallic iron fraction, it was possible to get the composition of the slag matrix in the slop material. These values are also given in Table 25. The major component of the slop was metallic iron. The ferrous and ferric levels in the slag matrix were relatively low. The slop material was quite acidic as evidenced by the low V-ratio. This further indicated that only a fraction of the lime added to the BOF had dissolved up to this point. The metallic iron content of the light slop material from the first mode was greater than that of the other slop samples. It averaged 43.1% whereas the heavier slop range had a mean metallic iron content of 28.9%. Differences were also noted in the ferric iron content of the two classes of slop. The light slop had a mean content of 3.9% whereas the heavier slop's average was 2.1%. The concentration levels of the other slag components were relatively similar for the two classes of slop.

By multiplying the individual, normalized slop weights by their respective total iron contents, it was possible to obtain a measure of the rates of iron loss at the 7 minute mark. For the slop data of the first mode, the average iron loss was 30.2 gm with a standard deviation of 21.7 gm. For the second slop mode, the mean iron loss was 162.0 gm with a standard deviation of 107.7 gm. For the case of droplets with fume, the mean weight of metallic iron was 5.3 gm with a standard deviation of 2.6 gm.

TABLE 25

SLOP ANALYSIS AT 7 MINUTE MARK
(N = 17)

COMPONENT	TOTAL SLOP ANALYSIS				SLAG FRACTION ANALYSIS[2]			
	Mean	Standard Deviation	Range Low	Range High	Mean	Standard Deviation	Range Low	Range High
CaO	23.3	4.0	16.7	29.3	33.9	2.6	29.8	39.9
SiO_2	18.3	4.1	10.3	23.4	26.2	3.1	20.4	29.9
Total Fe	35.6	10.8	23.3	59.4	-	-	-	-
Metallic Fe	31.4	10.3	20.0	53.6	-	-	-	-
Fe^{2+}	1.8	0.8	0.6	3.6	2.7	1.1	0.7	5.1
Fe^{3+}	2.4	1.3	0.1	4.5	3.8	2.5	0.1	9.6
V-ratio[1]	1.30	0.18	1.12	1.77	1.30	0.18	1.12	1.77

[1] $\text{V-ratio} = \frac{\text{Wt. \% CaO}}{\text{Wt. \% } SiO_2}$

[2] Obtained by discounting the metallic iron fraction.

4C4. SAMPLES AT 10 MINUTE MARK

In all the 28 regular heats sampled, the ejected materials collected at the 10 minute mark consisted entirely of slop. The sample weights varied from 40 to 500 gm. Two other samples taken at the 10 minute mark during the sample-testing period were combined with this data to form one distribution. The mean slop weight was 258.3 gm with a standard deviation of 116.2 gm. The X^2 test on this weight distribution is presented in Table 26. The level of significance at ≥50% is quite acceptable. Upon using the normalizing equation to obtain a better measure of the slop rate, the mean value changed to 447.7 gm with a standard deviation of 335.7 gm.

A Gaussian data distribution was found because of the random heat sampling method. The cases of large slopping rates were observed to differ from the others in one operating practice. Those heats with larger slop samples had a corresponding large bottom buildup in the furnace. This was to be expected since the buildup caused a reduction in available furnace volume. This has previously been shown to increase the frequency of slopping. This subject will be discussed later in greater detail (Section 4D).

Only two of the 28 slop samples had insufficient material for chemical analysis. The others were prepared by the method described in the previous section and were chemically analyzed for the same components. The results are presented in similar fashion in Table 27. The major slop component was again iron, principally of the metallic form. The ferrous and ferric contents were still low. The CaO content increased slightly from the previous concentration in the slop at 7 minutes, thereby causing the average V-ratio to increase to 1.48. The SiO_2 level was approximately the

TABLE 26

X^2 TEST ON DISTRIBUTION OF SLOP WEIGHT AT 10 MINUTE MARK

Range	fi	u	Pc	Pi	NPi	X^2
25-125	2	-1.1477	0.1256	0.1256	3.768	0.830
125-225	9	-0.2869	0.3871	0.2615	7.845	0.170
225-325	11	0.5738	0.7170	0.3299	9.897	0.123
325-425	6	1.4346	0.9243	0.2073	6.219	0.008
425-525	2	2.2954	0.9892	0.0649	1.947	0.001
				0.9892	29.676	1.132

N = 30

$\bar{x}$ = 258.33

s = 116.18

Degrees of freedom = 5 - 3 = 2

Level of Significance $\geq$ 50%

TABLE 27

SLOP ANALYSIS AT 10 MINUTE MARK

(N = 26)

COMPONENT	TOTAL SLOP ANALYSIS				SLAG FRACTION ANALYSIS			
	Mean	Standard Deviation	Range Low	Range High	Mean	Standard Deviation	Range Low	Range High
CaO	26.7	6.3	18.2	35.1	36.5	4.9	29.3	46.2
SiO_2	18.1	2.8	10.5	24.4	25.5	3.0	17.9	33.0
Total Fe	33.3	7.0	19.7	48.1	-	-	-	-
Metallic Fe	28.6	7.1	16.0	44.2	-	-	-	-
Fe^{2+}	2.3	1.0	0.6	4.8	3.2	1.4	0.7	6.3
Fe^{3+}	2.4	1.5	0.3	5.3	3.5	2.3	0.4	8.8
V-ratio	1.48	0.23	1.07	2.14	1.48	0.23	1.07	2.14

TABLE 28

X^2 TESTS ON SLOP COMPOSITION AT 10 MINUTE MARK

Component	Degrees of Freedom	X^2 Value	Level of Significance
CaO	2	0.750	≥70%
SiO_2	1	0.214	≥60%
Metallic Fe	1	0.240	≥60%
Fe^{2+}	2	1.263	≥50%
Fe^{3+}	2	0.736	≥60%

same as that at the 7 minute mark. A comparison of the two different slop samples has been presented using the average values. This marked the general behaviour in the heats sampled. A more detailed study of individual heats is presented later along with the slag analysis (Section 4G).

With these materials there was sufficient data to carry out a X^2 test on the representativeness of slop composition. This statistical test was conducted for the CaO, SiO_2, metallic iron, Fe^{2+} and Fe^{3+} fractions. The results are given in Table 28. All the components had a greater than 50% level of significance, attesting that the sample data represents the total population quite well.

The normalized slop weights were used in conjunction with the total iron content values to measure the rate of iron loss in the slop. The average iron loss was 135.1 gm with a standard deviation of 91.5 gm.

4C5. SAMPLES AT 13 MINUTE MARK

Two different classes of material were collected at this time period. In the samples of 28 heats, 20 yielded slop, 7 yielded metallics and one was lost.

(i) SLOP EJECTIONS

The slop weights varied from 40 to 270 gm. A mean value of 159.3 gm with a standard deviation of 69.0 gm was obtained with 25 measured points. The additional 5 came from early work during sampler-testing. A X^2 test on this data (Table 29) gave a reasonable level of significance of ≥40%. This data showed little evidence of the effect of bottom buildup on slop weights. This presumably was due to the small scatter of the data in comparison to the wide range observed at the 10 minute mark. Upon normalizing the ejection rates using equation 3.1, the mean slop weight increased to 210.4 gm with a standard deviation of 111.5 gm. These slop weights were considerably smaller than those measured at the 7 and 10 minute mark. At both 10 and 13 minutes, the oxygen blowing rate was normally 4000 m^3h^{-1} lower than that at 7 minutes as a corrective measure to reduce slopping.

Only one of the 20 slop samples proved unsuitable for chemical analysis. The results are given in Table 30. The iron component accounted for a large fraction of the slop composition. The metallic iron content was larger than that of slop taken at the 7 and 10 minute periods. The ferrous content was similar to other slop samples but the ferric content roughly doubled. The CaO and SiO_2 content of the slop dropped, but the V-ratio nevertheless increased. X^2 tests were carried out on the data distributions

TABLE 29

X^2 TEST ON DISTRIBUTION OF
SLOP WEIGHT AT 13 MINUTE MARK

Range	fi	u	Pc	Pi	NPi	X^2
0-75	3	-1.2218	0.1109	0.1109	2.773	0.019
75-150	8	-0.1350	0.4463	0.3354	8.385	0.018
150-225	9	0.9517	0.8293	0.3830	9.575	0.035
225-300	5	2.0384	0.9792	0.1499	3.748	0.419
				0.9792	28.481	0.491

N = 25

$\bar{x}$ = 159.32

s = 69.01

Degrees of freedom = 4 - 3 = 1

Level of Significance $\geq$ 40%

TABLE 30

SLOP ANALYSIS AT 13 MINUTE MARK
(N=19)

COMPONENT	TOTAL SLAG ANALYSIS				SLAG FRACTION ANALYSIS			
	Mean	Standard Deviation	Range Low	Range High	Mean	Standard Deviation	Range Low	Range High
CaO	21.9	3.4	15.8	27.5	34.9	2.4	31.1	39.1
SiO_2	14.0	4.0	9.4	22.5	22.7	4.8	15.5	29.2
Total Fe	42.7	8.9	23.6	58.1	-	-	-	-
Metallic Fe	36.7	8.6	17.9	52.2	-	-	-	-
Fe^{2+}	2.0	0.6	1.2	3.6	3.1	0.9	1.6	4.7
Fe^{3+}	4.0	2.3	1.6	7.9	6.3	3.6	2.3	14.3
V-ratio	1.64	0.38	1.22	2.41	1.64	0.38	1.22	2.41

TABLE 31

X^2 TESTS ON SLOP COMPOSITION AT 13 MINUTE MARK

Component	Degrees of Freedom	X^2 Value	Level of Significance
CaO	1	1.258	≈20%
SiO_2	1	0.418	≈50%
Metallic Fe	1	0.563	≈40%
Fe^{2+}	1	1.157	≈20%
Fe^{3+}	1	0.640	≈40%

for the various slop components. The results are presented in Table 31. SiO_2, metallic Fe and Fe^{3+} all had acceptable levels of significance. The CaO and Fe^{2+} distributions, with a level of significance of $\geq$20%, were not that representative of the total population. This discrepancy could not be explained.

The normalized slop weights were employed as previously described in measuring the rates of iron loss in the slop. The average iron loss was 89.6 gm with a standard deviation of 61.6 gm.

(ii) METAL EJECTIONS

The seven heats which yielded metal ejection samples at the 13 minute point in the blow had no evident differences in operational parameters. The phenomenon causing this behaviour must have arisen due to some differences in unobserved parameters. The 7 metal ejection samples varied in weight from 70 to 500 gm. The mean weight was 237.3 gm with a standard deviation of 155.4 gm. These samples varied from accumulations of fine droplets for the small weights (Figure 63) to combinations of fine droplets and larger splash material for the heavier samples (Figure 64). In those samples composed entirely of fine droplets, the particle size was typically less than 300μ. Some size distributions of this class of metal ejection are presented later (Sections 4C6 and 4C7). For samples with mixtures of droplets and splash, the maximum particle size was around one cm. This could only be estimated since the large droplets, which gave rise to the splash appearance, spread on contact with the sampler. The stated diameter was estimated from the width of the splash sections. The size distribution of this mixture of droplets could not be obtained because of the welding together of the material. The surface was also too uneven to employ a counting method.

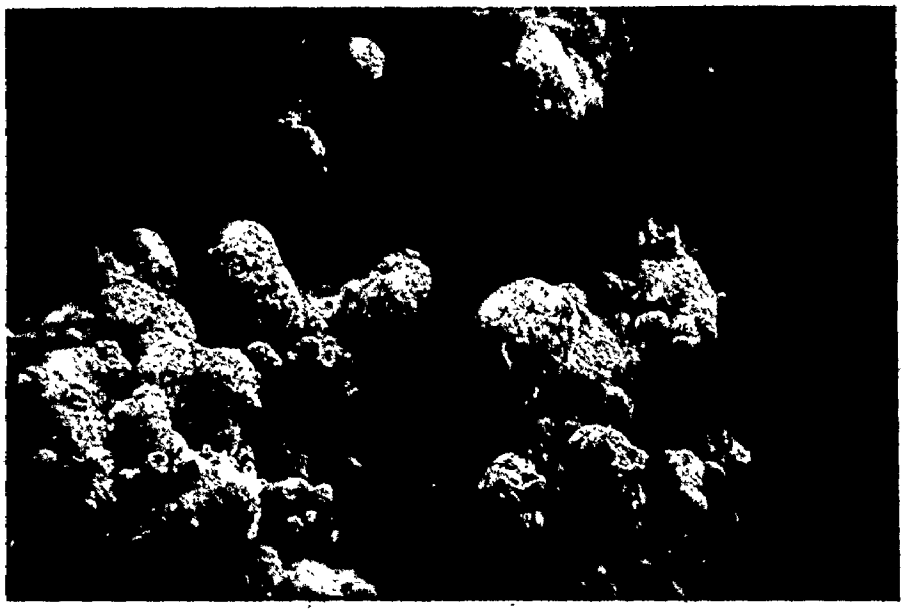

X80

Fig. 63. Metal ejection material from 13 minute mark containing only fine droplets.

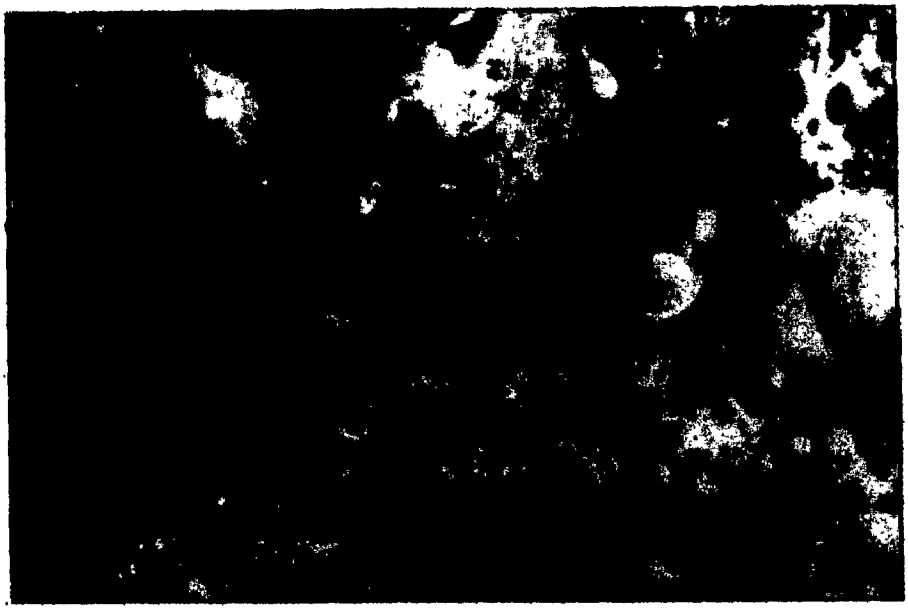

X20

Fig. 64. Metal ejection material from 13 minute mark consisting of splash and fine droplets.

Metallographic examination of the metal ejection samples indicated that they were almost entirely composed of iron. Chemical analyses for total iron content were performed on 5 metal ejection samples taken at random from the 13 to 19 minute mark of the blow. The results are given in Table 32. All these samples had iron contents greater than 95%. No further analyses were performed on metal ejection samples. The reasonable assumption that they were composed entirely of iron was made. Metal ejection samples were clearly distinguishable by their physical appearance and their high density in comparison to the other classes of material.

Etching of mounted specimens with 2% nital solution revealed the presence of carbon. The carbon content varied throughout the sample, ranging from mixtures of pearlite, cementite and ferrite in the various splash portions to mixtures of pearlite and ferrite in the smaller droplets (Figures 65a and b). Because of the mixed nature of this material, the carbon content was not further analyzed. The observations indicated that the splash and fine droplets were both generated from the metal bath in the BOF. The finer material however had some of its carbon removed by some mechanism before it was collected on the sampler. The larger droplets that gave rise to the splash had a carbon content more comparable to that of the bath.

The exposed surface of the metal ejection samples gave clear indication of the presence of an oxide film over the droplets. Fractured areas showed that the film thickness varied from 3 to 15μ (Figure 66). The thicker layer was observed on the larger droplets and splash portions. The inner layers of the ejection samples contained no observable surface oxide. Thus the film must have been iron oxide that had formed upon oxidation of the hot material after the sampler had been withdrawn from the furnace.

TABLE 32

TOTAL IRON CONTENT OF
METAL EJECTION SAMPLES

Heat	Time into Blow (min)	% Total Iron[1]
5	19	95.8
8	13	100.0
11	16	97.7
23	19	97.1
24	16	96.1

[1] determined by wet chemical analysis using method described for slag

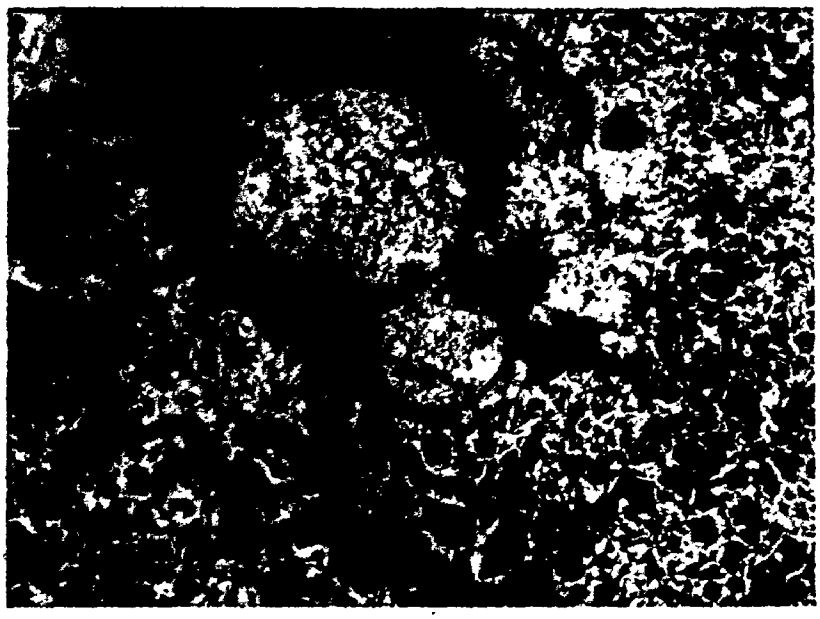

(A) X200

(B) X200

Fig. 65. Metallographic examination of etched metal ejection specimens from the 13 minute mark. (A) Splash and droplets - ferrite and pearlite (B) Droplets - ferrite. (Etched in 2% nital solution).

(A) X 500

(B) X 200

Fig. 66. Oxide films on metal ejections for (A) droplet and, (B) splash material.

4C6. SAMPLES AT 16 MINUTE MARK

Of the 28 regular heats sampled, 26 yielded metal ejection samples and 2 produced slop samples. The metal ejection weights varied from 30 to 1500 gm. The mean weight of metallics was 361.4 gm with an extremely high standard deviation of 384.2 gm. This discrepancy was evident in the data distribution presented in Table 33. The six points above 500 gm caused the high standard deviation. The data below 500 gm could be fitted to a Gaussian distribution. A bimodal behaviour similar to that present at the 7 minute mark might have been found had more observation points been available. The distribution of the data below 500 gm was tested for its representativeness by the X^2 method (Table 33). A low level of significance of $\geq$20% was found. The larger weights (500 gm) were encountered only in those heats where the bottom buildup exceeded one meter. This could be taken as the delineating mark between the two behaviour modes. The 20 points in the first range had a mean of 184.7 gm with a standard deviation of 121.0 gm. The 6 remaining points had a mean of 950.5 gm and a standard deviation of 375.8 gm. For these metal ejection samples, there was some apparent correlation between sample weight and extent of bottom buildup. This is examined later in conjunction with similar observations made on slop samples (Section 4D).

These metallics could again be classified into two different types. For the lighter samples only fine droplets were present. Heavier samples bore more splash material in conjunction with the fine droplets. Finally, for the extremely heavy ones, only splash was observed. Two size distributions of the finer material are presented in Figures 67 and 68. These were obtained by taking stereoscope photos and then size counting using the Zeiss instrument.

TABLE 33

METAL EJECTION WEIGHT
DISTRIBUTION AT 16 MINUTE MARK

Weight Range (gm)	Number of Observations
0 - 125	7
125 - 250	7
250 - 375	4
375 - 500	2
500 - 1000	3
1000 - 1500	2
1500 - 2000	1

$N = 26$

$\bar{x} = 361.4$

$s = 384.2$

X^2 TEST

Range	fi	u	Pc	Pi	NPi	X^2
0-125	7	-0.4934	0.3109	0.3109	6.218	0.098
125-250	7	0.5397	0.7053	0.3944	7.888	0.100
250-375	4	1.5727	0.9421	0.2368	4.736	0.114
375-500	2	2.6058	0.9954	0.0533	1.066	0.814
				0.9954	19.908	1.126

Degrees of freedom = 4 - 3 = 1

Level of Significance $\geq$ 20%

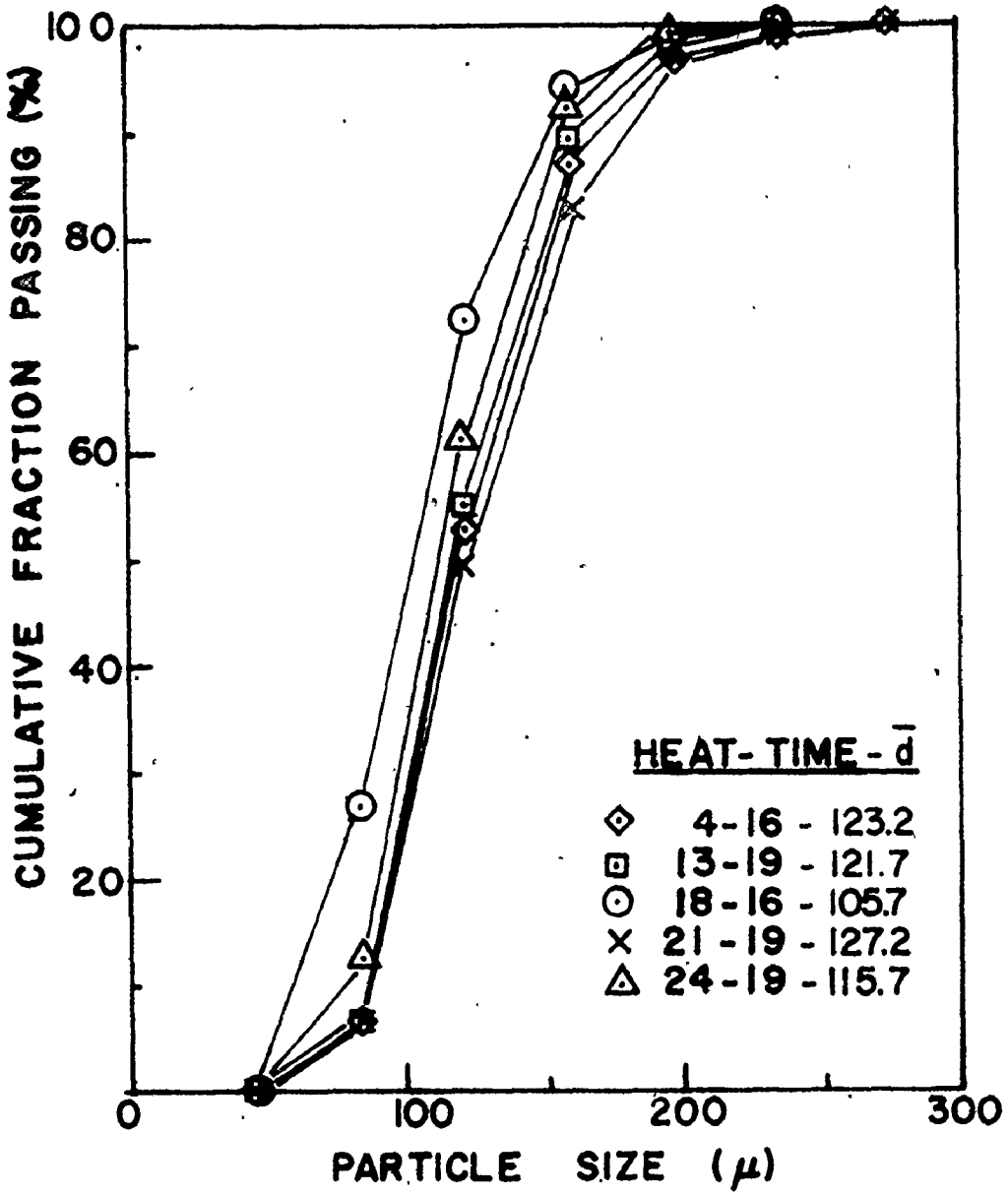

Fig. 67. Size distribution of metal droplet ejections from 16 and 19 minute marks based on the number distribution.

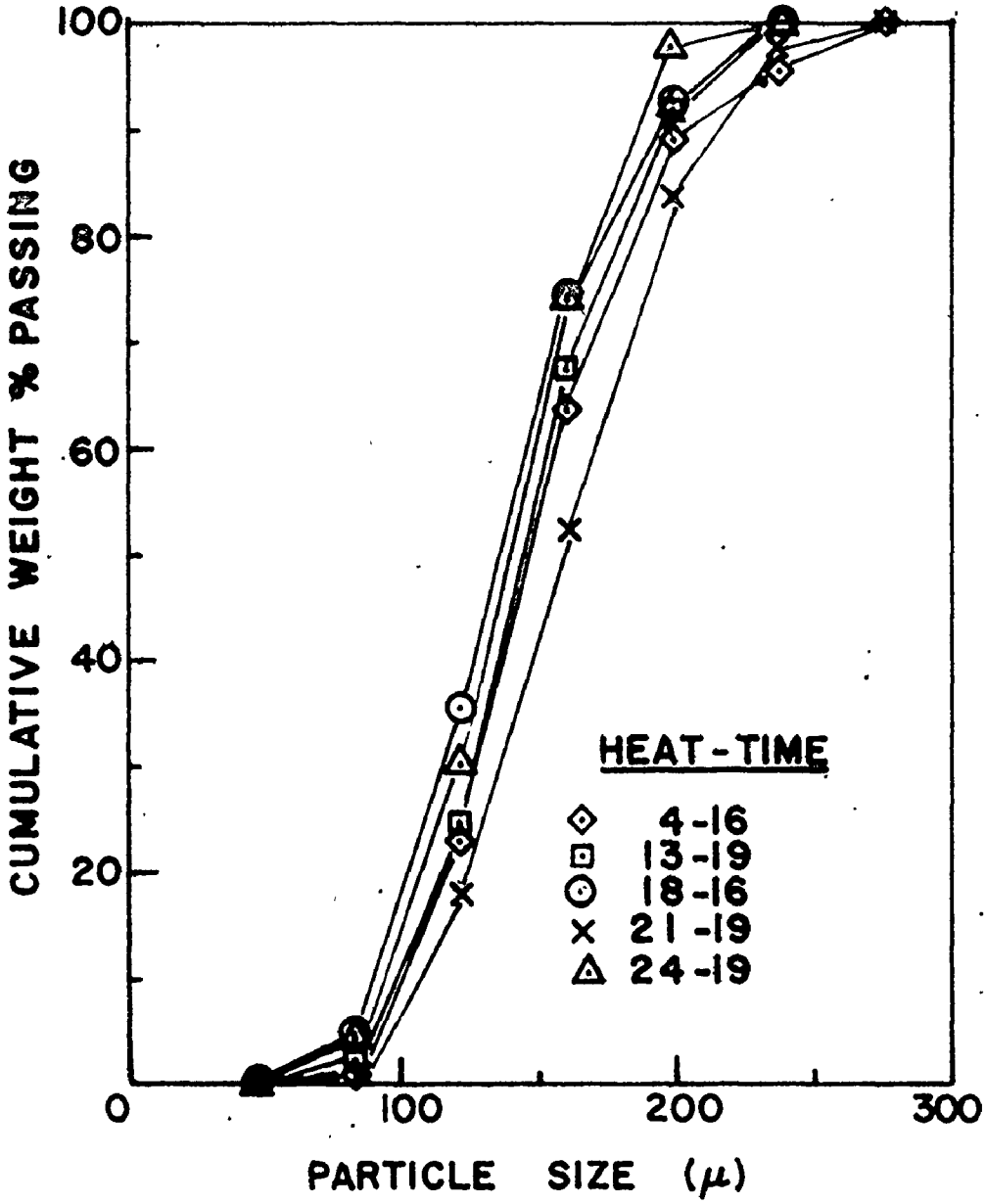

Fig. 68. Size distribution by weight of metal droplet ejections from 16 and 19 minute marks.

The maximum droplet size was 300μ, and the two average sizes based on the number distributions were 123μ and 106μ. The oxide film thickness was ignored in these calculations and a constant density was assumed in determining the weight distribution. The splash material again consisted of leveled droplets of less than 1 cm width. Surface oxide films similar to those described in the last section were again present.

Metallographic studies of some samples gave similar results to those of the metallics at the 13 minute mark. The splash material contained large amounts of carbon as evidenced by the presence of cementite and pearlite or pearlite plus some ferrite. The finer droplets had reduced carbon contents as indicated by their mainly ferritic structure.

The two slop samples obtained at the 16 minute mark had weights of 63 and 250 gm. Their composition was determined through chemical analysis and is presented in Table 34. No concrete statements could be made on the basis of just these two samples. Nevertheless it was evident that the CaO and SiO_2 levels were similar to those at the 13 minute mark. The material still had a low average V-ratio of 1.68. The principal component of the slop, as always, was metallic iron.

TABLE 34

SLOP ANALYSIS AT 16 MINUTE MARK
(N = 2)

Component	Total Slop Analysis		Slag Fraction Analysis	
	Sample 1	Sample 2	Sample 1	Sample 2
CaO	22.1	15.1	35.6	35.1
SiO_2	16.4	7.5	26.4	17.5
Total Fe	40.9	62.2	-	-
Metallic Fe	38.0	57.1	-	-
Fe^{2+}	2.8	0.9	4.5	2.0
Fe^{3+}	0.1	4.2	0.1	9.9
V-ratio	1.35	2.01	1.35	2.01

4C7. SAMPLES AT 19 MINUTE MARK

In all the 28 heats sampled, the ejected materials collected at the 19 minute mark consisted of metallics. The weights ranged from 40 to 1100 gm. These data points were combined with the metal ejection samples taken at the same approximate time after the beginning of the blow during stages of sampler-testing. Altogether 71 samples were obtained. The distribution of this data is presented in Table 35. A small bimodal type behaviour was observed. The mean weight of metallics was 239.2 gm with a standard deviation of 196.7 gm. A X^2 test on the data in the lower ranges (Table 35) showed it to have a small level of significance (>5%). As was the case with the samples obtained at the 16 minute mark, the weight of metal ejection was seen to increase with the extent of bottom buildup in the furnace. This is discussed later in greater detail (Section 4D).

These metal ejection samples were identical in almost all respects to those obtained at the 16 minute mark. The fine droplets present in the light samples had a similar size distribution as indicated by Figures 67 and 68. The mean droplet sizes were 116, 122 and 127μ. The heavier samples had large accretions of splash material. The metallographic structure of this splash was typically ferrite plus pearlite. The finer droplets were almost entirely composed of ferrite. Figure 69 shows the metallographic structures of metal ejections obtained from one heat at the 13, 16, 19 and 22 minute marks.

TABLE 35

METAL EJECTION WEIGHT
DISTRIBUTION AT 19 MINUTE MARK

Weight Range (gm)	Number of Observations
0 - 100	19
100 - 200	20
200 - 300	12
300 - 400	8
400 - 500	5
500 - 600	2
600 - 700	4
> 700	1

$N = 71$

$\bar{x} = 239.2$

$s = 196.7$

X^2 TEST

Range	fi	u	Pe	Pi	NPi	X^2
0-100	19	-0.7522	0.2259	0.2259	14.909	1.122
100-200	20	-0.0071	0.4972	0.2713	17.906	0.245
200-300	12	0.7380	0.7698	0.2726	17.992	1.995
300-400	8	1.4831	0.8310	0.1612	10.639	0.655
400-500	5	2.2282	0.9870	0.0560	3.696	0.460
500-600	2	2.9733	0.9985	0.0115	0.759	2.029
				0.9985	65.901	6.506

Degree of freedom = 6 - 3 = 3
Level of Significance ≥ 5%

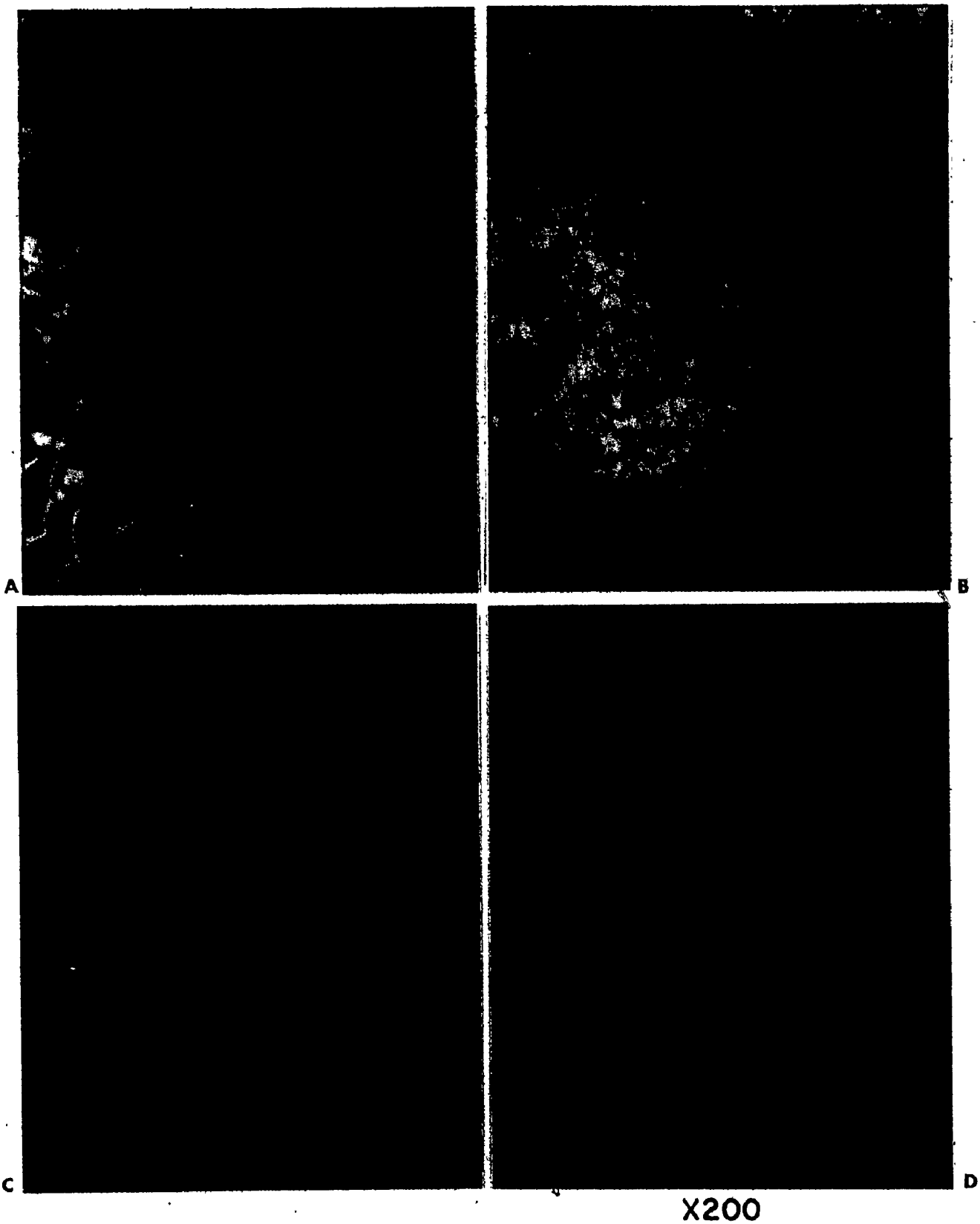

Fig. 69. Metallographic examination of metal splash from heat 27:

(A) 13 min. - cementite and pearlite
(B) 16 min. - pearlite and ferrite
(C) 19 min. - pearlite and ferrite
(D) 22 min. - ferrite and some pearlite.

4C8. SAMPLES AT 22 MINUTE MARK

The ejection samples obtained at the 22 minute mark were quite complex. Nine heats yielded metal ejection samples. In 4 heats, a light red powder material was obtained. Two heats were blown in less than 22 minutes so no sample could be taken. The 13 remaining heats yielded negligible quantities of ejections. Only specks of dark matter could be seen on the sampler's paint coating.

The 9 metal ejection samples had weights varying from 20 to 340 gm. The mean value was 157.3 gm with a standard deviation of 123.0 gm. As always, the lighter samples consisted of fine droplets while the heavier ones contained mixtures of droplets and splash. Both types of material had a similar metallographic structure. It was composed almost entirely of ferrite with only small quantities of pearlite. The heats having metal ejections occurred when the bottom had built up past 0.5 m.

The 4 red powder samples were found to contain fine metal droplets along with the fume. Analysis of this material for its metallic iron content gave an exact measure of the weight of droplets. The mean metallic iron weight was 1.1 gm, which was rather small. Because of the small weight, it was not possible to secure a large enough sample for size distribution studies.

The 2 heats blown in under 22 minutes deviated from the others in that the operator did not reduce the oxygen blowing rate at any time during the blow. Only light slopping had been present so the operator by-passed this normal corrective action.

The 13 heats where no material was captured did not have any distinguishing characteristics in terms of operation parameters. They occurred both

with a new furnace lining and when the bottom had built up past the 0.5 m level. The "red powder" heats also bore no distinguishing characteristics. The only clear observation was that metal ejection was more prevalent when there was moderate bottom buildup in the furnace.

4C9. CARBON REBLOW SAMPLES

Three ejection samples were taken during periods of reblow for further carbon removal. The reblow lasted for twenty seconds in two cases and for 50 seconds in the other at oxygen flow rates of 17000 to 21000 m^3h^{-1}. Red powder ejection samples were obtained in all these cases. However, the quantities present were very small. Fine metal droplets were again present in this powder. Chemical analysis showed, however, that the weights of droplets were rather small since the largest sample contained only 0.4 gm of iron.

4C10. PREDICTION CAPABILITIES OF RESULTS FOR BOF OPERATION

As was shown in Section 3F, the central sampling location proved to be roughly representative of the whole furnace mouth. It was therefore reasonable to calculate overall ejection rates of slop and metal at the sampling times based on the measured specific rates, subject to the errors in sampling and the measurement of the cross sectional area at the furnace mouth.

As mentioned previously ejection sampling was conducted on a random basis in the selection of heats for investigation. If the ejection rates measured in these sampled heats are to be adequate in predicting general BOF operation, at least in this melt shop, it must be substantiated that the collected data represented the total population of heats. This could be determined by testing for an expected Gauss distribution of some random variable which may be used to characterize individual heats, using the X^2 method. The various impurity concentrations in the blast furnace hot metal are among such variables. For those heats tested, the Si and Mn levels were always measured. X^2 tests were therefore conducted on these two variables (Tables 36 and 37). Both levels of significance were quite acceptable - 70% for Mn and 50% for Si. The distribution of hot metal temperature, another random heat variable, had a lower significance level (≥10%) because of its dependence on non-controllable exterior parameters such as transport time from the blast furnace and torpedo car lining thickness. Another variable, scrap percentage in the metallic charge, had an adequate level of significance (≥30% from Table 38). The lime and dolomite charge additions had low Gaussian significance levels (<1%) because the additions were altered frequently for furnace lining maintenance. For those variables that

TABLE 36

X^2 TEST ON DISTRIBUTION OF
Si IN HOT METAL FOR SAMPLE HEATS

Range	fi	u	Pc	Pi	NPi	X^2
0.58 - 0.68	4.5	-1.0089	0.1562	0.1562	4.686	0.007
0.68 - 0.78	9	-0.2967	0.3821	0.2259	6.777	0.729
0.78 - 0.88	5.5	0.4154	0.6628	0.2807	8.421	1.013
0.88 - 0.98	7	1.1276	0.8708	0.2080	6.240	0.093
0.98 - 1.08	3	1.8397	0.9671	0.0963	2.889	0.004
1.08 - 1.18	1	2.5519	0.9946	0.0275	0.825	0.037
				0.9946	29.838	1.883

N = 30

$\bar{x}$ = 0.822

s = 0.140

Degrees of freedom = 6 - 3 = 3

Level of Significance $\geq$ 50%

Table 37

X^2 TEST ON DISTRIBUTION OF Mn IN HOT METAL FOR SAMPLE HEATS

Range	fi	u	Pc	Pi	NPi	X^2
0.82 - 0.98	1.5	-1.5906	0.0559	0.0559	1.677	0.019
0.98 - 1.14	8	-0.4920	0.3121	0.2562	7.686	0.013
1.14 - 1.30	11.5	0.6065	0.7291	0.4170	12.510	0.082
1.30 - 1.46	8	1.7050	0.9554	0.2263	6.789	0.216
1.46 - 1.62	1	2.8035	0.9974	0.0420	1.260	0.054
				0.9974	29.922	0.384

$N = 30$

$\bar{x} = 1.212$

$s = 0.143$

Degrees of freedom = 5 - 3 = 2

Level of Significance $\geq$ 70%

TABLE 38

X^2 TEST ON DISTRIBUTION OF
% SCRAP IN THE SAMPLE HEATS

Range	fi	u	Pc	Pi	Npi	X^2
17.5 - 20.0	2	-1.8362	0.0332	0.0332	0.930	1.233
20.0 - 22.5	3	-0.9096	0.1815	0.1483	4.152	0.320
22.5 - 25.0	8	0.0170	0.5068	0.3253	9.108	0.135
25.0 - 27.5	10	0.9437	0.8273	0.3205	8.974	0.117
27.5 - 30.0	5	1.8703	0.9693	0.1420	3.976	0.264
				0.9693	27.140	2.069

$N = 28$[1]

$\bar{x} = 24.954$

$s = 2.698$

Degrees of freedom = 5 - 3 = 2

Level of Significance $\geq$ 30%

[1] only 28 heat values were used because 2 heats had special scrap charges.

were essentially random, the X^2 levels were all acceptable. For this reason it could be assumed that the test heats were representative of the population of all furnace heats. The measured ejection rates could therefore be used in predicting overall furnace behaviour.

No exact measure of the overall sampling error has been given till now because of the lack of a method of comparison. On the basis of the heats sampled, the predicted average rate of metal loss by ejection was 2.0 tons per heat. This figure can be employed in a yield inventory of all metal units. This is supplied in Table 39. The "Unaccountable" category was obtained by balancing the imput and output units. This value, 0.53 tons per heat, if ascribed to errors in ejection sampling, can serve as a rough measure of the overall sampling error. The error, measured on the basis of measured ejection rate, was 26.5% on the negative side. That is, not all the ejections were collected. This could be caused by the already described errors in sampling: i.e., lower sample collection efficiency with the small vs large sampler, and large deviations in the representativeness of the central sampling location of the whole furnace mouth.

TABLE 39

YIELD INVENTORY

No.	Category	Actual Weight Per Charge (tons)	Portion of Metallic Charge (%)
1.	Ingots	146.12	84.88
2.	Non-ferrous elements in hot metal and scrap removed in refining reactions	11.63	6.76
3.	Fe in slag	2.99	1.74
4.	Ingot butts and untapped steel	6.32	3.67
5.	Fuming	1.27	0.74
6.	Stool cavities, runners, skulls	1.28	0.74
7.	Slopping and metal ejection	2.00	1.16
8.	Unaccountable	0.53	0.31
	Total Metallic Charge	172.14	100.00

4D. EFFECT OF FURNACE BOTTOM BUILDUP ON EJECTION RATES

As noted previously on several occasions, bottom buildup during the course of a furnace campaign increased the slop and metal ejection rates. To present these findings in a more convenient manner, the measured bottom buildups were used to calculate the metal bath-to-mouth distance. For a new furnace with a standard charge, the bath to mouth height was 4.8m. In these simple calculations of changes in working volume due to buildup, it was assumed that there was no erosion of the sidewall in the furnace brickwear. This assumption was based on several actual bath-to-mouth measurements taken in conjunction with bottom buildup measurements. These tests showed that the bath was elevated with furnace bottom buildup in about the same proportions. Buildup on the lower sidewalls must have compensated for any erosion of the brickwear in the bath region.

The weight of each ejection sample expressed in grams for one minute sampling is numerically equal to the ejection rate in Kg min^{-1} for the furnace since the area of the furnace mouth is approximately 1000 times that of the sampler. In all the heats, only 2 or 3 samples of each type of material (slop or metallic) were collected. Since each ejection sample taken was representative of a 3 minute period, it was possible to predict overall material loss rates from the furnace. The slop weight, iron weight in the slop, metal ejection weight and combined iron loss were treated as separate variables. In calculating the total iron loss, it was assumed that metal ejections consisted of 100% iron. In determining the average slop weight, the normalized values were used. By multiplying the normalized slop weights by their total iron

content, as obtained from their individual analyses, it was possible to determine an average iron loss rate in the slop for each heat. For the metallics collected between the 13 and 22 minute mark, an average metal ejection rate was calculated.

Altogether, 28 observations were available from the heats studied. The minimum bath-to-mouth height was 3.7m. A linear least squares regression analysis was performed on all the 7 ejection variables described to test for correlation with bath-to-mouth height. The results are presented in Table 40. The correlation coefficients and T^2 values for all the regressions were statistically acceptable. The dependency of ejection rates on bath-to-mouth height was always negative. This was to be expected since a decrease in this height caused a reduction in the gas residence time. The ejected material also had a shorter path to travel in order to escape. There was also a reduction in the free furnace volume available for material collection. The additional quantities of slop and metal ejection generated per meter decrease in height were roughly similar, being 3.36 and 4.35 tons respectively. The effect of bath-to-mouth height on total iron loss was quite substantial, measuring 5.7 additional tons per 1m decrease. The plot of this variable dependence is presented in Figure 70 along with the calculated regression line.

TABLE 40

LEAST SQUARES REGRESSION ANALYSIS OF
BATH-TO-MOUTH HEIGHT vs. EJECTION RATES

Y Variable	Units	Average Y Value	Slope	Intercept	Correlation Coefficient	T^2 Value
Avg. Slopping Rate	Kg min^{-1}	371	-557	2714	-0.591	14.0
Avg. Fe Loss Rate in Slop	Kg min^{-1}	137	-216	1046	-0.532	10.2
Avg. Metal Ejection Rate	Kg min^{-1}	279	-474	2273	-0.694	24.1
Total Slop Loss	ton $heat^{-1}$	2.65	-3.36	16.77	-0.593	14.1
Total Fe Loss in Slop	ton $heat^{-1}$	0.99	-1.31	6.50	-0.526	9.9
Total Metal Ejection Loss	ton $heat^{-1}$	2.21	-4.35	20.50	-0.709	26.2
Total Fe Loss	ton $heat^{-1}$	3.21	-5.66	27.00	-0.720	28.0

[1] X variable was the metal bath-to-mouth height in meters. The average X-value was 4.21m. The equation fitted was of the form

$$Y = m X + b$$

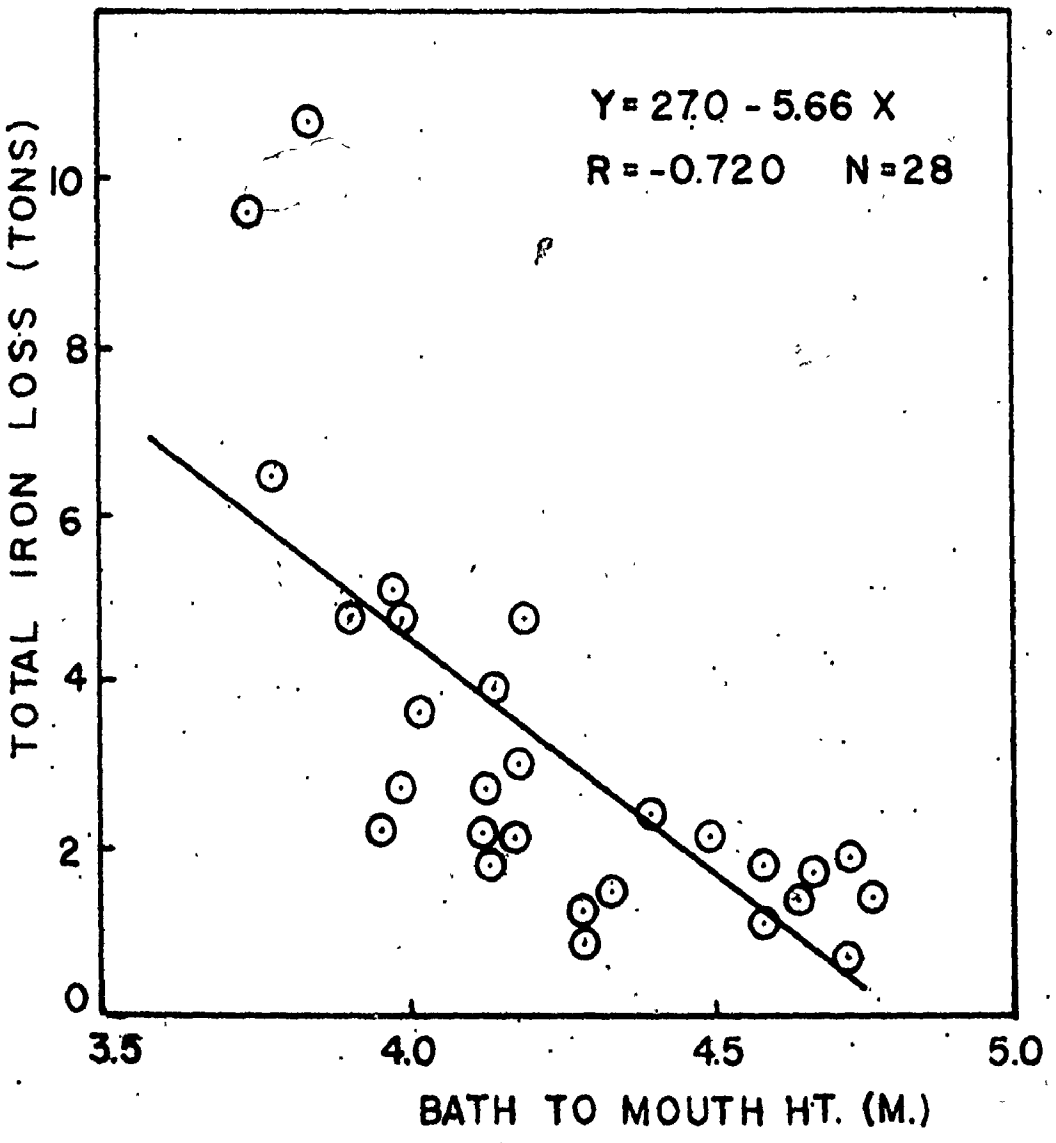

Fig. 70. Variation of total iron loss from the BOF by ejection with metal bath-to-mouth height.

4E. EFFECT OF OXYGEN FLOW SURGE ON EJECTIONS

As was noted with certain ejection samples taken at the 4 minute mark, rapid surges in the oxygen flow rate could create additional metal and slag ejections. This was also noticed in cases where the flow was increased from 17000 to 21000 m^3h^{-1} when slopping had terminated or subsided. One illustration of this is given in Figure 51b. The flow rate was normally increased in one step lasting 15 seconds. The bath could not absorb this added kinetic energy rapidly enough, some of it being transformed into additional material ejection. Special tests were conducted where the flow rate was increased more gradually. The material ejection rates before and after this increase were noted. Together with the observations recorded in the 28 regular heats sampled, a regression analysis was performed on the dependence of the change in material ejection quantity during this period to the length of the time period of oxygen increase. The data points and least squares regression line are presented in Figure 71. Though the correlation coefficient was low at -0.388, there was clear indication that a gradual rate of oxygen increase resulted in less ejections. The oxygen was more easily assimilated, with less kinetic energy going to material ejection.

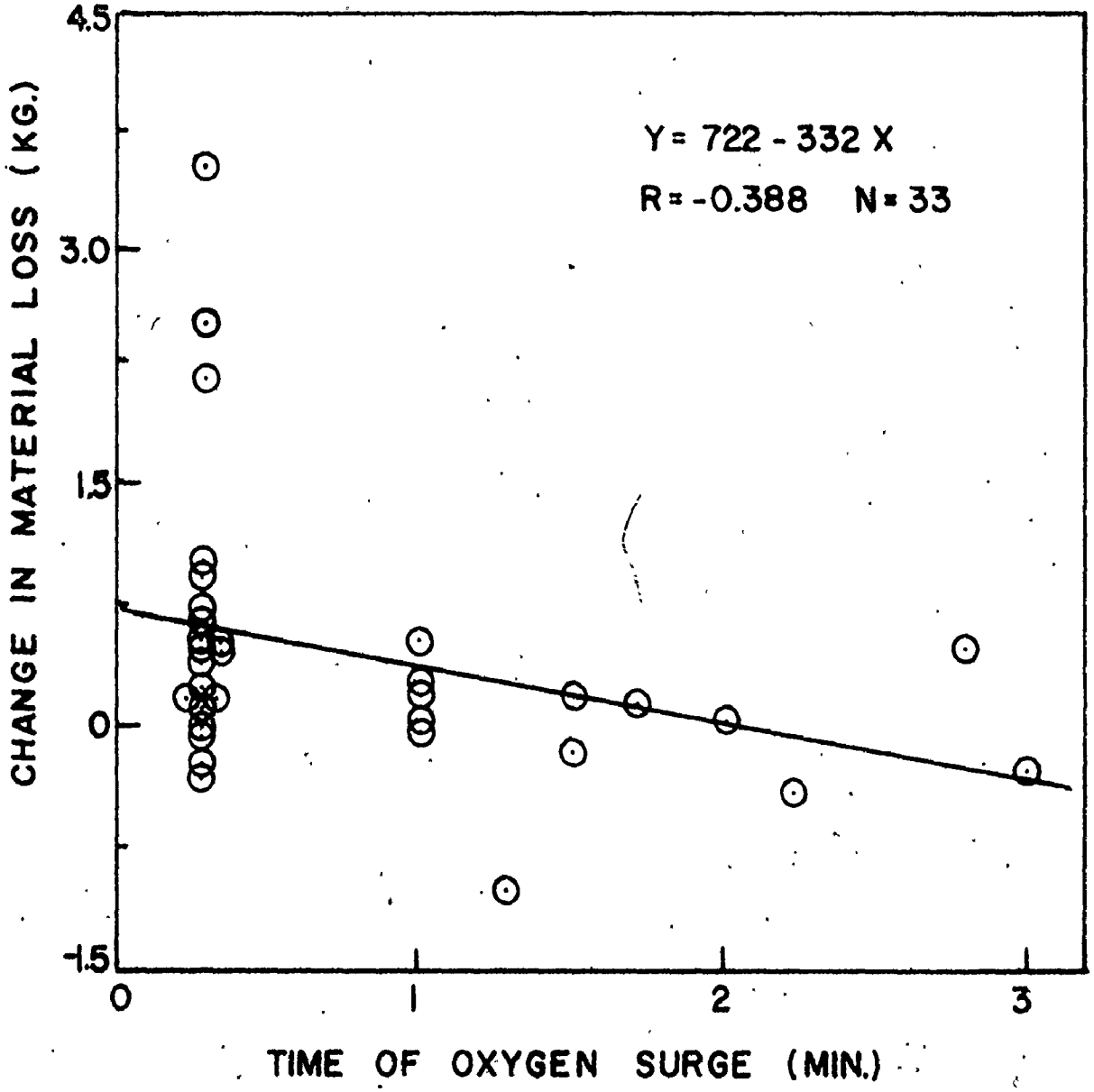

Fig. 71. Dependence of the change in material ejection quantity, between the 3 minute periods before and after the oxygen surge, on the length of the time period of oxygen increase.

4F. SPECIAL HEATS

As mentioned previously, two heats were sampled in which the charge was radically different. These heats had a 40% scrap content and were blown at oxygen flow rates of 25000 to 30000 m^3h^{-1} during certain periods of the heat. The total metal charge to the furnace was about 15 tons lower than the regular heats. The ejection and blowing pattern of these two heats is given in Figure 72. Red powder and fine metal droplet ejections were found in the early blowing stages just like in all the regular heats. No slopping occurred after this period. Rather, the 7, 10 and 13 minute mark samples produced metal ejections. These metal ejections varied in weight from 50 to 250 gm. This material was of a very similar nature to those metal ejections obtained in regular heat sampling. Thereafter, when the oxygen flow rate was increased, negligible amounts of ejection material were collected on the sampler.

The quantity of slag generated during the main blowing period was about 25% less in these two heats in comparison to the regular heats. Also, because the hot metal charge was so much smaller, the metal was refined more quickly. Metal samples taken at the 13 minute mark had less than 1% carbon. On the basis of calculations, like those described in Section 2D, the waste gas residence time for this operating condition was 1.05 seconds when the blowing rate was 21000 m^3h^{-1}. This was about 10% longer than the computed gas residence time for regular Dofasco operation (0.97 sec).

The slag samples taken in this heat were analyzed by the methods previously described. The results are tabulated in Table 41. A very interesting observation was that the combined ferrous and ferric level dropped substantially in the middle segment of the blow. These iron oxides were being utilized

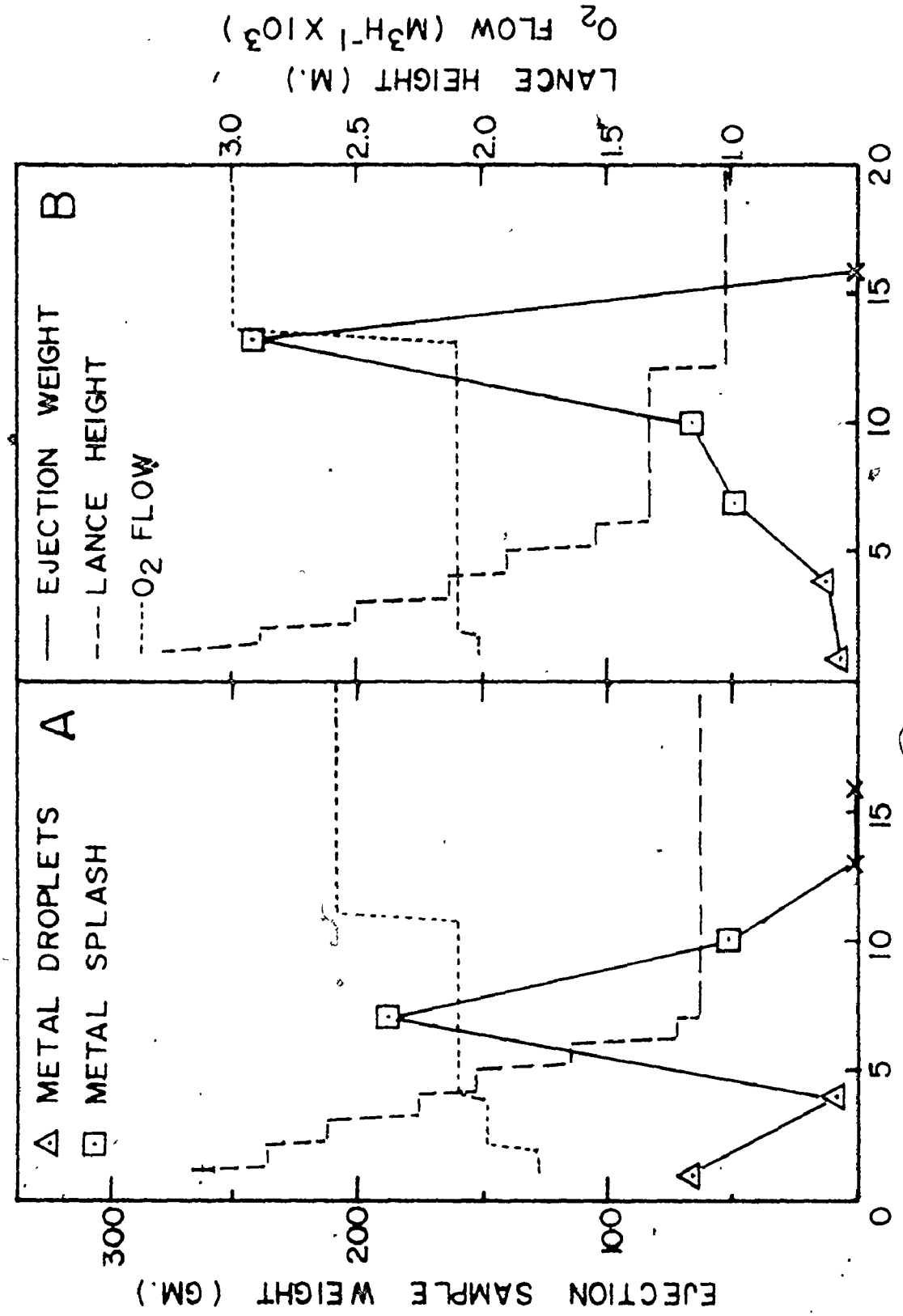

Fig. 72. Ejection and blowing pattern of two heats with special (40%) scrap charges. (A) Heat 14, (B) Heat 16.

TABLE 41

SLAG COMPOSITION FOR SPECIAL HEATS

Component	Heat 1			Heat 2			
	4 min	7 min	20 min	4 min	10 min	16 min	19 min
CaO	22.1	25.3	38.1	18.6	32.3	27.8	29.3
SiO_2	23.2	23.8	10.2	13.7	26.3	17.6	8.9
MnO	22.3	21.8	9.1	13.8	17.9	10.2	7.8
MgO	4.2	5.3	8.7	6.1	8.2	10.2	9.3
Fe^{2+}	10.2	9.4	20.8	16.1	3.2	18.0	25.9
Fe^{3+}	7.5	3.4	3.9	11.5	2.0	7.9	4.8
Metallic Fe[1]	28.2	20.9	15.8	28.0	13.3	12.7	12.6

[1] expressed as percent content of total slag-metal emulsion weight

as oxygen sources for decarburization. The V-ratio of the slag increased gradually over the first half of the blow and then rose rapidly as all the remaining lime dissolved. The SiO_2 and MnO levels dropped drastically in this time period because of extensive dilution. The MgO level increased gradually as the dolomite dissolved. The metal content of the emulsion appeared to drop gradually throughout the blow.

4G. SLAG AND METAL SAMPLES

During the 28 regular heats, a total of 121 slag samples were taken. They were obtained predominantly at the 4, 10, 16 minute and at first turndown. The average blowing time till first turndown was 24.5 minutes. Some samples were also taken at the 7, 13, 19 and 22 minute points of the blow. These slags were analyzed for CaO, SiO_2, MnO, MgO, metallic Fe, Fe^{2+} and Fe^{3+} by the methods described previously. The results are presented in Tables 42, 43 and 44. For all the components other than metallic iron, the composition given is that of the slag matrix alone. The weight of the metallic iron is expressed as a percentage of the whole metal-slag emulsion.

The CaO content of the slag increased gradually until the 19 minute mark whereupon fast lime dissolution took place. The SiO_2 level remained almost constant up to 19 minutes but then dropped quickly due mainly to dilution by the lime. The MnO content of the slag dropped off earlier due to MnO reversion to the metal. The slag started off with an appreciable level of MgO (5%) and this continued to increase gradually until the end of the blow. The ferrous ion content of the slag stayed rather uniform during the first 16 minutes of the blow but then increased as the carbon in the metal was depleted. The fastest rise was in the very last few minutes. The ferric ion content was very similar to the ferrous level for the first 19 minutes of the blow. Thereafter, the CaO and ferrous ion content of the slag increased rapidly, causing a drop in the ferric level.

The metallic iron content of the metal-slag emulsion was at its highest level in the first few minutes of the blow. The slag volume was low at this point so the oxygen jet could easily load up the slag with metal by its

TABLE 42

CaO AND SiO_2 CONTENT OF SLAG

Time into Blow (min)	Number of Samples	CaO Content				SiO_2 Content			
		Mean	Standard Deviation	Range Low	Range High	Mean	Standard Deviation	Range Low	Range High
4	24	28.5	6.3	12.6	41.7	25.7	4.3	17.7	33.0
7	12	31.2	5.6	17.5	41.5	25.9	2.8	21.3	30.1
10	19	34.4	3.1	26.9	40.2	26.1	2.4	20.6	31.5
13	12	35.8	1.9	32.2	38.3	25.4	1.2	23.1	27.4
16	18	38.6	2.2	36.0	43.2	24.6	2.0	21.6	28.0
19	9	36.8	2.8	32.3	40.3	24.3	2.2	21.6	28.5
22	2	41.7	1.2	40.8	42.5	19.7	5.2	16.0	23.3
TD	25	45.1	3.3	38.0	51.6	14.9	1.7	12.0	18.9

TABLE 43

MnO AND MgO CONTENT OF SLAG

Time into Blow (min)	Number of Samples	MnO Content				MgO Content			
		Mean	Standard Deviation	Range Low	Range High	Mean	Standard Deviation	Range Low	Range High
4	24	19.3	3.3	13.8	26.2	5.5	1.5	2.1	8.4
7	12	20.0	2.7	14.8	24.0	6.0	1.4	4.1	8.3
10	19	17.5	1.6	15.3	21.1	6.6	0.8	5.6	8.4
13	12	17.0	2.0	13.7	20.0	7.1	1.1	5.2	8.8
16	18	14.1	2.0	10.8	17.8	7.4	1.2	5.4	9.1
19	9	12.2	1.4	9.8	13.4	8.4	1.4	5.9	11.0
22	2	12.6	3.0	10.5	14.7	7.5	2.1	6.0	8.9
TD	25	9.1	1.3	7.0	11.4	9.7	1.2	7.3	11.9

TABLE 44

METALLIC Fe, Fe^{2+} and Fe^{3+} CONTENT OF SLAG

Time into Blow (min)	Number of Samples	Fe^{2+} Content				Fe^{3+} Content				Metallic Fe Content[1]			
		Mean	Standard Deviation	Range Low	Range High	Mean	Standard Deviation	Range Low	Range High	Mean	Standard Deviation	Range Low	Range High
4	24	3.3	2.3	0.6	7.2	3.6	2.2	0.3	7.5	23.5	6.2	10.8	33.6
7	12	3.5	1.6	1.5	6.6	3.2	2.2	0.0	7.3	21.7	3.6	16.0	27.4
10	19	3.2	1.2	0.6	5.0	2.9	1.3	0.6	5.6	13.5	2.8	8.4	20.0
13	12	2.6	0.7	1.5	3.7	2.5	1.9	0.0	6.7	17.9	5.5	12.4	28.7
16	18	2.7	1.1	1.3	5.0	3.3	1.7	0.6	6.7	20.8	7.1	11.0	37.1
19	9	4.5	2.4	2.7	10.1	5.0	1.4	3.4	7.2	21.3	8.0	13.5	34.8
22	2	5.8	2.3	4.1	7.4	2.9	0.6	2.4	3.3	15.2	1.4	14.2	16.2
TD	25	9.9	3.8	1.7	14.7	2.4	0.8	0.7	3.9	12.5	2.8	7.7	16.6

[1] expressed as percent content of total slag-metal emulsion weight.

TABLE 45

X^2 TESTS ON COMPONENT COMPOSITION DISTRIBUTION IN SLAG

Time into Blow (min)	Number of Samples	Component Level of Significance (%)						
		CaO	SiO_2	MnO	MgO	Fe^{2+}	Fe^{3+}	Fe^{o}
4	24	70	50	40	40	40	25	30
10	19	50	50	30	30	40	50	25
16	18	-[1]	70	60	35	30	60	30
TD	25	70	30	30	70	70	60	70

[1] could not be determined because 2 analyses were missing.

shearing action on the bath. The metal content dropped continually until the 10 minute mark as the slag volume increased. Thereafter it continued to increase until the 19 minute mark. This marked the period of active development of the metal-gas-slag emulsion. Decarburization was fastest in this period because of the assistance of the emulsion refining reactions in the total reaction scheme. As decarburization dropped off in the last minutes of the blow, so did the metallic iron content of the emulsion. The driving mechanisms for droplet formation became slower, thereby making it easier for the droplets to settle.

Sufficient slag samples were taken at the 4, 10, 16 minute and first turndown marks to permit X^2 analysis for sample representativeness. The results are given in Table 45. All the components for the different times exceeded a 25% level of significance. The major slag components, CaO and SiO_2 displayed the best degrees of representativeness.

These average slag compositions are plotted along with the average slag matrix composition of the slop in Figure 73. As can be seen, the CaO and SiO_2 contents for these two materials matched quite closely. The ferrous ion content was similar in both materials, but the ferric level in the slop was somewhat greater that of the slag, especially at the 13 minute mark. The metallic iron content of the slop exceeded that of the slag. At 7 minutes this difference was 9.7%, at 10 minutes it was 15.1%, at 13 minutes it was 18.8% and finally at 16 minutes it was 26.8%. However, the metallic iron content of the slop displayed a minimum similar to that of the slag at the 10 minute mark.

Plotting of average values can sometimes be misleading if the data does not follow a Gaussian distribution. In these cases, the slop and slag components have been shown to have reasonable levels of significance so this problem would not be expected. As further evidence of this behaviour, the

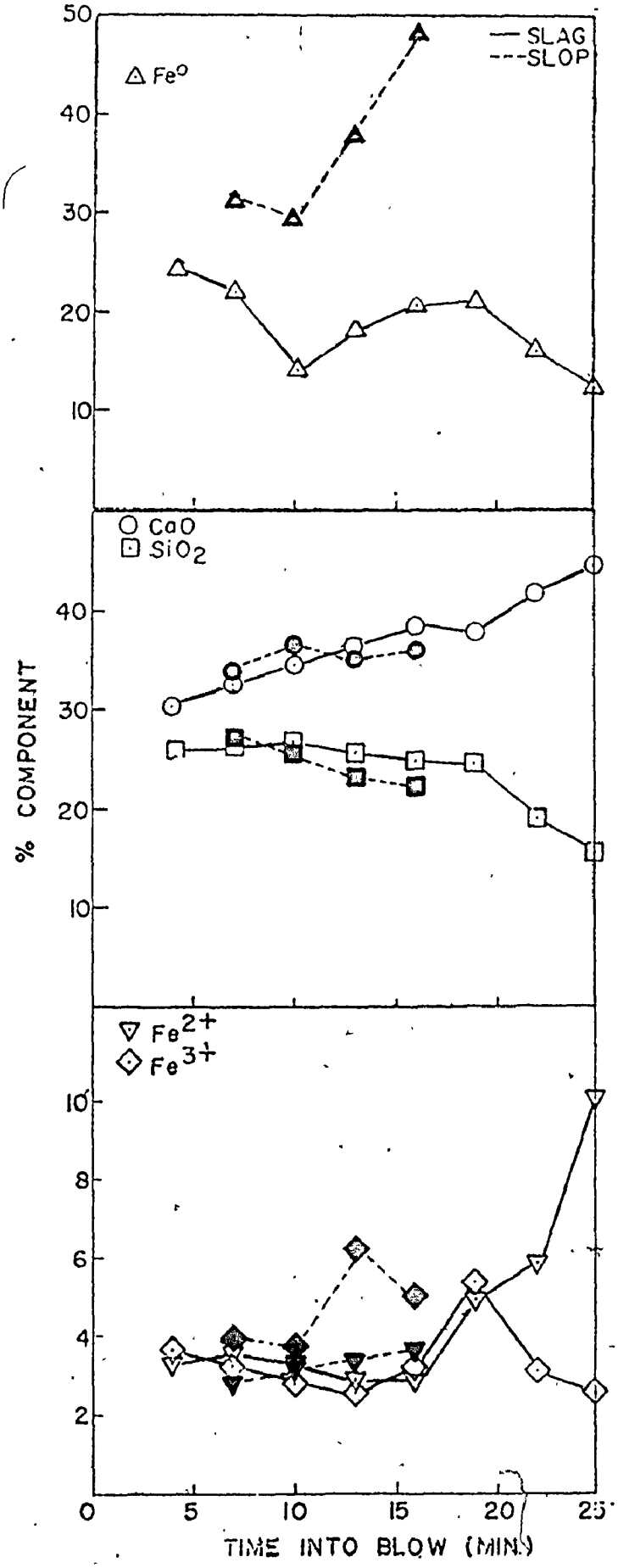

Fig. 73. Evolution of the average slag and slop composition during the blow for the 28 heats sampled.

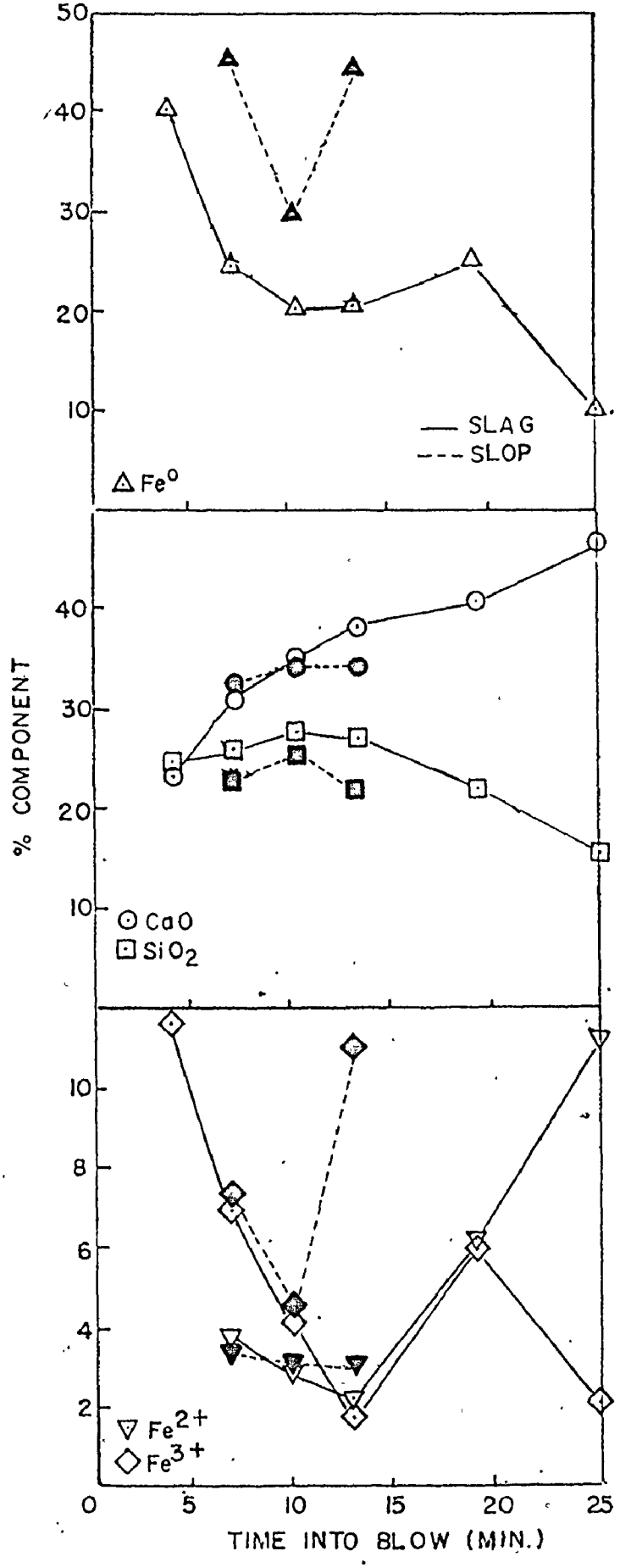

Fig. 74. Evolution of the slag and slop composition during the blow in heat 4.

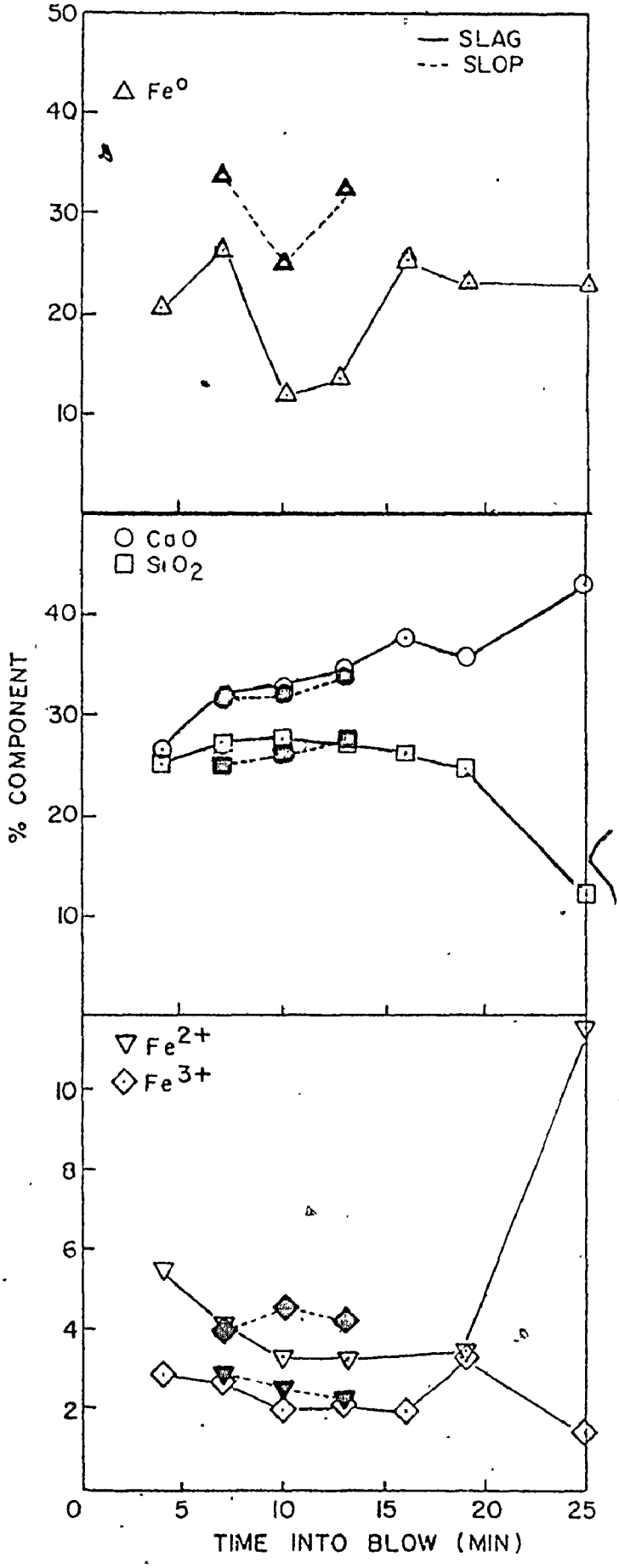

Fig. 75. Evolution of the slag and slop composition during the blow in heat 9.

analyses of these materials in two individual heats is presented in Figures 74 and 75. The same differences between slop and slag, as described using the average values, are seen to exist in the individual heats.

Along with the slag samples, 153 metal samples were taken. The number of samples taken at each sampling time was roughly the same at 20 except at the 22 minute mark where only 11 samples were successfully taken. At this moment, the sampler frequently contained a non-analyzable surface coating of metal because the bath was very hot. The oxygen jet blew out the metal from the sampler. The carbon, manganese and silicon levels at the different time periods are reported in Table 46. X^2 tests were run on the data where applicable and the results are presented in Table 47. The levels of significance were mixed between low and high values, but overall they were reasonable, except the carbon level at turndown. This, however, was due to the specification of end carbon contents.

The carbon content of the bath was low (3.2%) at the start of the blow in comparison to the hot metal carbon content. This however was due to a wide variety of factors: i.e., chilling of the bath by scrap resulting in graphite precipitation, and dilution by scrap dissolution. The rate of carbon drop was essentially constant between the 4 and 16 minute mark of the blow at about 0.15%C per minute. Between 16 and 19 minutes, the period of peak emulsion formation, a marked increase in carbon drop was noted. Over this period, decarburization sped up to 0.23%C per minute. Thereafter, this rate decreased to 0.15%C min^{-1} between 19 and 22 minutes. Between 22 minutes and the first turndown, the average decarburization rate was 0.06%C min^{-1}.

The manganese level dropped very quickly at the start of the blow due to preferential oxidation. By the 4 minute mark it had decreased from an average starting value of 1.21% to 0.26%. It continued to decrease but more

TABLE 46

METAL COMPOSITION DURING THE BOF BLOW

Time into Blow (min)	Number of Samples	C Content				Mn Content				Si Content			
		Mean	Standard Deviation	Range Low	Range High	Mean	Standard Deviation	Range Low	Range High	Mean	Standard Deviation	Range Low	Range High
4	22	3.23	0.30	2.65	3.65	0.26	0.09	0.12	0.40	0.10	0.05	0.03	0.19
7	18	2.80	0.38	2.01	3.25	0.14	0.04	0.07	0.24	0.015	0.005	0.005	0.024
10	20	2.25	0.33	1.69	2.81	0.14	0.04	0.07	0.21	-	-	-	-
13	19	1.83	0.29	1.28	2.35	0.18	0.05	0.11	0.30	-	-	-	-
16	20	1.39	0.24	0.95	1.93	0.23	0.06	0.12	0.33	-	-	-	-
19	18	0.69	0.28	0.27	1.22	0.23	0.05	0.12	0.31	-	-	-	-
22	11	0.24	0.15	0.05	0.53	0.20	0.06	0.10	0.30	-	-	-	-
TD	24	0.07	0.03	0.04	0.15	0.19	0.04	0.12	0.30	-	-	-	-

TABLE 47

X^2 TESTS ON COMPONENT
COMPOSITION DISTRIBUTION IN METAL

Time into Blow (min)	Number of Samples	Component Level of Significance (%)		
		Carbon	Manganese	Silicon
4	22	70	20	70
7	18	30	50	30
10	20	20	40	-
13	19	60	20	-
16	20	25	25	-
19	18	50	40	-
22	11	-	-	-
TD	24	1	30	-

slowly, reaching a lower limit of 0.14% by 7 minutes. This level stayed constant for a few minutes and then manganese reversion set in. Manganese reversion reached a peak at around 16 minutes where the level was 0.23%. A slow rate of decrease continued on to the end of the blow.

The silicon was also oxidized very quickly. It dropped from 0.82% to 0.10% in the first 4 minutes. Between 4 and 7 minutes, silicon removal slowed down reaching 0.015% at the end of this period. At all subsequent times, the silicon level was essentially trace.

By combining the information obtained about the slag and metal composition, it was possible to roughly calculate the slag weight as a function of time. A silicon balance was used in this calculation. The simplifying assumptions made were: the hot metal silicon content accounted for 80% of the total charged silicon; 30% of the scrap was dissolved at 4 minutes; 40% scrap was dissolved at 7 minutes; and after 7 minutes, the silicon content of the metal was negligible. The slag weight and weight of the various components are given in Table 48. The quantity of dissolved lime in the slag and the total slag weight increased, especially in the last few minutes. The SiO_2 weight, since it formed the basis of the calculation, stayed constant over the main period of the blow. The MnO weight displayed its typical reversion pattern as manganese returned to the metal. The MgO weight increased gradually over the largest part of the blow, but then rose rapidly as the major fraction of dolomite dissolved. The FeO weight stayed constant over two thirds of the blow, but then increased rapidly as the carbon in the metal was depleted. The Fe_2O_3 weight displayed a slight dip over the first half, but then continued to increase. The Fe_2O_3 at 19 minutes is most probably incorrect since there appears to be no cause for a peak. Rather, it is best to ignore this value and assume a gradually increasing Fe_2O_3 weight. The weight

TABLE 48

CALCULATED SLAG AND COMPONENT WEIGHTS IN BOF SLAG

Time into Blow (min)	Slag Weight (t)	Component Weight (t)						
		CaO	SiO_2	MnO	MgO	FeO[1]	Fe_2O_3[2]	Fe^o (in emulsion)
4	9.57	2.72	2.46	1.85	0.52	0.41	0.49	2.94
7	10.49	3.27	2.72	2.09	0.63	0.47	0.48	2.91
10	10.60	3.65	2.76	1.86	0.69	0.43	0.43	1.66
13	10.89	3.99	2.76	1.85	0.77	0.37	0.39	2.37
16	11.27	4.34	2.76	1.59	0.83	0.39	0.53	2.95
19	11.38	4.19	2.76	1.39	0.95	0.65	0.81[3]	3.07
22	14.07	5.86	2.76	1.77	1.05	1.04	0.57	2.52
TD	18.53	8.35	2.76	1.68	1.79	2.37	0.62	2.64

[1] calculated on basis of Fe^{2+} content

[2] calculated on basis of Fe^{3+} content

[3] value best ignored. See section 4G.

of metal droplets in the emulsion followed a similar pattern to its composition profile. It decreased over the first few minutes, then rose to a peak in the main decarburization period, followed by a slow tapering off. Over most of the blow, there was between 2.5 - 3.0 tons of metal in the form of droplets present in the emulsion.

5. DISCUSSION

(i) MATERIAL LOSSES

This study was prompted in an attempt to reduce the material ejection rates from one melt shop operation. As shown, a substantial reduction could be achieved by preventing bottom buildup in the furnace (Section 4D) and by eliminating surges in the oxygen flow rate (Section 4E). The lowering of oxygen flow during the slopping period also proved to be a proper corrective procedure since the ejection rate decreased (Tables 24, 26 and 29). By employing these findings in melt shop practice, material ejection can be reduced but not eliminated. This last goal can only be achieved if the causes for ejection are first known. The studies carried out offer insights into these causes.

An overview of the average measured rates of iron loss throughout the blow is given in Figure 76. In those periods where more than one type of material was collected, the probability of incidence of each type is given. These cases where oxygen surges caused disturbances in the regular ejection profile were not considered in determining these probabilities. The two incidences of slop at the 16 minute mark were not noted because they represented a frequency of occurrence of less than 10%. The path of highest probability is marked in Figure 76 by the solid line. The dotted lines indicate other possible routes. No noticeable differences were found in the operation parameters to explain these different routes. However several hypotheses could be made on the basis of the information gathered.

(ii) SLAG FREE vs SLAG BOUND METAL EJECTIONS AT ONE MINUTE

At the one minute mark, two types of metal droplets were obtained, one free of and the other tied up with slag. The droplets with the slag were

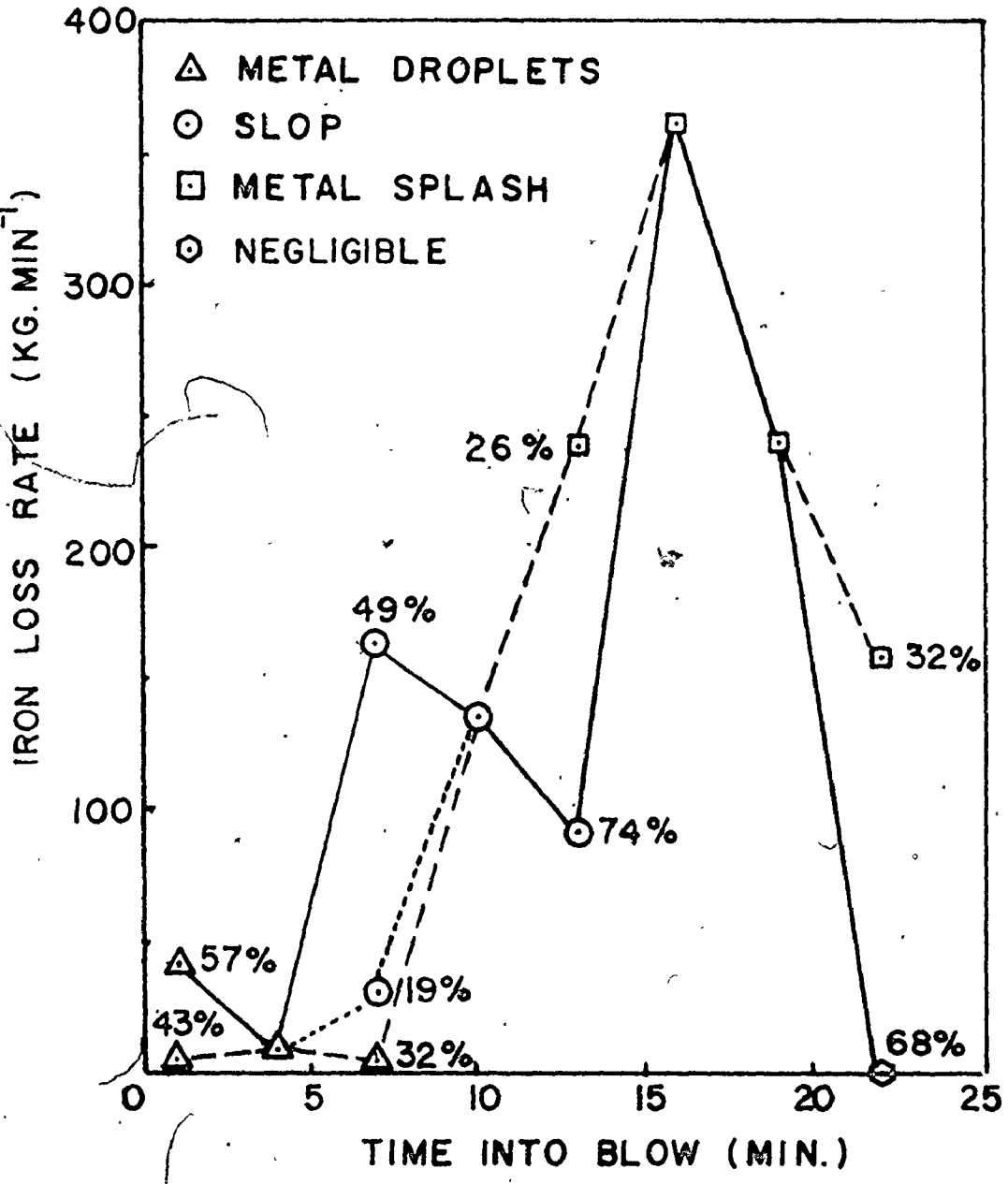

Fig. 76. Average metal loss rates during the blow. Percentages indicate the frequency of occurrence.

considerably larger, having a mean diameter of 100μ compared with the other case of 30μ. The weight ratio of the metal droplets collected was roughly 10 (large/small). No explanations could be found upon examination of the steelmaking practices to account for the presence of these two different materials. Similar physical differences between two classes of droplets have been noted in a study by Li[25] on the effect of a foam cover on the splashing of liquid in water model studies. He noted that when a foam cover was present, the droplets from the splashing mode were larger and fewer than that formed without such a cover.

The source of both classes of metal ejections has been established as the shearing of the metal in the jet impact area[112-123]. The slag tied up with the one class of ejections must have been present in this cavity region. Unlike the water study, slag was present in the furnace for both these cases. Some difference in slag properties must therefore have caused the slag to be ejected in one case and not the other. A clue as to what caused this was available from the one accidental heat in which lime was added after the 5 minute mark. In this case both the one and 4 minute ejection samples consisted of the finer, slag free, metal droplets. The CaO content of the slag could therefore be the influencing factor.

Dissolved CaO in the slag combined with suspended lime particles could make the slag viscous, allowing it to be pushed aside from the cavity region so that it is not ejected. Lower CaO levels, as present in the initial blast furnace carry-over slags, make the slag more fluid. In this way the slag can enter the cavity region and be ejected. This presence of slag could reduce the rate of oxygen assimilation by covering up some of the potential reaction sites. More oxygen would be deflected, taking with it larger metal droplets because of the increased shearing force. The weight of metal would also be larger. The metal droplets bound with slag exhibited both these characteristics, giving

credence to this explanation. Lime addition should therefore be made as early as possible if this particular ejection material is to be reduced. For the case of the fine, slagless droplets, a larger portion of the oxygen jet must have been absorbed in the cavity region by the various refining reactions, leaving a smaller deflected jet stream for material ejection since CO evolution was relatively low at this point in the blow.

Both types of droplets were very low in carbon as was indicated by their mainly ferritic structure. There are two major schemes to explain this behaviour. The cavity area where these droplets were ejected from may be largely depleted in all the elements other than iron by the oxidizing action of the oxygen. The other possibility is that these droplets are refined in the furnace atmosphere which initially has some free oxygen and a larger proportion of CO_2 to CO as compared to later stages in the blow. The first explanation is somewhat more plausible in light of the completely refined nature of some slag coated droplets. Nevertheless both mechanism could be active along with the added possibility of some droplet refining by slag-metal reactions for the case of the larger slag coated droplets.

The heterogeneity of the slag fragments tied up with the larger droplets (Figure 55) showed the slag complexity at the one minute mark. This slag was formed in the furnace by a multiplicity of interactions. The amount of blast furnace slag carry-over could vary in normal practice from 0.3 to 1.2 tons. The time the flux addition started also varied from 30 seconds to 1.5 minutes into the blow. The amount of fluorospar added with this also varied. The combination of all these parameters could make the slag properties very variable at the one minute mark. This could account for the two types of ejections as already described.

(iii) JET INTERACTION WITH THE METAL BATH IN THE EARLY BLOWING PERIOD

A slag free class of metal droplet ejections was obtained at the 1, 4 and 7 minute mark of the blow. These droplets were very similar both physically and chemically as already shown. Their quantities did not vary substantially: 4 Kg min^{-1} at 1 min., 6.8 Kg min^{-1} at 4 min. and 5.3 Kg min^{-1} at 7 minutes. Because of these similarities, only one mode of metal bath-jet interaction would most likely be active over this period. Yet, the oxygen flow rate had been increased from 17000 to 21000 $m^3 h^{-1}$ and the lance was lowered from 3.0 to 1.4 meters during this period. With this change would naturally come a drastic variation in the jet impact velocity. This was seen to cause a large variation (1 to 2 orders of magnitude; Figures 28 and 29) in the ejection rates in cold model studies [10, 14]. In contradiction a relatively constant ejection profile was observed in the commercial furnace. Some mechanism must therefore be compensating for these increased impact velocities by absorbing to a higher degree the more concentrated impulse energy.

The slag could in no way act as a compensating mechanism because of its observed similarity in composition and quantity over this time period. It's absence in the ejection sample also indicated that it was not directly present in the cavity impact area. The only alternative medium for energy absorption is the metal bath itself. One possibility is that the impact energy is transmitted to an ever increasing expanse of fluid motion. This area grows during the early stages of the blow until it covers the whole bath volume (See Figure 77). The small quantity of metal droplet ejections suggests that a very significant portion of the oxygen in the jet was assimilated for forming oxides in condensed phases. Thus, only a small portion of the jet's kinetic energy or the slow rate of carbon monoxide evolution was responsible for shearing the metal in the cavity region.

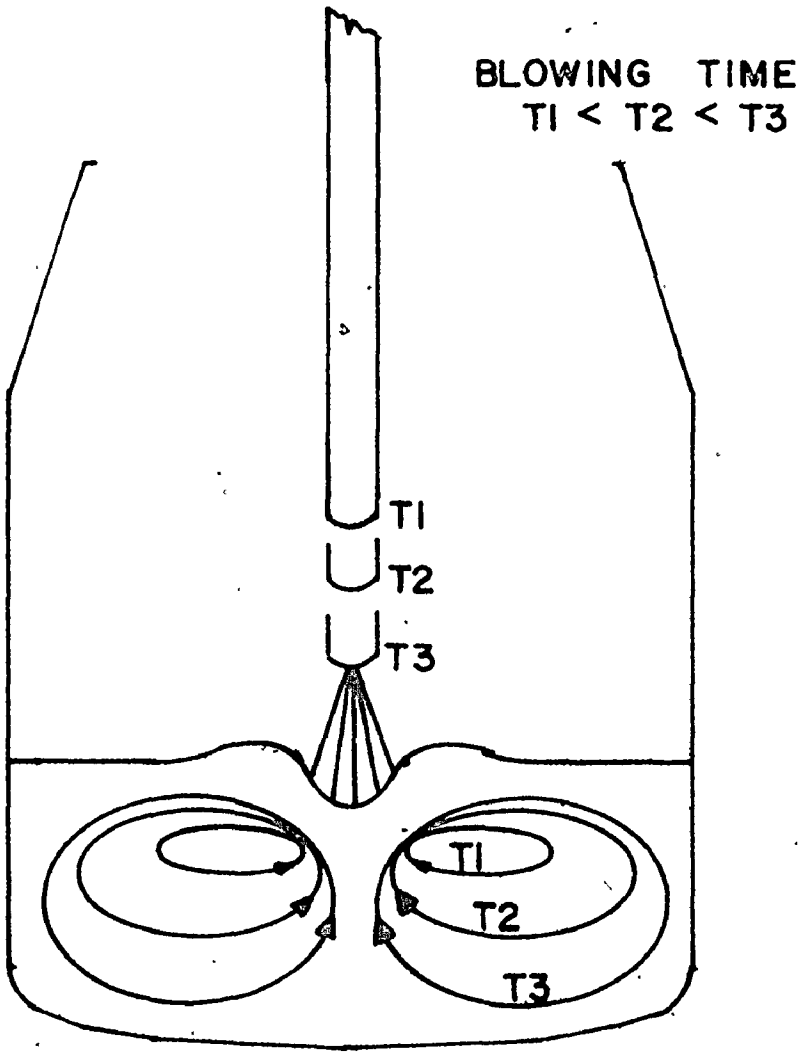

Fig. 77. Expanding front of fluid motion during the first third of the blow.

A question that may arise, and one that has been proposed by different experimentalists[14, 32, 38], is whether the quantity of droplets generated inside the vessel could be much greater than those collected at the furnace mouth. Perhaps the main portion of the ejections was directed towards the furnace walls and never escaped[15]. Measurements made by blowing oxygen on slag free hot metal suggest high ejection rates of 500 Kg min^{-1} in a 6 ton furnace[38]. Higher rates than those measured could not have occurred in the commercial furnace since, as will be proved later, the carbon monoxide evolution rates (0.05 to 0.15%C min^{-1}) present during this period could break up liquid metal films to cause entrainment of molten metal droplets of 200 to 600μ diameter. Droplets of such size can readily be carried away in the gas stream and be caught in the ejection sampler. The observed droplet sizes ranged considerably below these values at 15-45μ; of course these could be originated from larger droplets through explosions. It would be unlikely however that the metal droplet quantity present in the furnace atmosphere could largely exceed the collected amounts since it could be and would be carried out by the waste gas flow. The contradictory evidence obtained by these experimentalists could be created by an erroneous sampling method. In their small scale furnaces, a lance was introduced over a metal bath with the ejection samples being taken on a pan inside the furnace as soon as the oxygen flow was started. Such a surge in flow has been shown to cause increased ejection. Starting with a motionless bath as in these experiments, this deviation would be more easily manifested since the input gas would be initially deflected without any energy absorption. Large quantities of droplets were thereby incorrectly formed and measured[14, 32, 38]. This behaviour was visually observed in commercial operations just before and after ignition.

(iv) CAUSES FOR SLOPPING

Slopping was first observed at the 7 minute sampling. It persisted throughout the 10 and 13 minute points of the blow. The most important cause for slopping might be the highly overoxidized state of the slag. Throughout this period, the ferric to ferrous ratio in the slag sampled by the slag sampler was around one with the total concentration varying slightly between 5 and 7%. This ratio is considerably larger than values quoted by other authors[51, 73] (between 0.1 to 0.5) for operations free of slopping. Similar evidence of the effect of this composition ratio on slopping occurrence was obtained in this study. As shown in Table 40, two special heats noted for the absence of slopping had a maximum ferric to ferrous ratio of 0.6 during this time period. Furthermore, three regular heats, in which only metal ejection was present at the 7 minute mark and whose corresponding slags had been analyzed, had ratios of 0.55, 0.43 and 0.54. These observations indicate the importance of maintaining a ferric to ferrous ratio of less than 0.6 to avoid slopping. The operation parameters which cause these different slag conditions could not be identified. They would most probably be terms involving slag development, lance height, blowing rate and metal and slag temperature.

The existence of a high ferric to ferrous ratio in the slag is not sufficient by itself to cause slop. This was indicated by the absence of slop at the 4 and 16 minute points in the blow where this ratio was also around one. The only apparent difference in slag composition was the V-ratio variation. Between the 7 and 13 minute mark, the slag V-ratio (between 1.1 and 1.4) was in the active foaming region as noted in Figure 12. This slag could reach higher levels in the vessel, thereby permitting some slag-metal emulsion to escape if there was any suddenly excessive gas release in localized areas. CO release of this sort could occur because of the low metal droplet temperatures and the

relatively high carbon concentration. The oxygen concentration could build up in the droplets under these conditions to certain supersaturation levels as required for homogeneous nucleation of CO. Explosive gas release could thus result.

The cause for the variation in the intensity of slopping (light and heavy) at the 7 minute mark could not be determined. One explanation, variance in ferric to ferrous ratio, could not be checked out because of insufficient slag analyses. Anotner possible explanation, variation in the decarburization profile as in Figure 16, could not be studied because of the rather poor information rendered by metal analysis. The instantaneous decarburization profile, as obtained from waste gas analysis, would have been more useful. Further work would have to be done in this area to make any concrete statements.

(v) BACKGROUND METAL EJECTION DURING SLOPPING

In considering the slop material, it was noted (Section 4G) that it contained a larger amount of metallic iron than the corresponding slag-metal emulsion in all the time periods. These excess iron droplets could be considered to arise from another source, but they could not be physically isolated from the emulsion slop. By taking into account the composition differences it was possible to calculate the hypothetical background metal ejection rates during slopping. The corresponding results are plotted in a fashion similar to Figure 76 in Figure 78. As can be seen this metal ejection rate was almost constant during the slopping period.

The source of this metal would have to be the metal bath since the slag matrix composition of the slop material was essentially the same as that of the furnace slag taken by the slag sampler for most of its components. The one deviation, higher ferric levels in the slop, could be accounted for by oxidation of the extra metal. The surface of these metal droplets could have been

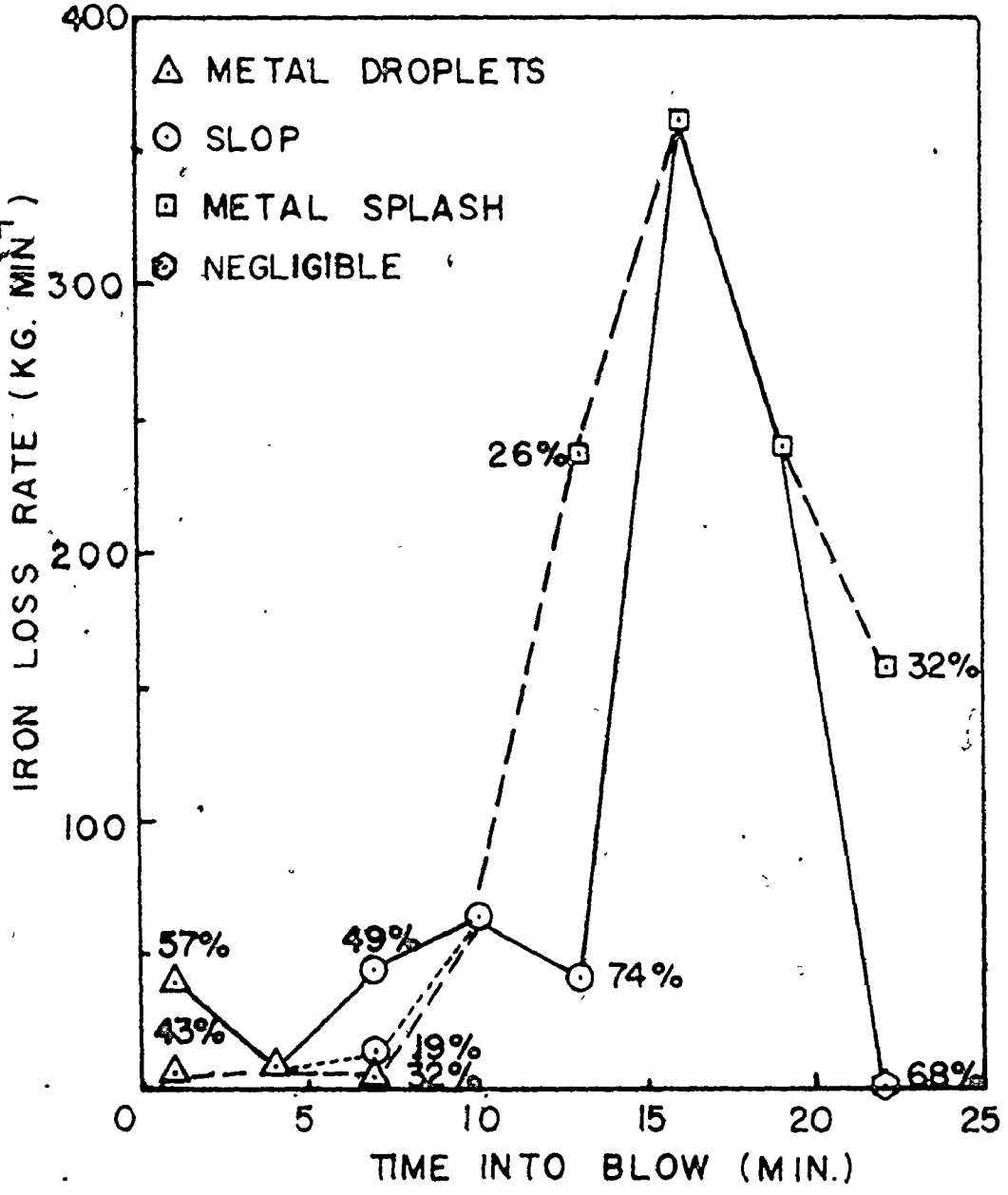

Fig. 78. Average metal loss rates by ejection from the central cavity zone during the blow. Percentages indicate the frequency of occurrence.

oxidized during the collection process or after its removal from the furnace and before it cooled in air. The higher ferric content of light slop in comparison to heavy slop at the 7 minute mark and the excessive ferric content (6.8%) of slop at 13 minutes was due to the larger excess metal proportion in both materials.

The background metal ejection must have arisen from the jet impact area. This was the only place where metal droplets free from slag could be generated. The existence of an open channel for metal release through the emulsion is necessary for any mechanism to be proposed. Oxygen deflection in the impact area is not likely to be the dominant mechanism since the assimilation rate by refining reactions is close to 100%. However, off gas being released from the cavity area may be fast enough to carry along these substantial quantities (40 to 60 Kg min^{-1}) of metal. This mechanism is supported by the fact that from the 7 to 13 minute mark, decarburization increases in prominence since nearly all the silicon and manganese have been oxidized. Further supporting evidence is available from the observation that only metal ejection occurred in the latter stages of the blow where decarburization is the predominant refining reaction.

(vi) THE INCIDENCE AND MECHANISM OF METAL EJECTION

Slopping gave way to metal-only ejections of greater quantity at either the 13 or 16 minute mark. The average metal ejection rates at 13, 19 and 22 minutes were quite similar. The peak observed at the 16 minute mark was most likely due to the surge in oxygen flow normally taking place between 14 and 16 minutes. The cause for this transition to metal ejections was not observed in any operation parameters. The slag ferric to ferrous ratio was still around one in the early time periods of metal ejection. One hypothesis

for this behaviour is a change in the slag properties occurring simultaneously with a peak decarburization level. As the V-ratio of the slag increased, the capacity for foaming decreased (Figure 12) causing the emulsion to subside somewhat. No emulsion was thereby ejected. The rate of decarburization was maintained at a peak level during this time period (Figure 17), utilizing almost all the supplied oxygen. The rapid CO evolution from the cavity region could supply the shearing force to produce these large quantities of metal ejection. This gas could escape along the walls of the cavity area or through an alternate gas channel in the metal bath as depicted in Figure 26e. This secondary channel has been observed to form during peak decarburization rates to physically accommodate the rapid gas release[112-123].

Several observations point to the importance of decarburization rate on metal ejection. Firstly, there was a similarity between the metal loss by direct ejection as a function of time (Figure 78) and the decarburization (Figure 17) profiles. Both increased with time, but not in a constant proportion, until the latter stages of the blow. At this 22 minute mark, negligible ejection quantities were generally noted along with a decreased decarburization rate. This was also observed for cases of carbon reblow. There was no slag cover in this last case because of the operating practice of dumping slag before carbon reblows. Slag cover is thus seen to be unimportant in reducing metal ejections by entrapment as long as the decarburization rate is low. This was also observed in the early blowing periods (0-6 min), where oxygen predominantly forms oxides in condensed phases.

However slag cover is an important term when considering the peak decarburization period. The metal ejections had to pass through some sort of channel around the lance area since no slag was found with the metal. This channel could have been formed by the oxygen jet pushing away the viscous

slag towards the furnace walls. An alternative might be that the gas release from the cavity area was so large that it formed its own channel through the slag layer. Any metal sheared from the cavity area could thus escape through this opening without being trapped by the slag.

The metal ejection material had a maximum droplet size of around 1 cm. However, on the basis of gas entrainment studies (Appendix 3), the maximum size droplet that could be carried in the waste gas stream during the peak decarburization period (0.23%C min^{-1}) was only 0.09 cm (See Figure 79). This is smaller than the observed diameter by one order of magnitude. Some mechanism that supplies sufficient momentum to these droplets to allow them to escape directly from the furnace must therefore be active. Rapid CO gas release from the cavity region or through the secondary bath channel, either of a continual or periodic nature, could supply the necessary momentum through its shearing action. The mixture of droplet and larger splash sizes in the metal ejection material could be explained as being the result of varying intensities of shear in the two source regions.

(vii) THE RELATIVE IMPORTANCE OF REFINING REACTIONS IN THE EMULSION

During the BOF blow, metal refining takes place at a variety of reaction sites: directly under the jet, in the slag-metal-gas emulsion, along the trajectory of CO bubbles within the bulk metal, and at the metal bath-slag interface. It is difficult to assess the quantitative contribution of each of these mechanisms because of the system's complexity. The emulsion site has been ascribed various degrees of significance[51-65]. Slag is circulated in the BOF by the action of the oxygen jet (Figure 24). Metal droplets are supplied to it to form an emulsion by a variety of mechanisms: i.e., shearing action of oxygen jet in cavity region, metal coating on rising CO bubbles (Figure 13). Metal droplets of bath composition are continually renewed while the refined ones settle out. The droplets are refined in the emulsion by slag-metal and gas-metal reactions.

The exact reaction path a droplet follows and the degree of refining in each cycle have not been fully determined. Some authors[53] claim that emulsion reactions account for the majority of the metal refining, whereas others[56, 66] estimate that it can, at maximum, be responsible for 30% of the overall scheme. Its degree of importance will vary during the blowing period.

In this study, based on the sampling of emulsified materials, the metal present in the emulsion as droplets varied between 1.8 and 3 tons during the blow. The average was 2.8 tons. This metal droplet content, if a 1 to 2 minute-droplet in slag-residence time is assumed[51-53], represents the passage of 35 to 70 tons of metal through the emulsion. If it is assumed that the metal droplets are refined completely during their residence in the emulsified state, an estimate can be made of the maximum possible contribution of emulsion reactions. This estimate is somewhat dubious in that it ignores the fact that the bath concentration is continually changing and unlikely to be uniform. Along with the variation in the amount and properties of slag, the droplets residence time and intensity of reactions would also change during the course of the blow. However, under the assumptions stated, it could be said that it is very likely that less than half of the total impurities are removed from the metal phase by refining reactions in the emulsified state.

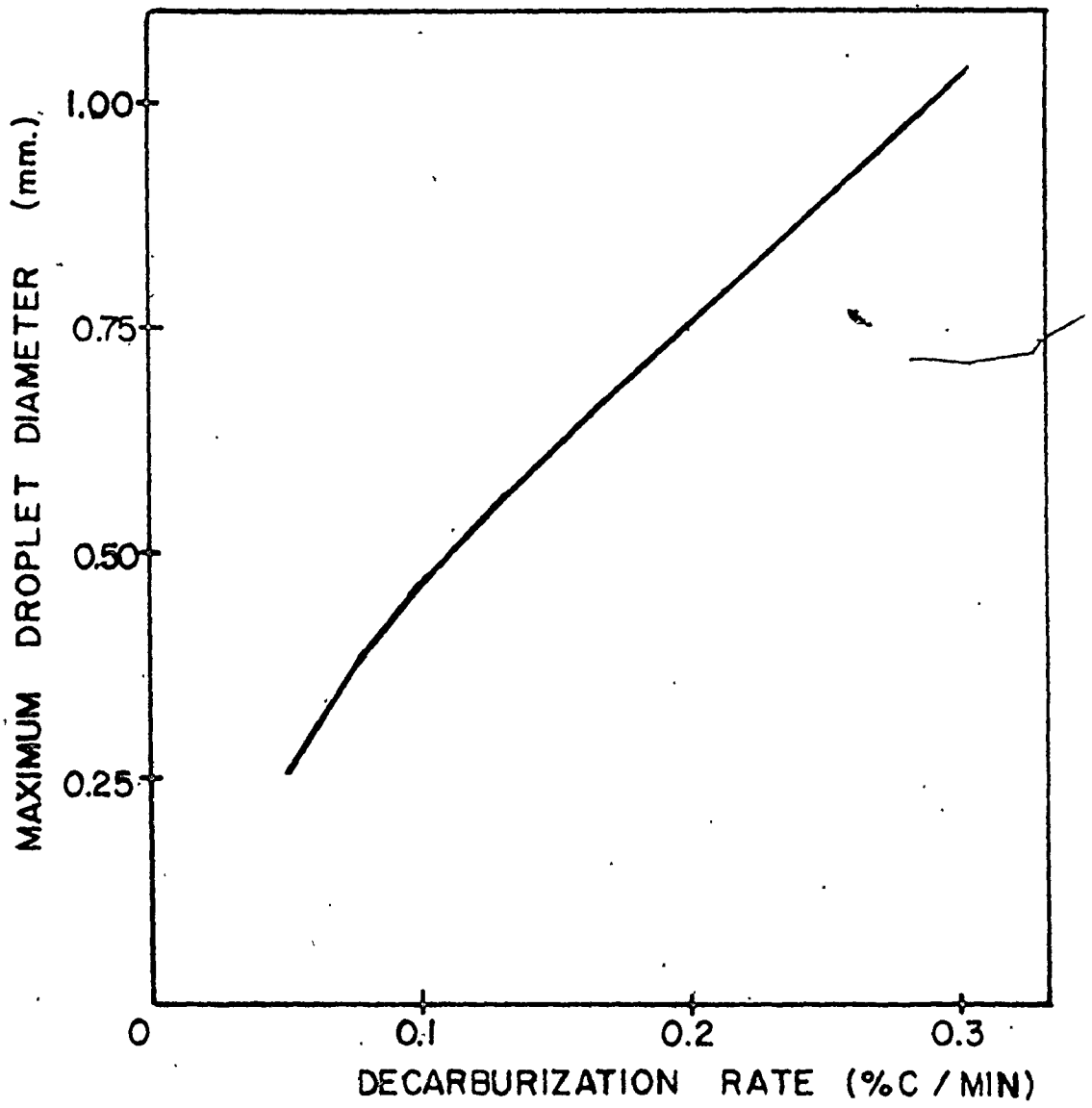

Fig. 79. Plot of the maximum size metal droplet that can be entrained in the off gas stream. (Appendix 3).

6. CONCLUSIONS

In view of the complexity of the industrial system and the limited number of measurements, nevertheless, in the present work, the following conclusions have been reached.

1. Two sampling devices, one for measuring ejection rates and the other for obtaining slag and metal samples, were developed. The various tests conducted showed the samplers to be accurate and reliable for the purpose such as that of the present work.
2. Three periods of material ejection were noted in the BOF blow with characteristic and predictable ejection rates. These consisted of a fine metal ejection stage (0-6 min), a slopping stage (6-15 min) and a heavy metal ejection stage (15-21 min). The remaining time period in the blow normally yielded very little ejections.
3. The iron loss rate by ejection from the furnace was found to be directly affected by the distance from the surface of the metal bath to the mouth of the BOF, the shorter the distance the stronger the ejection.
4. Sudden surges in oxygen flow, which were not readily assimilated by the bath, caused large increases in ejection rates.
5. The first stage of material ejection had low, constant metal loss rates because of the large extent of assimilation of the oxygen flow by non-gas producing reactions. Cavity shearing was not very active in this time period. An increase in the jet impact velocity did not increase the metal ejection rate because of the absorption of the kinetic energy by an expanding front of fluid motion.

6. Slopping was caused by a combination of factors: a relatively high ferric to ferrous ratio in the slag, a slag V-ratio between 1.1 and 1.4, and a low spectic furnace refining volume (0.52 $m^3 t^{-1}$). A reduction in the oxygen flow reduced the slopping rate. Slopping - emulsion ejection - was accompanied by metal ejection from the bath. The oxidation of this metal caused higher ferric levels in the slop material.
7. Metal ejection passes through an open channel around the lance region. The metal could be ejected from the cavity region or from an alternate gas hole. High decarburization rates were present during the period of heavy metal ejection, thereby strengthening the concept that CO gas release rates determine the intensity of metal ejection.
8. The slag composition was determined for the entire blowing period. The high metal droplet content suggests that emulsion reactions may be very important in the refining process.

FUTURE WORK

All the information supplied in this thesis was based on one melt shop operation. The findings need not be restrictive because of this, since the BOF process is rather common for most other shops. Using the simple devices that were designed in this work, it was possible to extract a lot of information about slag development, slopping and metal ejection. Certain insights were gained on the causes of material ejection but no concrete conclusions were reached. A more intensive study consisting of more frequent sampling and analysis of ejections and slag could possibly supply some answers. This could be run in conjunction with a continuous monitering of the carbon evolution rate through waste gas analysis, and with sound intensity measurements to determine the degree of slag cover. A correlation between these two variables and the material ejection rate was suggested in this thesis; by monitering these variables the hypothesis could be proved or disproved. A measurement of the emulsion level at the different sampling periods could also supply useful information on the effect of gas residence time on ejection rates. All these studies could be used to form a more complete picture of the BOF process.

BIBLIOGRAPHY

1. Itaoka, T., Proc. I.I.S.I., p. 32, 1976.

2. Oakey, J. D. and Hunter, P. B., Proc. I.I.S.I., p. 73, 1976.

3. Lait, J. E., Heyer, K. W. and Cuthill, G. K., "The Role of Slag in Basic Oxygen Steelmaking Processes", W-k. Lu (Ed.), McMaster University Press, Hamilton, Paper 8, 1976.

4. Okhotskii, V. B. et al, Steel in the USSR, 4, p. 187, 1974.

5. Sheridan, A. T., Mackenzie, J. and Fitzgerald, F., Fuel and Furnace Research, Report 5561, 1967.

6. Jervais, P., Stewart, I. and Sheridan, A. T., Fuel and Furnace Research, Report 5561, 1967.

7. Rosler, R. S. and Stewart, G. H., J. Fluid Mech., 31, p. 163, 1968.

8. Molloy, N. A., J.I.S.I., 208, p. 943, 1970.

9. Mathieu, F., Revue Universelle Mines de la Metallurgie, 18, p. 482, 1962.

10. Chedaille, J., "Congres Intern. Acieries a l'Oxygene", Le Touquet, p. 222, 1963.

11. Kluth, K. H. and Maatsch, J., Techn. Mitt. Krupp. Forsch. Ber., 22, p. 93, 1964.

12. Ishikawa, H. et al, Tetsu to Hagane, 58, p. 76, 1972.

13. Holden, C. and Hogg, A., J.I.S.I., 196, p. 318, 1960.

14. Chatterjee, A. and Bradshaw, A. V., J.I.S.I., 210, p. 179, 1972.

15. Robertson, A. D. and Sheridan, A. T., J.I.S.I., 208, p. 625, 1970.

16. Van Langen, J. M., J.I.S.I., 196, p. 262, 1960.

17. Aniola, J. and Bien, A., Hutnik, 32, p. 35, 1965.

18. Bacan, N. P. et al, J.I.S.I., 195, p. 286, 1960.

19. Turkdogan, E. T., Chem. Eng. Sci., 21, p. 1133, 1966.

20. Banks, R. B. and Chandrasekhara, D. V., J. Fluid Mech., 15, p. 13, 1963.

21. Davenport, W. G. et al, "Proc. of Symposium on Heat and Mass Transfer in Process Metallurgy", I.M.M., London, p. 207, 1966.

22. Inada, S. and Watanabe, T., Trans. I.S.I.J., 17, p. 59, 1977.

23. Inada, S. and Watanabe, T., Trans. I.S.I.J., 17, p. 67, 1977.

24. Szekely, J. and Asai, S., Met. Trans., 5, p. 463, 1974.

25. Li, K., J.I.S.I., 196, p. 275, 1960.

26. Holmes, B. S. and Thring, M. W., J.I.S.I., 196, p. 259, 1960.

27. Segawa, K. et al, Tetsu to Hagane, 44, p. 1056, 1958.

28. Ogryskin, E. M., Inzhenerno-Fizicheskii, 11, p. 97, 1959.

29. Philbrook, W. O., Open Hearth Proc., 44, p. 376, 1961.

30. Block, H. R., Masui, A. and Stolzenberg, G., Arch. Eissenhuttenwes, 44, p. 357, 1973.

31. Ogryzkin, E. M., Izvest. Akad. Nauk SSSR, p. 17, 1963.

32. Flinn, R. A. et al, Trans. Met. Soc. A.I.M.E., 239, p. 1776, 1967.

33. Kootz, T., J.I.S.I., 196, p. 253, 1960.

34. Kootz, T. and Behrens, K., Neue Hutte, 11, p. 207, 1966.

35. Kleppe, W. and Oeters, F., Arch. Eisenhuttenwes, 47, p. 271, 1976.

36. Hammer, R., Kootz, T. and Sittard, J., Stahl und Eisen, 77, p. 1303, 1957.

37. Yavoiskii, V. A. et al, Steel in the USSR, 6, p. 17, 1976.

38. Chatterjee, A., Lindfors, N. O. and Wester, J. A., I.&S.M., 1, p. 21, 1976.

39. Baker, R., BSC Report, code CAPL/SM/A/31/74.

40. Nilles, P. et al, C.R.M., 27, p. 3, 1971.

41. Dauby, P. and Boelens, J., C.R.M., 33, p. 3, 1972.

42. Meyer, F. and Kaell, N., "The Role of Slag in Basic Oxygen Steelmaking Processes", W-K. Lu (Ed.), McMaster University Press, Hamilton, Paper 5, 1976.

43. Iyengar, R. K. and Aukrust, E., Open Hearth Proc., 57, p. 152, 1974.

44. Klein, A. L. et al, Stal', 3, p. 215, 1975.

45. Gorelov, V. F. et al, Izv. VUZ Chern. Met., p. 50, 1976.

46. Yamada, K. et al, "The Role of Slag in Basic Oxygen Steelmaking Processes", W-K. Lu (Ed.), McMaster University Press, Hamilton, Paper 3, 1976.

47. van Hoorn, A. I. et al, ibid, Paper 2.

48. Cosma, D. et al, ibid, Paper 4.

49. Turkenich, D. I. et al, Steel in the USSR, 2, p. 270, 1972.

50. Szekely, J. and Todd, M. R., Trans. Met. Soc. A.I.M.E., 239, p. 1664, 1967.

51. Kozakevitch, P., J. Metals, 21, p. 57, 1969.

52. Trentini, B., Trans. Met. Soc. A.I.M.E., 242, p. 2377, 1968.

53. Meyer, H. W. et al, J. Metals, 20, p. 35, 1968.

54. Nilles, P. and Denis, E. M., J. Metals, 21, p. 74, 1969.

55. Kozakevitch, P. et al, "Congres Intern Acieries a l'Oxygene", Le Tuoquet, p. 248, 1963.

56. Price, D. J., "Chemical Metallurgy of Iron and Steel", I.S.I. Publication, London, p. 8, 1973.

57. Meyer, H. W., J.I.S.I., 207, p. 781, 1969.

58. Zarvin, E. Y. et al, Steel in the USSR, 2, p. 616, 1972.

59. Poggi, D., Minto, R. and Davenport, W. G., J. Metals, 21, p. 40, 1969.

60. Goto, K. S. and Eketorp, S., Scand. J. Metallurgy, 3, p. 1, 1974.

61. Urquhart, R. C. and Davenport, W. G., J. Metals, 22, p. 36, 1970.

62. Gaye, H. and Riboud, P. V., I.R.S.I.D. Report.

63. Okhotskii, V. B., Steel in the USSR, 3, p. 473, 1973.

64. Bardenheuer, H., Stahl und Eisen, 95, p. 1023, 1975.

65. Walker, R. D. and Anderson, D., Iron and Steel, 45, p. 271, 1972.

66. Okano, S. et al, Proc. I.C.S.T.I.S., Suppl. Trans. I.S.I.J., vol. 2, p. 227, 1971.

67. Muchi, E. et al, ibid, p. 347.

68. Mulholland, E. W., Hazeldean, G. S. F. and Davies, M. W., J.I.S.I., 211, p. 632, 1973.

69. Weeks, R., "Kinetics of Metallurgical Processes in Steelmaking", Dusseldorf, p. 103, 1975.

70. Middleton, J. R. and Rolls, R., ibid, p. 117.

71. Oeters, F., ibid, p. 97.

72. Kuznetsov, A. F. et al, Steel in the USSR, 2, p. 516, 1972.

73. Krainer, H., Borowski, K. and Maatsch, J., Krupp Technical Review, 23, p. 53, 1965.

74. Kol'tsov, A. T. and Yakoveev, V. V. Stal', 9, p. 799, 1976.

75. Geiger, G. H., Kozakevitch, P., Olette, M. and Riboud, P. V., "Theory of BOF Reaction Rates", BOF Series, Book 2, A.I.M.E. Publication, 1975.

76. Baptizmanskii, V. I. et al, Stal in English, p. 293, 1967.

77. Meyer, H. W., "Proc. of Symposium on Heat and Mass Transfer in Process Metallurgy", I.M.M., London, p. 173, 1966.

78. Nilles, P. et al, C.R.M., 15, p. 81, 1968.

79. Hayashi, S., I. & S. M., 3, p. 13, 1976.

80. Meyer, H. W. et al, J. Metals, 16, p. 501, 1964.

81. Voll, H. and Ramelot, D., C.R.M., 33, p. 11, 1972.

82. Dauby, P. et al, C.R.M., 15, p. 51, 1968.

83. Koga, K. et al, I. & S. M., 3, p. 146, 1976.

84. Coheur, J. P. and Nilles, P., C.R.M., 12, p. 43, 1967.

85. Trentini, B. et al, J. Metals, 16, p. 508, 1964.

86. Nilles, P. and Holper, R., C.R.M., 35, p. 23, 1973.

87. Decker, A. and Nilles, P., C.R.M. 40, p. 3, 1974.

88. Nagano, Y et al, Proc. I.C.S.T.I.S., p. 354, 1971.

89. Dauby, P. and Scouvement, J., C.R.M., 34, p. 3, 1973.

90. Iyengar, R. K. and Petrilli, F. C., J. Metals, 25, p. 21, 1973.

91. Tret'yakov, E. V. et al, Metallurg , 14, p. 21, 1969.

92. Zarvin, E. Y. et al, Steel in the USSR, 5, p. 76, 1975.

93. Baptizmanskii, V. I. et al, Steel in the USSR, 3, p. 634, 1973.

94. Itaoka, T. et al, Tetsu to Hagane, 50, p. 412, 1964.

95. Elliott, J. F., Elec. Furn. Proc., 32, p. 293, 1974.

96. Zarvin, E. Y. et al, Izvest. VUZ Chern. Met., 13, p. 47, 1970.

97. Fitterer, G. R., Open Hearth Proc., 52, p. 124, 1969.

98. Plockinger, E. and Wahlster, M., Stahl und Eisen, 80, p. 407, 1960.

99. Rellermeyer, H. and Kootz, T., Stahl und Eisen, 74, p. 390, 1954.

100. Kootz, T. and Altgeld, A., Proc. I.C.S.T.I.S., p. 528, 1971.

101. Bardenheuer, F. et al, Blast Furnace and Steel Plant, 58, p. 401, 1970.

102. Rote, F. E. and Flinn, R. A., Met. Trans., 3, p. 1373, 1972.

103. Krainer, H. et al, Open Hearth Proc., 45, p. 494, 1962.

104. McBride, D. L., J. Metals, 12, p. 531, 1960.

105. Myrtsymov, A. F., Stal in English, p. 794, 1965.

106. Ichinoe, M. et al, Proc. I.C.S.T.I.S., p. 232, 1971.

107. Kawakami, K., Open Hearth Proc., 49, p. 59, 1966.

108. Smith, G. C., ibid, p. 71.

109. Chatterjee, A., Iron and Steel, 45, p. 627, 1972.

110. Lee, C. K. et al, Iron and Steel Int., 50, p. 175, 1977.

111. Denis, E., C.R.M., 8, p. 17, 1966.

112. Okhotskii, V. B. et al, Steel in the USSR, 3, p. 630, 1973.

113. Sharma, S. K., Hlinka, J. W. and Kern, D. W., I. & S.M., 4, p. 7, 1977.

114. Kapalun, P. R. et al, Izv. VUZ Chern. Met., p. 43, 1974.

115. Zarvin, E. Y. et al, ibid, p. 33.

116. Yavoiskii, V. I. et al, Steel in the USSR, 4, p. 20, 1974.

117. Baptizmanskii, V. I. and Shchedrin, G. A., Steel in the USSR, 3, p. 14, 1973.

118. Afanas'ev, S. G. et al, Steel in the USSR, 1, p. 515, 1971.

119. Baptizmanskii, V. I. et al, Steel in the USSR, 5, p. 540, 1975.

120. Baptizmanskii, V. I. and Paniotov, Y. S., Steel in the USSR, 4, p. 801, 1974.

121. Chernyatevich, A. G. et al, Steel in the USSR, 5, p. 79, 1975.

122. Okhotskii, V. B. et al, Steel in the USSR, 2, p. 443, 1972.

123. Ogryzkin, E. M., Izvest. Akad. Nauk SSSR, p. 17, 1963.

124. Kreyger, P. J., Stahl und Eisen, 96, p. 957, 1976.

125. Rinesch, R. F., Steel Times, 193, p. 783, 1966.

126. Reichmayr, J., Iron and Steel Eng., p. 146, April, 1964.

127. Ward, M. D., J.I.S.I., 208, p. 445, 1970.

128. Obst, K. H. et al, ibid, p. 450.

129. Nilles, P. et al, J. Metals, 19, p. 18, 1967.

130. Baptizmanskii, V. I. et al, Steel in the USSR, 5, p. 71, 1975.

131. den Hartog, H. W., Kreyger, P. J. and Snoeijer, A. B., C.R.M., 37, p. 13, 1973.

132. Bondarenko, V. P. and Afanas'ev, S. G., Steel in the USSR, 1, p. 785, 1971.

133. Asai, S. and Muchi, I., Trans. I.S.I.J., 11, p. 107, 1971.

134. Private communication from Dante Cosma, Dofasco.

135. Allen, T., "Particle Size Measurement", Chapman and Hall, London, 1974.

136. Didkovskii, U. K. et al, Steel in the USSR, 4, p. 873, 1974.

APPENDIX 1: CHI-SQUARE TEST FOR DISTRIBUTION NORMALITY

The frequency distribution of a small number of measurements generally provides only sketchy information about the parent distribution whose characteristics are sought. The problem is to decide whether or not the experimental distribution can be satisfactorily assumed to be a sample from a normal parent distribution.

A very useful quantitative test for the goodness of fit of the experimental distribution is the so-called X^2 (Chi-Square) test. The X^2 test gives a single numerical measure of the over-all goodness of fit for the entire range of deviations. In a general view, the X^2 test determines the probability that a purely random sample set of measurements taken from the assumed model parent distribution would show better agreement with the model than is shown by the actual set. This probability is called the level of significance of the distribution.

In performing this test, a minimum of about 20 measurements is normally required. The mean and standard deviation of the data points are first obtained. The entire range of observations is divided into M intervals, normally of the same size. Ideally, each interval should contain more than five measurements but this is not possible with small data sets. In this test, the observed frequencies (f_{obs}) in the intervals are compared with the theoretical model values (f_{th}). These theoretical values are obtained from a normal distribution model based on the calculated mean and standard deviation values. The quantity X^2 is defined as the sum :

$$X^2 = \sum_{j=1}^{M} \frac{\left[(f_{obs})_j - (f_{th})_j \right]^2}{(f_{th})_j}$$

Based on this X^2 value and M-3 degrees of freedom, the level of significance of the experimental distribution can be obtained from Table 1.

An example of a computation of the level of significance is now given.

EXAMPLE

1. DATA SET: number of observations = N = 18

13.5	13.8	11.2
14.5	14.5	10.8
17.8	12.8	13.0
16.4	15.5	14.1
17.6	11.9	14.1
15.8	14.5	12.3

$$\text{mean} = \bar{X} = \frac{\Sigma X}{N} = 14.12$$

$$\text{standard deviation} = s = \left[\frac{\Sigma(X - \bar{X})^2}{N - 1}\right]^{0.5} = 1.99$$

2. FREQUENCY DISTRIBUTION:

Date Range	Number of observations in Interval
10-12	3
12-14	5
14-16	7
16-18	3

3. X^2 TEST

Range	f_{obs}	U_i	Pc_i	P_i	NPi	X^2
10-12	3	-1.0644	0.1436	0.1436	2.585	0.066
12-14	5	-0.0588	0.4766	0.3330	5.994	0.165
14-16	7	0.9467	0.8271	0.3505	6.309	0.076
16-18	3	1.9522	0.9745	0.1474	2.653	0.045
				0.9745	17.541	0.352

$$U = \frac{X_i^1 - \bar{X}}{s} \quad \text{where } X_i^1 = \text{right hand interval end point}$$

$Pc_i = 0.5 \pm (U_i)$ Table 2

$P_i = Pc_i - Pc_{i-1}$ $\quad (Pc_o = 0)$

$$X^2 = \frac{(NP_i - f_{obs})^2}{NP_i}$$

The total X^2 value is 0.354. The degrees of freedom is M-3 or 1. Therefore from Table 1 the level of significance $\geq$ 50%.

TABLE I

VALUES OF χ^2

P equals the probability of exceeding a given value of χ^2 corresponding to n degrees of freedom

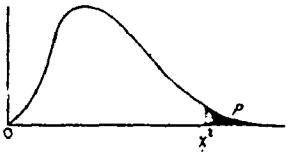

n \ P	0.99	0.98	0.95	0.90	0.50	0.10	0.05	0.02	0.01
1	0.0002	0.0006	0.0039	0.0158	0.455	2.706	3.841	5.412	6.635
2	0.0201	0.0404	0.103	0.211	1.386	4.605	5.991	7.824	9.210
3	0.115	0.185	0.352	0.584	2.366	6.251	7.815	9.837	11.34
4	0.297	0.429	0.711	1.064	3.357	7.779	9.488	11.67	13.28
5	0.554	0.752	1.145	1.610	4.351	9.236	11.07	13.39	15.09
6	0.872	1.134	1.635	2.204	5.348	10.64	12.59	15.03	16.81
7	1.239	1.564	2.167	2.833	6.346	12.02	14.07	16.62	18.48
8	1.646	2.032	2.733	3.490	7.344	13.36	15.51	18.17	20.09
9	2.088	2.532	3.325	4.168	8.343	14.68	16.92	19.68	21.67
10	2.558	3.059	3.940	4.865	9.342	15.99	18.31	21.16	23.21
11	3.053	3.609	4.575	5.578	10.34	17.28	19.68	22.62	24.72
12	3.571	4.178	5.226	6.304	11.34	18.55	21.03	24.05	26.22
13	4.107	4.765	5.892	7.042	12.34	19.81	22.36	25.47	27.69
14	4.660	5.368	6.571	7.790	13.34	21.06	23.68	26.87	29.14
15	5.229	5.985	7.261	8.547	14.34	22.31	25.00	28.26	30.58
16	5.812	6.614	7.962	9.312	15.34	23.54	26.30	29.63	32.00
17	6.408	7.255	8.672	10.08	16.34	24.77	27.59	31.00	33.41
18	7.015	7.906	9.390	10.86	17.34	25.99	28.87	32.35	34.80
19	7.633	8.567	10.12	11.65	18.34	27.20	30.14	33.69	36.19
20	8.260	9.237	10.85	12.44	19.34	28.41	31.41	35.02	37.57
21	8.897	9.915	11.59	13.24	20.34	29.62	32.67	36.34	38.93
22	9.542	10.60	12.34	14.04	21.34	30.81	33.92	37.66	40.29
23	10.20	11.29	13.09	14.85	22.34	32.01	35.17	38.97	41.64
24	10.86	11.99	13.85	15.66	23.34	33.20	36.42	40.27	42.98
25	11.52	12.70	14.61	16.47	24.34	34.38	37.65	41.57	44.31
26	12.20	13.41	15.38	17.29	25.34	35.56	38.88	42.86	45.64
27	12.88	14.13	16.15	18.11	26.34	36.74	40.11	44.14	46.96
28	13.57	14.85	16.93	18.94	27.34	37.92	41.34	45.42	48.28
29	14.26	15.57	17.71	19.77	28.34	39.09	42.56	46.69	49.59
30	14.95	16.31	18.49	20.60	29.34	40.26	43.77	47.96	50.89
n \ P	0.99	0.98	0.95	0.90	0.50	0.10	0.05	0.02	0.01

C

TABLE II

NORMAL CURVE AREAS

Area under the standard normal curve from 0 to z, shown shaded is $A(z)$

Examples If Z is the standard normal random variable and $z = 1.64$, then

$A(z) = P(0 < Z < z) = .4582,$
$P(Z > z) = .0618,$
$P(Z < z) = .9382,$
$P(|Z| < z) = .8764$

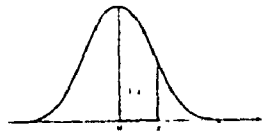

z	.00	.01	.02	.03	.04	.05	.06	.07	.08	.09
0.0	.0000	.0040	.0080	.0120	.0160	.0199	.0239	.0279	.0319	.0359
0.1	.0398	.0438	.0478	.0517	.0557	.0596	.0636	.0675	.0714	.0753
0.2	.0793	.0832	.0871	.0910	.0948	.0987	.1026	.1064	.1103	.1141
0.3	.1179	.1217	.1255	.1293	.1331	.1368	.1406	.1443	.1480	.1517
0.4	.1554	.1591	.1628	.1664	.1700	.1736	.1772	.1808	.1844	.1879
0.5	.1915	.1950	.1985	.2019	.2054	.2088	.2123	.2157	.2190	.2224
0.6	.2257	.2291	.2324	.2357	.2389	.2422	.2454	.2486	.2517	.2549
0.7	.2580	.2611	.2642	.2673	.2704	.2734	.2764	.2794	.2823	.2852
0.8	.2881	.2910	.2939	.2967	.2995	.3023	.3051	.3078	.3106	.3133
0.9	.3159	.3186	.3212	.3238	.3264	.3289	.3315	.3340	.3365	.3389
1.0	.3413	.3438	.3461	.3485	.3508	.3531	.3554	.3577	.3599	.3621
1.1	.3643	.3665	.3686	.3708	.3729	.3749	.3770	.3790	.3810	.3830
1.2	.3849	.3869	.3888	.3907	.3925	.3944	.3962	.3980	.3997	.4015
1.3	.4032	.4049	.4066	.4082	.4099	.4115	.4131	.4147	.4162	.4177
1.4	.4192	.4207	.4222	.4236	.4251	.4265	.4279	.4292	.4306	.4319
1.5	.4332	.4345	.4357	.4370	.4382	.4394	.4406	.4418	.4429	.4441
1.6	.4452	.4463	.4474	.4484	.4495	.4505	.4515	.4525	.4535	.4545
1.7	.4554	.4564	.4573	.4582	.4591	.4599	.4608	.4616	.4625	.4633
1.8	.4641	.4649	.4656	.4664	.4671	.4678	.4686	.4693	.4699	.4706
1.9	.4713	.4719	.4726	.4732	.4738	.4744	.4750	.4756	.4761	.4767
2.0	.4772	.4778	.4783	.4788	.4793	.4798	.4803	.4808	.4812	.4817
2.1	.4821	.4826	.4830	.4834	.4838	.4842	.4846	.4850	.4854	.4857
2.2	.4861	.4864	.4868	.4871	.4875	.4878	.4881	.4884	.4887	.4890
2.3	.4893	.4896	.4898	.4901	.4904	.4906	.4909	.4911	.4913	.4916
2.4	.4918	.4920	.4922	.4925	.4927	.4929	.4931	.4932	.4934	.4936
2.5	.4938	.4940	.4941	.4943	.4945	.4946	.4948	.4949	.4951	.4952
2.6	.4953	.4955	.4956	.4957	.4959	.4960	.4961	.4962	.4963	.4964
2.7	.4965	.4966	.4967	.4968	.4969	.4970	.4971	.4972	.4973	.4974
2.8	.4974	.4975	.4976	.4977	.4977	.4978	.4979	.4979	.4980	.4981
2.9	.4981	.4982	.4982	.4983	.4984	.4984	.4985	.4985	.4986	.4986
3.0	.4987	.4987	.4987	.4988	.4988	.4989	.4989	.4989	.4990	.4990

APPENDIX 2: NORMALIZING EQUATION FOR TRUE SLOPPING RATE

Several assumptions are made in deriving this model

(1) that the slopping rate was constant during the one minute sampling period

(2) that only that material entering through the free area was collected

(3) that a linear relationship existed between the final sample weight and its thickness.

Let:

$\dot{R}''$	=	material ejection rate per unit area	(gm $cm^{-2} min^{-1}$)
W	=	weight of material collected at any time t	(gm)
W_f	=	final weight of material after one minute	(gm)
h	=	thickness of material accumulation at any time t	(cm)
h_f	=	final thickness of material accumulation after one minute	(cm)
X_i	=	tube sampler's side length	(cm)
m	=	slope in regression analysis equation of form $h_f = mW_f$	(cm gm^{-1})
t	=	time	(min)
E	=	corrected weight of ejection material after one minute sampling	(gm)

A differential equation can be set up on the basis that during a small time interval, dt, additional material of weight, dW, and thickness, dh, is collected.

$$dW = \dot{R}'' (X_i - 2h)^2 \, dt \qquad (1)$$

The regression equation (2) can also be differentiated:

$$h_f = m W_f \qquad (2)$$

$$dh = m \, dW \qquad (3)$$

Upon substituting equ. (3) into equ. (1):

$$\frac{dh}{(X_i - 2h)^2} = m \ddot{R} \, dt \qquad (4)$$

Using the appropriate integration constants:

$$\int_0^{h_f} \frac{dh}{(X_i - 2h)^2} = \int_0^1 m \ddot{R} \, dt \qquad (5)$$

$$\frac{1}{X_i - 2h_f} - \frac{1}{X_i} = 2m \ddot{R} \qquad (6)$$

Substituting in equ. (2):

$$\ddot{R} = \frac{W_f}{X_i (X_i - 2 m W_f)} \qquad (7)$$

The corrected ejection weight is given by:

$$E = \ddot{R} \times X_i^2 \times 1\text{min} \qquad (8)$$

Therefore

$$E = \frac{X_i W_f}{X_i - 2 m W_f} \qquad (9)$$

Using the appropriate values for the variables

($X_i = 7$ cm, $m = 4.382 \times 10^{-3}$ cm. gm^{-1})

the final equation that results is:

$$E = \frac{1597 W_f}{1597 - 2 W_f} \qquad (10)$$

APPENDIX 3: DETERMINATION OF MAXIMUM SIZE DROPLET ENTRAINED IN BOF OFF GAS STREAM

List of Symbols:

M	=	droplet mass	(gm)
G	=	gravitational constant = 981	(cm sec^{-2})
d	=	droplet diameter	(cm)
ρ_L	=	droplet density	(gm cm^{-3})
C_D	=	drag coefficient	(unitless)
Pg	=	gas density	(gm cm^{-3})
Ug	=	gas velocity	(cm sec^{-1})
Re	=	Reynolds Number	(unitless)
μ	=	dynamic gas viscosity	(gm cm^{-1} sec^{-1})
C_1, C_2, C_3	=	constants	(unitless)
Vg	=	volume of gas exiting furnace per unit time	(cm^3 sec^{-1})
A	=	inner area of BOF	(cm^2)
$\dot{N}_c$	=	moles of carbon evolved as CO	(gm atom sec^{-1})
R	=	gas constant = 82.3	(cm^3 atm gm $mole^{-1}K^{-1}$)
T	=	temperature	(°K)
X_{co}	=	mole fraction of CO in gas	(unitless)
X_{co2}	=	mole fraction of CO_2 in gas	(unitless)
MW_{co}	=	molecular weight of CO = 28	(gm.gm $mole^{-1}$)
MW_{co2}	=	molecular weight of CO_2 = 44	(gm.gm $mole^{-1}$)
D	=	BOF mouth diameter = 250	(cm)
F_G	=	gravitational force	(gm cm sec^{-2})
F_D	=	drag force	(gm cm sec^{-2})
W	=	weight of metal = 1.45×10^8	(gm)
$\%C$	=	fractional decarburization rate	(sec^{-1})
NW_c	=	atomic weight of carbon = 12	(gm.gm $atom^{-1}$)
P	=	gas pressure	(atm.)

The assumption is made, that in the BOF, metal droplets are delivered to that area in the furnace above the slag by various mechanism. All these droplets are acted on by the drag force (F_D) of the gas. If this drag force is sufficiently large to overcome the gravitational force (F_G) on the droplet, then the droplet will be carried or ejected out of the furnace.

F_D can be obtained from a mathematical expression of Stokes Law:

$$F_G = M \cdot G = \frac{\pi d^3}{6} \rho_L G \qquad (1)$$

$$F_D = C_D \rho_g U_g^2 \frac{\pi d^2}{8} \qquad (2)$$

The gas velocity, Wg, employed in this equation corresponds to the gas velocity at the furnace mouth since it is greatest at this point, thereby exerting the largest drag force. The condition that must be satisfied to determine the largest droplet to be carried out in the gas stream is:

$$F_D > F_G \qquad (3)$$

The drag coefficient (C_D) is a function of the droplet's Reynolds Number (Re). It can be expressed as:

$$Re = \frac{U_g \rho_g d}{\mu} \qquad (4)$$

$$\text{where} \quad U_g = \frac{V_g}{A} \qquad (4A)$$

Functional relationships[1] of the following form are available to determine the drag coefficient for different ranges of Reynolds Number:

$$C_D = \frac{C_1}{Re} - \frac{C_2}{Re^2} + C_3 \qquad (5)$$

where C_1, C_2 and C_3 are unitless constants.

Substituting into equ. (3):

$$\frac{4}{3} \rho_L G d^3 - \frac{C_3 \rho_g V_g^2}{A^2} d^2 - \frac{C_1 \mu V_g}{A} d + \frac{C_2 \mu^2}{\rho_g} < 0 \qquad (6)$$

---

1. Morsi, S. A. and Alexander, A. J., J. Fluid Mech., 55, p. 193, 1972.

To find the maximum size droplet, these terms can be evaluated for various decarburization rates (% $\bar{C}$). The gas velocity varies with these different rates. The gas exiting the furnace is assumed to have a temperature of 1600°C, with a composition of 5% CO_2 and 95% CO. The diameter of the mouth (d) of the BOF is 250 cm. The gas pressure (P) is assumed to be one atmosphere. The quantity of molten metal (W) being decarburized is assumed to be 145 tons. The terms in the trinomial equation can be evaluated on the basis of these assumptions.

$$Nc = \frac{\bar{\%}\, C \cdot W}{AW_c} \qquad (7)$$

$$Vg = \frac{\dot{N}c \cdot R \cdot T}{P} \qquad (8)$$

$$p_g = \left[X_{co} \cdot MW_{co} + X_{co_2} MW_{co_2}\right] \frac{P}{RT} \qquad (9)$$

$$= 1.87 \times 10^{-4} \text{ gm cm}^{-3}$$

$$A = \frac{\pi D^2}{4} \qquad (10)$$

$$= 4.91 \times 10^{4} \text{ cm}^2$$

The values for the constants were obtained from appropriate sources.

$$\rho_s = 7.0 \text{ gm cm}^{-3} \qquad \text{(Reference 2)}$$

$$\mu = 6.16 \times 10^{-4} \text{ gm cm}^{-1} \text{ sec}^{-1} \qquad \text{(Reference 3)}$$

These values were substituted into equation (6) for different decarburization rates. The last term $\frac{(C_2 \mu^2)}{\rho_g}$ was negligible so it was ignored. This allowed a simple solution to be found for the reduced binomial equation. Upon finding the maximum size droplet diameter, a check was carried out to make sure its Reynolds Number was in the assumed range as applied in determining the drag coefficient. The results of these computations are given in Figure 79.

---

2. McGannon, H. E., "The Making, Shaping, and Treating of Steel", 8th Edition, 1964, p. 300.
3. Raznjevic, K., "Handbook of Thermodynamic Tables and Charts", 1976, p. 297.